Modeling mechanisms of nociception using the African mole-rat family

Inaugural-Dissertation
to obtain the academic degree
Doctor rerum naturalium (Dr. rer. nat.)

submitted to the Department of Biology, Chemistry, Pharmacy
of Freie Universität Berlin

by

Karlien Yvonne Berte Debus

2020

The present work was carried out under the supervision of Prof. Dr. Gary R. Lewin from February 2016 to September 2020 at the Max Delbrück Center for Molecular Medicine in the Helmholtz Association.

1st Reviewer: Prof. Dr. Gary R. Lewin

2nd Reviewer: Prof. Dr. Ursula Koch

Date of defense: 14.01.2021

ACKNOWLEDGEMENTS

I would like to thank Prof. Dr. Gary Lewin for giving me the opportunity to conduct my research in his lab. His expert advice and enthusiastic interest for the project throughout the ebb and flow of my own motivation drove me to pursue this PhD. I am very grateful that I got the opportunity to travel to the University of Pretoria (South Africa) and the University of Illinois in Chicago (USA) to perform research, meet interesting people and learn and grow from these different cultures. Special thanks go to Prof. Dr. Nigel Bennett and Prof. Dr. Thomas Park who allowed me to work with their teams and introduced me into their labs, universities and even countries. I also would like to thank Prof. Dr. Ursula Koch, *my Doktermutter*, for the input and guidance in writing and finishing this thesis.

This project would have been impossible without the contribution of many colleagues. First of all, thank you to Ole Eigenbrod and Alison Barker for the scientific collaboration as well as the office talks, travel experiences and friendship during my PhD. Thanks to Daniel Hart for being a great scientific collaborator as well as an incredible host in Pretoria. I feel grateful to have had the chance to work with many scientists who have given me space for developing ideas, helped me performing experiments, reviewed my thesis or were there for me personally: thank you to Jane, Damir, Oscar, Fred, Johannes, Sam, Dimitra, Lisa, Jan, Conni and many others.

This PhD project was also a personal experience with many ups and downs. I wouldn't have reached this point in my life and career without the help of Charlotte, Sirri, Laura, Jana, Carina and Marzena. Thank you so much for your listening, your genuine support, your jokes and everything that best friends do.

My father, my mother, my sister Liesbet and brother Bob have been an unconditional support in this journey. I feel blessed to have gotten all the opportunities and support that have brought me to where I am now. I love you and will never forget that.

Finally, I would like to direct my gratefulness and love to Jean-Yves. You have supported me in every way possible in the last four years, whether it was listening, giving advice, being the best boyfriend or an incredible dad to our daughter Léa Eveline Akoua.

PUBLICATIONS

Parts of this thesis have been published in

Eigenbrod, O. *et al.* (2019) '**Rapid molecular evolution of pain insensitivity in multiple African rodents.**' *Science (New York, N.Y.). American Association for the Advancement of Science*, 364(6443), pp. 852–859. doi: 10.1126/science.aau0236.

ABSTRACT

Algogens are chemically noxious substances produced by animals and plants for their protection against predators. Through behavioral tests on nine closely related African mole-rats (*Bathyergidae*), the naked mole-rat, the East African root rat and C57BL/6N mice, we identified novel insensitivities to three algogens: acid, capsaicin and mustard oil (allyl isothiocyanate, AITC). In parallel, we performed RNAseq on various tissues of these species including tissues of the nervous system, such as dorsal root ganglion (DRG) and spinal cord. This allowed us to investigate the algogen insensitivities by looking at differences in amino acid sequences and expression levels to identify key proteins of interest.

We found that the Highveld mole-rat, unlike its closely related species, is behaviorally insensitive to AITC and weak acids and show impaired behavioral response to formalin. Multiple sequence alignments of the AITC receptor TRPA1, revealed three cysteine changes in the AITC binding site of several species of the mole-rat family. Calcium imaging experiments uncovered a decreased sensitivity for AITC activation through the channels exhibiting one of these amino acid changes. However, since four African mole-rat species have this mutation, an additional adaptation must have taken place in the Highveld mole-rat. RNAseq data identified *nalcn* as the only upregulated gene in the Highveld mole-rats compared to the other mole-rats. NALCN is a sodium leak channel important for establishing the resting membrane potential in neurons and we suggest that an upregulation of the channel protein makes nociceptors less likely to be excited by a noxious stimulus. To evaluate the contribution of NALCN to the observed AITC insensitivity *in vivo*, we looked at the nocifensive behavior towards AITC following an i.p. administration of Verapamil, an L-type calcium channel blocker known to block NALCN *in vitro*. Remarkably, the Highveld mole-rat responded to all algogens to which it had displayed insensitivity. Furthermore, we hypothesized that environmental challenges in the natural habitat of the species have led to an adaptation in the TRPA1 sequence and NALCN expression. Confirming this hypothesis, we identified roots in the burrows of the Highveld mole-rat containing TRPA1 activating substances as well as aggressive biting ants to which the Highveld mole-rat was impervious.

Besides the naked mole-rat who is known to be behaviorally insensitive to acid and capsaicin, we also found two African mole-rats, the Natal mole-rat and Potwe mole-rat, that did not respond to capsaicin injection. Similar, to the naked mole-rat, we identified a functional TRPV1 channel in the Natal mole-rat. Therefore, further investigation is needed to dissect the molecular and evolutionary explanation of the insensitivity in these three species.

ZUSAMMENFASSUNG

Algogene sind chemisch schädliche Substanzen, die von Tieren und Pflanzen zum Schutz gegen Räuber produziert werden. Durch Verhaltensuntersuchungen mit neun eng verwandten Sandgräbern (*Bathyergidae*), Nacktmullen, der Ostafrikanische Maulwurfsratte und C57BL/6N Mäusen haben wir neue Insensitivitäten für drei Algogene: Säure, Capsaicin und Senföl (Allylisothiocyanat, AITC) identifiziert. Gleichzeitig haben wir RNAseq von diversen Geweben dieser Arten durchgeführt, inklusive Geweben des peripheren Nervensystems wie den Hinterwurzelganglien (DRG) und dem Rückenmark. Hierdurch konnten wir die Algogen-Insensitivitäten untersuchen und Unterschiede in den Aminosäure-Sequenzen und Expressionsleveln von Proteinen identifizieren.

Wir fanden heraus, dass der Highveld-Graumull, im Unterschied zu ihm eng verwandten Arten, verhaltensunempfindlich gegenüber AITC sowie schwachen Säuren war und und eine gestörte Verhaltensreaktion auf Formalin zeigte. Mehrfache Sequenz-Angleichungen des AITC-Rezeptors TRPA1 enthüllten drei Cystein-Änderungen in der AITC-Bindungsstelle in mehreren Spezies der Graumull-Familie. Kalzium-Imaging Experimente enthüllten eine herabgesetzte Sensitivität der Kanäle mit einer dieser drei Aminosäuren-Änderung für die Aktivierung durch AITC. Da diese Mutation jedoch in vier Arten der Graumull-Familie vorkommt, muss ein zusätzlicher Adaptationsprozess bei den Highveld-Graumullen stattgefunden haben. RNAseq-Daten identifizierten *Nalcn* als das einzige hochregulierte Gen der Highveld-Graumulle im Vergleich zu den anderen Mullen. NALCN ist ein Natrium Leck-Kanal, der wichtig ist, um das Ruhemembranpotenzial in Neuronen herzustellen, und wir folgern, dass eine Hochregulierung des Kanalproteins die Wahrscheinlichkeit verringert, mit der Nozizeptoren von einem schädlichen Reiz angeregt werden können. Um den Beitrag von NALCN zur beobachteten AITC-Insensitivität in vivo zu ergründen, untersuchten wir das nocifensive Verhalten gegenüber AITC nach einer i.p. Verabreichung von Verapamil, einem L-Typ-Calciumkanalblocker, der bekanntermaßen NALCN in vitro blockiert. Bemerkenswerterweise reagierte der Highveld-Graumull danach auf alle Algogene, auf die er vorher Insensitivitäten gezeigt hatte. Zusätzlich vermuteten wir, dass Herausforderungen im natürlichen Lebensraum der Art zu einer Anpassung der TRPA1-Sequenz und der NALCN-Expression geführt haben. Diese Hypothese

bestätigend, identifizierten wir Wurzeln in den Bauen der Highveld-Graumulle, die TRPA1-aktivierende Substanzen sowie aggressiv beißende Ameisen enthielten, denen gegenüber die Highveld-Graumulle unempfindlich waren.

Neben dem Nacktmull, welcher bekanntlich verhaltensunempfindlich gegenüber Säure und Capsaicin ist, fanden wir zwei weitere Sandgräber: den Natal-Graumull und den Potwe-Mull, die nicht auf Capsaicin-Injektionen reagierten. Wie beim Nacktmull identifizierten wir einen funktionellen TRPV1-Kanal im Natal-Graumull. Dies macht weitere Untersuchungen erforderlich, um die molekularen und evolutionären Mechanismen der Insensitivität bei diesen drei Arten zu ergründen.

LIST OF ABBREVIATIONS

AITC = Allyl Isothiocyanate
ANOVA = Analysis of Variance
ARD = Ankyrin Repeat Domain
ASIC = Acid Sensing Ion Channel
CaV channel = Voltage-gated Calcium channel
CNS = Central Nervous System
DRG = Dorsal Root Ganglion
EGFP = Enhanced Green Fluorescent Protein
IEG = Immediate Early Genes
i.p. = intraperitoneal
ITC = Isothiocyanate
KV channel = Voltage-gated Potassium channel
K2P channel = Two-Pore-Domain Potassium channel
MHR = TRPM Homology Region
Mya = Million years ago
NALCN = Sodium Leak Channel, Non-selective
NaV channel = Voltage-gated Sodium channel
PAG = Periaqueductal Gray
PBN = Parabrachial Nucleus
PCR = Polymerase Chain Reaction
PFA = Paraformaldehyde
PKC = Protein Kinase C
PLC = Phospholipase C
PNS = Peripheral Nervous System
PS-GPCR = Proton-Sensitive G Protein Coupled Receptor
RMP = Resting Membrane Potential
ROS = Reactive Oxygen Species
RT = Room Temperature
SC = Spinal Cord
SEM = Standard Error of the Mean
SLIC = Sequence and Ligation-Independent Cloning

TMD = Transmembrane Domain

TG = Trigeminal Ganglion

TM = Transmembrane

TRP = Transient Receptor Potential

TRPA = Transient Receptor Potential Ankyrin

TRPM = Transient Receptor Potential Melastatin

TRPV = Transient Receptor Potential Vanilloid

LIST OF FIGURES

LIST OF TABLES

TABLE OF CONTENTS

1. INTRODUCTION

1.1. NOCICEPTION

1.1.1. GENERAL PRINCIPLES

The ability to detect and respond to a damaging stimulus is a highly conserved evolutionary trait that serves as a protective mechanism to prevent (further) damage of tissue. Noxious stimuli are detected by peripheral high-threshold receptors (nociceptors) via sensory transduction mechanisms. Nociceptive signaling is relayed from the periphery along the axon to a central synapse in the central nervous system (CNS). Further processing in distinct brain areas allows the translation of the electrical signal into a painful sensation. Pain perception differs with the nature of the noxious stimulus, i.e. mechanical, chemical or thermal. In response to it, a perceptual, autonomic or behavioral response can be triggered (Tiemann *et al.*, 2018). In the beginning of the 20th century in his publication '*The integrative action of the nervous system',* Charles Scot Sherrington coined the animal's response to stimuli expected to produce pain as a 'purposive neural mechanism' which could be explained by Darwin's natural selection theory (Charles Scott Sherrington, 1906; Burke, 2006). Knowledge of a possible danger gives one a tactical advantage as described by the Latin proverb *"Praemonitus, Praemunitus*" or freely translated "Forewarned is forearmed".

Although *E. coli* are known to have mechanosensitive channels and sea anemones (Cnidarian) respond to mechanical stimulation of their sensory organ, it is conventionally thought that only species with a more organized CNS are able to centrally process information following a noxious stimulus (Smith and Lewin, 2009). It is therefore generally agreed upon that nociception developed in bilateral symmetrical species with a distinct peripheral nervous system (PNS) and CNS (Sneddon, 2018). Later in evolution, different ecological environments made it possible for species to further develop advantageous, specialized and complex nervous systems in order to protect against tissue damage.

The mammalian PNS consists of different classes of pseudo-unipolar neurons connecting somatic tissue such as the skin, muscle or visceral tissue to the CNS. The

cell bodies of these peripheral nerve endings are clustered in the dorsal root ganglia (DRG) or the trigeminal ganglia (TG) that project to the dorsal horn of the spinal cord or to the trigeminal nucleus in the brain stem, respectively (Schmidt and Willis, 2007). The function of these afferent neurons is to transduce sensory modalities such as touch, thermal sensation, etc. and send the information to the CNS. On an anatomical and morphological level, three major groups of peripheral sensory afferents can be distinguished: large myelinated Aβ-fibers; medium sized myelinated Aδ-fibers and small unmyelinated C-fibers (Julius and Basbaum, 2001). Aβ-fibers make up 22% of the total number of afferents (Lewin and Moshourab, 2004). They serve as low-threshold mechanoreceptors and are able to conduct information about touch and light pressure with a fast conduction velocity due to their large axonal diameter and thick myelin sheath. Aβ-fibers innervate known epithelial tactile structures including Merkel cells, Ruffini corpuscles, Meissner corpuscles, Pacinian corpuscles and guard hairs (Glatte *et al.*, 2019). Medium sized Aδ-fibers comprise 18% of the afferents and can be divided into D-hairs, low-threshold mechanoreceptors and high-threshold mechanonociceptors (Lewin and Moshourab, 2004). These fibers have “free” nerve endings in different layers of the (epi)dermis or innervate different types of hair follicles such as auchene and zigzag (Glatte *et al.*, 2019). The third and largest group of afferents is C-fibers, which are slow conducting because they lack myelin and are known to transduce noxious information (Dubin and Patapoutian, 2010). Most of these fibers are polymodal, a phenomenon first described by Ed Perl (Bessou and Perl, 1969), meaning that a neuron can be activated by a combination of different high-threshold stimuli, whether mechanical, thermal and/or chemical. Unlike these nociceptive stimuli leading to an unpleasant sensation, a small portion of C-fibers respond to low-threshold mechanical stimuli, which has been postulated to encode “pleasant touch” (Löken *et al.*, 2009). Lastly, a subset of C-fibers is ‘silent’, meaning these are inactive under normal circumstances, but start transducing noxious information after becoming sensitized (Prato *et al.*, 2017). This sensitization process is mostly caused by inflammatory mediators and can be initiated by different mechanisms such as direct stimulation of nociceptors, unmasking silent nociceptors or a reduction of the threshold of action potential generation (Woolf and Ma, 2007). C-like terminals are generally found in the skin as free nerve-endings, and more recently it was shown that some cutaneous Schwann cells are sensitive to noxious mechanical stimuli and transmit this information to associated C-fibers (Abdo *et al.*, 2019). Nociceptors can also be classified based on

the type of noxious stimuli that activate them and by their differential expression of key molecular proteins. These proteins are most often sensory detectors or transducers including ion channels and receptors that are directly or indirectly activated by the noxious stimulus and whose activation triggers an action potential. Whilst mechanical and thermal nociception are important aspects of physiology, this thesis will focus on chemical nociception.

In summary, mammals possess a variety of nociceptors tuned to detect specific stimuli as summarized in *Table 1* (Cain, Khasabov and Simone, 2001; Basbaum *et al.*, 2009).

Fiber	**Type**	**Type of noxious stimulus**
Aδ	A-mechanonociceptors (A-M)	mechanical
	A-mechanoheat nociceptors (A-MH)	mechanical and thermal
C	C-polymodal nociceptors	mechanical, thermal and chemical
	C-mechanonociceptors (C-M)	mechanical
	C-mechanoheat nociceptors (C-MH)	mechanical and thermal
	C-mechanocold nociceptors (C-MC)	mechanical and cold
	C-heat nociceptors (C-H)	thermal
	C-"silent"	mechanical and thermal after sensitization

***Table 1**: Overview of the existing mammalian nociceptor types* (Fleischer, Handwerker and Joukhadar, 1983)

1.1.2. PAIN AND NOCIFENSIVE BEHAVIOR

The International Association for the Study of Pain (IASP) defines pain as 'an aversive sensory and emotional experience typically caused by, or resembling that caused by, actual or potential tissue injury'. For the survival of an organism, it is important to perceive and interpret pain as well as to respond and learn from a painful experience to prevent any (further) tissue damage. Central processing of the peripheral signals is complex and many open questions remain about the contribution of different brain areas in perceiving and learning from a pain experience. From the periphery, the

signal generated after a noxious stimulation ascends through the spinal cord to either the parabrachial nucleus (PBN), the periaqueductal gray (PAG) or to nuclei in the thalamus (Hunt and Mantyh, 2001). Nociceptive signals arriving in these areas are in turn relayed to different higher brain areas such as cortex, amygdala, PAG, hypothalamus etc., which are involved in the quantification of pain (i.e. intensity and location) as well as in perceiving the affective and autonomous components (Gauriau and Bernard, 2002; Cortelli *et al.*, 2013; Han *et al.*, 2015). The interconnectivity between the different parts of the brain shows the complex mechanisms of input and output, processing and modulation of nociceptive signals necessary to consciously feel pain, contextualize it and display the appropriate behavior (Barik *et al.*, 2018). A connection between neurons from the PBN and the medulla was recently suggested to be crucial for this behavior, called nocifensive behavior (Baliki and Apkarian, 2015; Barik *et al.*, 2018).

For ethical and practical reasons, pain and nocifensive behavior is often studied in animals rather than humans, with the most studied species being mice and rats (Mogil, 2009; Deuis, Dvorakova and Vetter, 2017). In addition to the fact that the physiology of nociceptors is highly conserved across species from mouse to human, many of these animals' behaviors (such as reflexive withdrawal from painful stimuli) are easy to quantify. Researchers also have the advantage of genetically modifying mice to look at the contribution of single proteins to nocifensive behavior (Mogil, 2009; Gregory *et al.*, 2013). Distinct types of assays have been established based on different types of existing pain. Two major categories of pain are inflammatory and neuropathic pain, which can be acute or persistent depending on the duration of applied noxious stimuli.

For inflammatory and neuropathic pain, several mouse or rat models have been developed where specific manipulations including injury or application of chemical substances produce nociception to model human clinical conditions. Subsequent to the insult, a behavioral response, mimicking the naturally occurring pain experience is measured (Gregory *et al.*, 2013). To evaluate inflammatory pain, the animals are subjected to a manipulation activating the immune system or mimicking or initiating an inflammatory response in diverse tissues such as the skin, joint or muscle. An injection with complete Freund's adjuvant (CFA), a *Mycobacterium tuberculosis* oil suspension or carrageenan, a mixture of polysaccharides are examples of a chemically induced inflammatory models (Zhang and Ren, 2011). Additionally inflammation can be induced in rodents by paw incisions (Pogatzki and Raja, 2003), UV radiation (Bishop *et al.*, 2007)

or burn injuries (Nozaki-Taguchi and Yaksh, 1998). Many diverse experimental models for neuropathic pain have been developed including injury-induced, chemically-induced and disease-induced neuropathic pain. In injury-induced models nerve injuries are made by surgically damaging the nerve such as in partial sciatic nerve ligation (Seltzer, Dubner and Shir, 1990) or spared nerve injury (Decosterd and Woolf, 2000) or sciatic nerve constriction (Bennett and Xie, 1988). Neuropathic pain can be chemically induced by injecting a chemotherapeutic drug (Akbarzadeh *et al.*, 2007) or viruses (such as varicella-zoster or HIV) (Jaggi, Jain and Singh, 2011).

In order to evaluate the pain behavior in these models, several reflexive (e.g. withdrawal), spontaneous (e.g. biting or flinching) and operant (e.g. learned escape or place aversion) assays have been developed (for a detailed review see Deuis, Dvorakova and Vetter, 2017 and Gregory *et al.*, 2013). Reflexive behaviors are measured with assays such as the Hot-Plate test, a test where the animals' paw is placed on a hotplate and the latency of the spinal reflex to withdraw the paw is measured. It can evaluate inflammatory pain as well as neuropathic pain models to measure allodynia, thermal hyperalgesia or spontaneous pain as well as the effectiveness of analgesics on thermal nociception (Eddy and Leimbach, 1953). Similarly, the Hargreaves heat test (Hargreaves *et al.*, 1988) and cold plate test (Jasmin *et al.*, 1998) were developed to detect deficits in thermal sensation. Mechanical stimuli are applied to a mouse or rat by applying calibrated pressure with von Frey elements of pressure application measurement device to identify mechanical allodynia or hyperalgesia (Bradman *et al.*, 2015). A spontaneous behavior such as lifting or licking the paw is used to assess ongoing pain, while operant behaviors and more complex responses are more often used to evaluate the learned aversive nature of pain (Gregory *et al.*, 2013). Conditioned place preference (CPP) for example, is a test where pre-conditioned animals have learned to associate a certain place in the experimental set-up with an analgesic. In Davoody *et al.*, 2011, the researchers used CPP to compare rats with spinal nerve lesions and healthy rats and found a clear place preference in the injured animals for the room with an analgesic, indicating the animals experienced pain was relieved.

There is an important distinction to make between inflammatory and neuropathic models and between acute and persistent pain. In the case of persistent pain, the initial cause of nociception has healed, but the experience remains. It has been found that

distinct neurochemical circuits contribute to the generation of an acute or persistent pain experience (Basbaum, 1999). It is unclear what is the threshold after which pain becomes persistent, however it is generally thought that peripheral sensitization leads to central sensitization triggering plastic changes of peripheral and central neurons which is a pre-requisite for persistent pain (Latremoliere and Woolf, 2009; Sun *et al.*, 2019).

Although using rodent pain models has its limitations, such as the lack of actual evidence for the true origin of the behavior, the partially subjective scoring system or the presence of spontaneous reflexes, it remains a widely used experimental method to investigate pain, the behavior related to it and pharmacology of new analgesics (Gregory *et al.*, 2013).

1.1.3. MOLECULAR MECHANISMS OF CHEMICAL NOCICEPTION

Noxious chemical stimuli, also known as algogens, can be generated by plants or insects as a defense mechanism against foraging animals or predators (Basbaum *et al.*, 2009; Julius, 2013). Well-known examples are capsaicin from chili peppers (Janscó, Kiraly and Janscó-Gábor, 1977) and bee venoms (Chen and Lariviere, 2010). Skin contact with these substances activates nociceptive peripheral endings directly through chemical binding or indirectly by initiating an inflammatory process and/or increasing expression of ion channels. Capsaicin binding to the transient receptor potential vanilloid 1 (TRPV1) receptor causing an electrical signal is an example of direct chemical binding (Jordt and Julius, 2002). In the case of inflammation, a directed immune response causes local plasma extravasation and recruitment of inflammatory cells into the tissue. The release of pro-inflammatory substances including protons, substance P, prostaglandins, bradykinin and cytokines from inflammatory cells (such as mast cells, macrophages, Schwann cells, etc.), causes direct or indirect activation of different receptors and a cascade of downstream pathways, which sensitize nociceptors (Woller *et al.*, 2017). Bradykinin for example, is known to sensitize TRPV1. Doing patch clamp recordings on isolated rat DRG neurons, researchers found an application of bradykinin increased the heat-evoked current and proposed the activation of phospholipase C (PLC) which stimulates a protein kinase C (PKC) mediates this heat sensitization (Burgess *et al.*, 1989; Cesare and Mcnaughton, 1996). Similar experiments with HEK293

cells expressing rat TRPV1 confirmed that the channel is sensitized by bradykinin through a PLC dependent pathway (Chuang *et al.*, 2001). Thus, chemical nociception has enabled many species to detect 'warning signals' from environmental algogens as well as through endogenously produced inflammatory substances in order to prevent any further harm.

Two of the most thoroughly characterized molecular transducers of chemical stimuli are the channels of the Transient Receptor Potential (TRP) channel family and acid-sensing ion channels (Julius, 2013). The TRP channels are highly conserved in the kingdom Animalia, with some mammalian equivalents known to be key proteins in chemical nociception. The mammalian TRP channels involved in chemical nociception will be discussed in more detail in Introduction 1.1.4. The acid-sensing ion channels are able to detect changes in pH since a stable and controlled regulation of acid inside and outside of the cell is important for enzymatic activity and ion homeostasis. Activation of proton-sensitive receptors expressed in nociceptors can evoke nocifensive behavior (Leffler, Mönter and Koltzenburg, 2006). An overview of acid sensors will be given in Introduction 1.1.5.

1.1.4. TRP CHANNELS IN SOMATOSENSATION AND CHEMICAL NOCICEPTION

Intense research on the role of TRP channels in nociception followed the discovery of a light-activated and sustained current in the photoreceptors of the fruit fly (*D. melanogaster*) eye. The mutation of the channel responsible for this current resulted in the a transient depolarization, thus leading to its name "transient receptor potential channel A" or dTRPA (Montell and Rubin, 1989; Smani *et al.*, 2015).

The family of known mammalian TRP channels has grown to over 30 members (Julius, 2013). The channels have significant variations in structure, selectivity, activation and function despite their similarities in subunit composition (i.e. four subunits, each containing six transmembrane segments and cation permeability) *(Figure 1)* (Venkatachalam and Montell, 2007). Based on sequence and topology, the TRP family can be divided into 7 subfamilies in 2 groups: group 1 (greater sequence homology

dTRPA): TRPC, TRPV, TRPM, TRPA, TRPN (not present in mammals) and group 2 (low homology to dTRPA): TRPP and TRPML. These Ca^{2+} permeable ion channels are activated by either chemical (environmental or endogenous substances) or physical (light, sound, temperature, stretch) stimuli (Julius, 2013; Zheng, 2013). TRP channels are a large family of ion channels involved in taste, olfaction, thermo- and mechanosensitivity in many different tissues of humans and most animals. Several members of the mammalian TRP family are notable for their direct gating by algogens, e.g. TRPA1, TRPV1, TRPM2 and TRPM8.

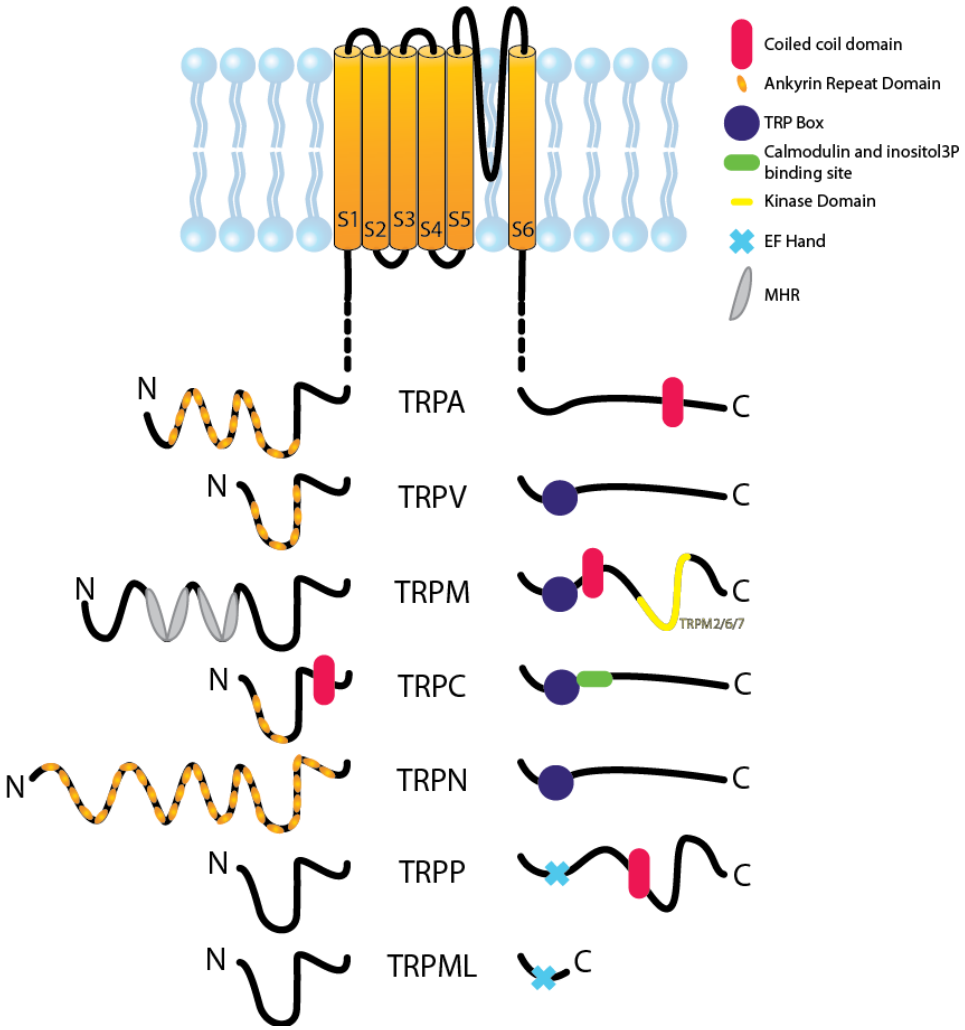

Figure 1: *The general TRP channel structure (S1-S6) with N- and C-terminals indicated for the different subfamilies. Adapted from Blair et al., 2019.*

1.1.4.1. TRPA1, TRANSIENT RECEPTOR POTENTIAL CATION CHANNEL SUBFAMILY A MEMBER 1

The mammalian TRPA1 channel (originally called “ANKTM1”; (Jaquemar, Schenker and Trueb, 1999) is the sole member of the TRPA subfamily. Like all other TRP channels, every subunit has six transmembrane segments (S1-S6). When the subunits form a tetrameric protein, S5, S6 and the transmembrane loop (P loop) shape the ion conducting pore of the channel with amino acid D915, E920 and E924 determining the specificity for mono- or divalent cations (Christensen, Akyuz and Corey, 2016) (*Figure 1* and *Figure 2*). Gating of these channels by endogenous and exogenous ligands enables electrical signaling initiation. All TRP channels have a TRP domain adjacent to S6, which is likely involved in pore gating regulation. Specific to TRPA1 is a large cytoplasmic N-terminal ankyrin repeat domain (ARD). At least 14 repeats of the 33 amino-acid ankyrin sequence-motifs have been identified, compared to only six repeats found in the TRPV and four or five in the TRPC channels (Gaudet, 2008). The region has been determined to be an important site for chemical and thermal activation. In addition, the C-terminal coiled-coil structures from every subunit interact with each other for tetramerization (Clapham, 2015). TRPA1 is expressed in a subset of primary sensory neurons, the peptidergic C-fibers. These nociceptive neurons are known to express Substance P, calcitonin-gene related peptides (CGRP), and the bradykinin receptor, are involved in the transduction of acute noxious stimulation and inflammation (Chen and Hackos, 2015).

External irritants and endogenously produced substances can chemically activate TRPA1, and this can happen in three different ways. The first and most studied type of chemical activation is by covalent modification. Many of the known TRPA1 agonists are exogenous algogens, such as the compound isothiocyanates (ITCs) from the wasabi root and garlic (Jordt *et al.*, 2004) or acrolein from exhaust gas. Tear gas has been weaponized because it contains highly potent TRPA1 activators and the use of it exemplifies the extremity of physiological responses to direct activation of TRPA1 channels (Laursen, Bagriantsev and Gracheva, 2014). Furthermore, endogenous prostaglandin 15d-PGJ2 has been shown to bind via a similar chemical reaction (Takahashi *et al.*, 2008). A more complete list of TRPA1 agonists can be found in *Table 2*.These substances are chemically reactive because of their strong electrophilic

moieties and can therefore interact with the nucleophilic thiol groups of cysteines (*Figure 2*). Cysteines at positions 421, 621, 641 and 661 (human TRPA1 numbering) have been identified to be important for TRPA1 reactivity to electrophilic substances together with one lysine at position 708. All of these cysteines are located on the N-terminus in the ARD or in the linker with S1 (*Figure 2*). The link responsible for the conformational change of the channel and its gating is unknown (Hinman *et al.*, 2006; Macpherson, Dubin, *et al.*, 2007; Chen and Hackos, 2015). The sensitivity to AITC and other algogens is a trait conserved in evolution and seen in all mammals (Jordt *et al.*, 2004), planaria (Arenas *et al.*, 2017), flies (Kang *et al.*, 2010), zebrafish (Oda *et al.*, 2016) and birds (Saito *et al.*, 2014).

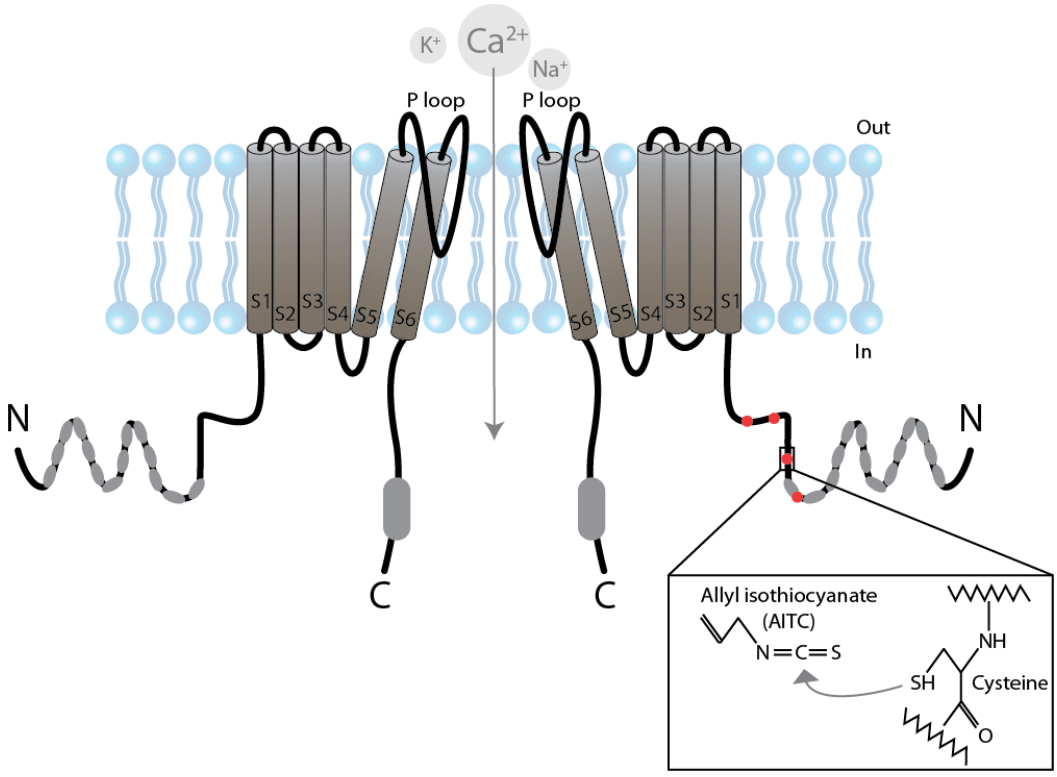

Figure 2: *The general molecular structure of TRPA1. Cysteines identified to be important in the activation by AITC are indicated in red. The covalent modification reaction between a cysteine residue and AITC is shown in detail.*

Some substances directly activate TRPA1 in a non-covalent manner. These include environmental pollutants, benzoquinone produced as a defensive compound by arthropods (Ibarra and Blair, 2013) or weak acids including formic acid (Wang *et al.*, 2011). A mutant TRPA1 channel lacking the reactive cysteines could still be activated by these compounds, however the precise molecular activation mechanism remains elusive (Wang *et al.*, 2011). Thirdly, TRPA1 acts as a 'receptor-operated' channel and is activated via the phospholipase C (PLC) pathway through neurotransmitters, growth factors and other inflammatory substances (e.g. bradykinin activates its G-protein coupled receptor which on its turn modulates TRPA1 activation) (Bandell et al., 2004). It remains unclear how the PLC pathway is coupled to TRPA1 activation. Various hypotheses have been suggested ranging from the action of PIP_2 hydrolysis, and lipid metabolite production to calcium release from intracellular stores (Hinman *et al.*, 2006; Laursen, Bagriantsev and Gracheva, 2014).

Agonist/Antagonist	**Reference**
AP18	(Petrus *et al.*, 2007)
Camphor	(Xu, Blair and Clapham, 2005)
Gadolinium	(Nagata *et al.*, 2005; Bang *et al.*, 2007)
HC-030031	(McNamara *et al.*, 2007)
Ruthenium red	(Story *et al.*, 2003)
15-deoxy-Δ12,14-Prostaglandin J2 5,8,111,14 eicosatetraynoic acid Clordantoin Disulfiram Farnesyl thioacetic acid Farnesyl thiosalicylic acid	(Maher *et al.*, 2008)
15-deoxy-Δ 12,14-Prostaglandin J2, isoprostane 8-iso prostaglandin A2, PGD2 metabolites (A and J)	(Taylor-Clark, Undem, *et al.*, 2008)
2-aminophenyl borane (2-APB)	(Hinman *et al.*, 2006)
4-HHE (4-hydroxyhexenal) 4-ONE (4-oxononenal)	(Taylor-Clark, McAlexander, *et al.*, 2008)
4-HNE (4-hydroxynonenal)	(Macpherson, Dubin, *et al.*, 2007)
Acetaldehyd	(Bang *et al.*, 2007)

2-pentanal Acrolein (2-propenal)	(Bautista *et al.*, 2006)
Allyl isothiocyanates (Mustard oil, AITC) Eugenol Gingerol Methyl salicylate (wintergreen oil)	(Bandell *et al.*, 2004; Jordt *et al.*, 2004)
Benzyl isothiocyanate (BITC)	(Hinman *et al.*, 2006)
Bradykinin	(Bandell *et al.*, 2004; Bautista *et al.*, 2006)
Cannabinoid WIN 55,212-2	(Jeske *et al.*, 2006)
Chlorine	(Bessac *et al.*, 2008)
Cinnamaldehyde	(Bandell *et al.*, 2004)
Citral (inhibition at higher concentrations)	(Stotz *et al.*, 2008)
Clotrimazole	(Meseguer *et al.*, 2008)
Crotonaldehyde cigarette smoke aqueous extract (CSE)	(Andrè *et al.*, 2008)
Delta-9-tetrahydrocannabinol (THC)	(Jordt *et al.*, 2004)
Formalin	(Macpherson, Xiao, *et al.*, 2007; McNamara *et al.*, 2007)
Garlic (allicin)	(Bautista *et al.*, 2005; Macpherson *et al.*, 2005)
Hydrogen peroxide (H2O2)	(Andersson *et al.*, 2008; Bessac *et al.*, 2008; Sawada *et al.*, 2008)
Hydrogen sulfide H2S NaHS (donor of H2S)	(Streng *et al.*, 2008)
Icilin	(Story *et al.*, 2003)
Iodoacetamide IA	(Macpherson, Xiao, *et al.*, 2007)
Isovelleral polygodial (sesquiterpene)	(Escalera *et al.*, 2008)
Lidocaine	(Leffler *et al.*, 2008)
Menthol (inhibition at higher concentrations)	(Macpherson *et al.*, 2006; Karashima *et al.*, 2007)
Morphantridine tear gases (CN, CR, CS, EBA, CABBC)	(Brône *et al.*, 2008)
MTSEA methane thiosuphonate	(Hinman *et al.*, 2006; Macpherson, Dubin, *et al.*, 2007)

Nifedipine	(Fajardo *et al.*, 2008)
N-methyl maleimide (NMM)	(Hinman *et al.*, 2006)
Parabens Methylp-hydroxybenzoate	(Fujita *et al.*, 2007)
Phytocannabinoids	(De Petrocellis *et al.*, 2008)
Reactive oxygen species reactive nitrogen species nitric oxide	(Sawada *et al.*, 2008)
Thymol 2-tert-butyl-5-methylphenol carvacrol 2,6-dimethylphenol 2,5-dimethylphenol	(Lee *et al.*, 2008)
Trinitrophenol Toxin GsMTx-4	(Hill and Schaefer, 2007)

***Table 2**: Overview of the published TRPA1 agonists and antagonists (adapted from* Zurborg *et al.*, 2009)

A fourth type of activation of mammalian TRPA1 channel by direct thermal stimulation has been hypothesized, but remains controversial. Since the early 2000s, conflicting results have emerged concerning the involvement of TRPA1 in the perception of noxious cold (Story *et al.*, 2003; Bautista *et al.*, 2006; Kwan *et al.*, 2006). Furthermore, non-mammalian TRPA1 channels from fruit flies were shown to detect innocuous warmth while frog, lizard, and snake TRPA1 are directly activated by noxious heat (Kang *et al.*, 2011; Laursen, Bagriantsev and Gracheva, 2014). Recent studies have demonstrated that deletion of TRPA1, TRPV1 and TRPM8 receptors in mice causes a lack of nociceptive responses at hot, normally noxious temperatures, suggesting the combination of the three channels is essential for noxious heat perception (Vandewauw *et al.*, 2018). Lastly, mechanosensitivity of TRPA1 has also been suggested. Amphipathic molecules such as the spider toxin GsMTX-4 and trinitrophenol are known to alter the shape of a cell membrane and therefore activate or inhibit mechanosensitive channels. As the human TRPA1 channel in heterologous systems shows current upon stimulation with these molecules, it has been suggested that the channel might be involved in direct mechanosensation (Hill and Schaefer, 2007).

In summary, TRPA1 functions as a ‘polymodal signal integrator’, able to detect a variety of stimuli dependent on an animal’s evolutionary adaptions to its unique habitat (Basbaum *et al.*, 2009).

Besides pharmacological evidence, behavioral testing has demonstrated that mice show nocifensive responses upon TRPA1 agonist administration. Application of AITC, the active substance in mustard oil (Jiang and Gebhart, 1998), cinnamaldehyde (Bandell *et al.*, 2004) and other substances causes the animal to show pain, discomfort and/or defensive behavior (Schmidt and Willis, 2007). This behavior is tested by scientists through injection of the algogens in the paw of the mice. The immediate behavior of these animals would be to lick, lift or avoid walking on the injected paw, responses that can be quantified and compared between different groups of wild-type and mutant mice. TRPA1 is also thought to be involved in the response following the formalin test. Formalin is a 37% diluted solution of formaldehyde. An injection of 1-2% formalin into an animals’ paw will cause a biphasic response where the first short phase (5-15 minutes) is thought to be caused by direct activation of chemoreceptors such as TRPA1. A second longer phase (up to 1 hour) is suggested to be an effect of central sensitization (Abbott, Franklin and Westbrook, 1995; McNamara *et al.*, 2007). Genetically deleting the *trpa1* gene in mice strongly reduces the behavioral response to AITC application as well as reduces inflammatory reactions such as swelling and hyperalgesia caused by it (Bautista *et al.*, 2006). The same study showed no difference in responses to noxious heat or cold. Also an attenuated nocifensive response to formalin was observed in mice where TRPA1 was pharmacologically or genetically disrupted (McNamara *et al.*, 2007). Interestingly, both the first and the second phase of the behavioral response were diminished. Knocking out TRPA1 in rat by using CRISPR technology completely abolished the response to AITC injection in the paw. Other assays testing acute (such as capsaicin and heat), inflammatory and neuropathic pain as well as some specific disease pain models were unaltered (Reese *et al.*, 2020).

1.1.4.2. TRPV1, TRANSIENT RECEPTOR POTENTIAL CATION CHANNEL SUBFAMILY V MEMBER 1

Another channel often studied in nociception is TRPV1. The first mammalian TRPV1 channel was identified when searching for the mechanism behind noxious heat perception and the spicy chili pepper substance capsaicin (Caterina *et al.*, 1997). The receptor is a polymodal signal integrator which is mainly expressed in nociceptors and is activated by stimuli including noxious heat (>43°C), inflammatory and vanilloid substances and acid (Julius, 2013). As with other TRP channels, it also has the tetrameric structure with 4x6 transmembrane segments where S5-6 forms the pore, passing mono- and divalent cations. Furthermore, the TRPV1 channel contains six ARDs in the N-terminal region which are known to be binding sites for ATP and Calmodulin involved in desensitizing the channel (Gaudet, 2008). Like TRPN, TRPM and TRPC subfamilies, TRPV channels have a TRP box region found to be important for tetramerization (García-Sanz *et al.*, 2004; Gaudet, 2006; Liao *et al.*, 2013) (*Figure 1*). The 'V' in the subfamily name is a reference to a "vanilloid pocket" in S2-4, responsible for the activation by capsaicin and other vanilloid substances. It is proposed that the vanillyl group binds with hydrophobic residues in the intracellular loop between S2 and S3 (Jordt and Julius, 2002; Yang *et al.*, 2015). The activation mechanism upon application of noxious heat and the exact location of the temperature sensing domain in TRPV1 is unknown. Different research groups have identified contrasting regions such as the pore region (Zhang *et al.*, 2018), a region between TM5 and the pore helix (Yang *et al.*, 2010), C-terminus (Brauchi *et al.*, 2006) or N-terminus (Yao, Liu and Qin, 2011) to be essential for the temperature sensing properties of TRPV1.

TRPV1 has been described as a detector for deviations from the physiological pH (~7.6). An increase in pH to a more basic environment or the presence of an alkaline substance has been shown to activate the channel through residue H378 in the intracellular N-terminus (Dhaka *et al.*, 2009). Protons are known to activate many different types of proteins in nociceptors including ASICs and vanilloid receptors (Jordt, Tominaga and Julius, 2000). A direct activation of TRPV1 takes place at a low pH (<6) (Leffler, Mönter and Koltzenburg, 2006). At a milder pH (6-7), protons are thought to increase the sensitivity of TRPV1 to capsaicin and decrease the temperature threshold (~43°C) to non-noxious temperatures (Tominaga *et al.*, 1998; Holzer, 2009).

Extracellular residues E600 and E648 in the link between S5 and the pore region are known to be involved in this direct and indirect activation (Jordt, Tominaga and Julius, 2000). A mild acidic condition is often seen in inflamed tissue where together with protons, other inflammatory substances (such as NGF and bradykinin) produced at the injury act on C-fiber nerve endings by sensitizing or activating receptors such as TRPV1 through activation of G-protein coupled receptors (Chuang *et al.*, 2001; McMahon, Bennett and Bevan, 2006). These GPCRs activate PLC which on its turn metabolizes membrane lipid PIP_2 and depletion of PIP_2 leads to sensitization of TRPV1 (Rohacs, Thyagarajan and Lukacs, 2008).

In addition, allyl isothiocyanate (AITC), a known agonist of the TRPA1 channel, has been shown to activate and sensitize the TRPV1 channel, however much less than TRPA1 (Everaerts *et al.*, 2011; Gees *et al.*, 2013; Alpizar *et al.*, 2014). Everaerts *et al.* showed a reduced behavioral response in mice with a genetic ablation of TRPV1. After observing that cysteine-less rTRPV1 in a heterologous expression system is still activated by AITC, Gees *et al.* proposes a direct activation mechanism with the vanilloid domain. A sensitization of the channel after an inflammatory process caused by AITC is suggested by Alpizar *et al*. In this study, an increase in heat sensitivity was observed after AITC administration during patch clamp recordings on HEK293T cells heterologously expressing mouse TRPV1 and calcium imaging on *Trpa1* knock out mice DRGs.

As with TRPA1, behavioral testing has demonstrated that animals show nocifensive behavior upon administration of TRPV1 activating substances. Subcutaneous administration of capsaicin evokes a relatively short lasting burning sensation (Caterina *et al.*, 1997). When initially tested in mice or rats, the injection was done in the plantar skin of the hind paw and animals would lift or lick the injected paw intensely for five to ten minutes. Following this nocifensive response, neurogenic inflammation around the injection site occurs, which is characterized by local edema, flare and hypersensitivity (Van Der Schueren *et al.*, 2007). The hyperalgesic area has a decreased thermal and mechanical threshold (Russell and Burchiel, 1984; O'Neill *et al.*, 2012). *Trpv1* deletion in mice causes several changes in nocifensive behavior. Firstly, the animals show a reduced paw licking and lifting behavior as well as a reduced inflammation and aversion to vanilloid compounds such as capsaicin. Also, responses to proton administration were reduced. In the same animals, thermal nociception seems to

be impaired but not eliminated and there is no thermal hyperalgesia after inflammation (Caterina and Julius, 2000; Caterina *et al.*, 2000; Davis *et al.*, 2000).

1.1.4.3. TRPM8 AND TRPM2

The TRPM subfamily is a large and heterogeneous group of channels, with some common structural features (*Figure 1*) (Fleig and Penner, 2004). Besides the usual TRP structures with six TMDs where S5, S6 and the P loop form the cation conducting channel pore, the TRPM subfamily members contain 4 N-terminal TRPM homology regions (MHRs). These domains are highly conserved in TRPM channels and are not found in other TRP channels and harbor binding sites for small molecules (Gaudet, 2006). At the C-terminal end a coiled-coil structure was identified to be important for tetramerization (Huang *et al.*, 2020) as well as a TRP box, involved in channel activation and inhibition (Diver, Cheng and Julius, 2019; Huang *et al.*, 2020). For some channels it is known that the C-terminus contains a sequence with enzymatic activity. TRPM2, TRPM6 and TRPM7 are examples of these type of channels often called ‘chanzymes’. In TRPM6 and TRPM7 this is a serine/threonine kinase domain which phosphorylates several proteins and subsequently regulates gene transcription, it is however not completely clear which genes are modulated (Runnels, 2011; Krapivinsky *et al.*, 2014) . In TRPM2 a NUDT9-H domain has been characterized, the function of this ADP ribose binding site will be discussed below (Huang *et al.*, 2020). Ion-selectivity of the TRPM pores are very different due to different lengths in the selectivity filters which determines the permeability for divalent cations (Huang *et al.*, 2020). Within the TRPM subfamily, TRPM2 and TRPM8 channels are highly linked to chemical nociception, as described below.

The TRPM8 channel is expressed in cold-sensitive C-fibers and some Aδ-fibers (Julius, 2013; Almaraz *et al.*, 2014). Activated by temperatures lower than 24°C, it is a crucial sensor for cool, non-noxious temperatures (15-24°C) and cold, noxious temperatures (5-15°C). TRPM8 knockout mice show impaired cold sensation until 5°C and cold hypersensitivity (Bautista *et al.*, 2007; Cohen and Moiseenkova-Bell, 2014; Milenkovic *et al.*, 2014). Furthermore, a few cooling agents chemically activate the TRPM8 channel and are perceived as painful when administered at very high

concentrations (McKemy, 2007). These include menthol and icillin which bind to a region in the transmembrane helices S2 and S3 (Almaraz *et al.*, 2014). Recently researchers found that TRPM8 is also involved in the detection of non-noxious warm temperatures (Paricio-Montesinos *et al.*, 2020). They suggested that the decreased spiking of cool-sensitive TRPM8 expressing C-fibers is necessary to perceive warmth. These fibers are absent in *trpm8*$^{-/-}$ mice making them unable to detect warm temperatures. Unlike other TRPM channels, the TRPM8 is a voltage-dependent channel. Gating of the channel following chemical or thermal stimulation is thought to be achieved through a shift in voltage dependence of the channel towards the resting membrane potential (Voets *et al.*, 2004, 2007). Several types of modulations of the channel have been described, including a calcium dependent desensitization after prolonged stimulation. Sustained calcium influx after TRPM8 activation in turn activates the PLC pathway to the breakdown of PIP2, a positive regulator of the channel, and therefore desensitizes the channel (Diver, Cheng and Julius, 2019). Additionally, acidic pH also increases channel activation threshold for icilin and temperature. Since inflammation is often associated with acidosis, the channel is likely to be less sensitive in an inflammatory environment (Andersson, Chase and Bevan, 2004).

Many tissues express the TRPM2 channel, but it is primarily expressed in the hypothalamus and in DRG C-fibers (Fleig and Penner, 2004). The channel functions as a cellular sensor for oxidative stress and has a role in inflammatory pain. H_2O_2 and Reactive Oxygen Species (ROS) molecules generated via inflammatory processes produce ADP ribose which interacts with the C-terminal enzymatic region NUDT9H to activate TRPM2 (Perraud *et al.*, 2001; Belrose and Jackson, 2018; Jang *et al.*, 2018). In contrast to TRPM8, the TRPM2 channel does not have a voltage-dependent gating mechanism. TRPM2 gating is calcium-dependent, where intracellular calcium binds Calmodulin which binds a region in the N-terminus of TRPM2 and makes gating possible. Many modulatory mechanisms have been described, such as protons which inhibit channel gating (Sumoza-Toledo and Penner, 2011; Belrose and Jackson, 2018). An important role of TRPM2 in nociception has been suggested after showing a decreased sensitivity to inflammatory pain in TRPM2 knockout mice (Haraguchi *et al.*, 2012). Mice lacking TRPM2 also show a blunted non-painful warm perception confirming that the channel is also known as a warming detector, important for body temperature

homeostasis regulated in the hypothalamus (Song *et al.*, 2016; Tan and McNaughton, 2018; Paricio-Montesinos *et al.*, 2020).

1.1.4.4. CLINICAL AND THERAPEUTIC RELEVANCE

TRP channels are important in many physiological processes and within the focus of this thesis, some are important for nociception following chemical stimulation. Dysregulation of TRP channel function, expression and localization has pathophysiological implications, making them clinically relevant (Smani *et al.*, 2015). In the case of TRPA1, TRPV1, TRPM2 and TRPM8 pathological implications may impair the somatosensory system in mammals; including humans (Julius, 2013). For example, a gain of function point mutation in TRPA1 has been described to cause Familial Episodic Pain Syndrome (FEPS), a disease characterized by upper body pain (Kremeyer *et al.*, 2010). Many mutational studies of TRPV1 have shown increased or decreased activity upon stimulation (Boukalova *et al.*, 2014; Duo *et al.*, 2018). In this way, acquired information about the channel gating could be valuable in the search of analgesics targeting these TRP channels. Furthermore, many of the endogenous agonists activating these channels are elevated in pathological conditions such as inflammation, making them interesting targets for analgesic development (Chen and Hackos, 2015).

One of the primary motivations of the current pain research is the need for specific and targeted analgesics. The currently available treatments cause many side effects and in the case of opioids, a highly addictive pain drug, its abuse has caused a true public health crisis in the United States (Skolnick, 2018). A study showed that roughly 4% of the nation's population misused prescription opioids in 2016 and found more than 33,000 Americans died as a consequence of opioid overdose in 2015 (Saha *et al.*, 2016). A pressing lack of alternatives has led scientist to study the therapeutic relevance of key proteins in nociception, including TRP channels. Only ten years after the first cloning and identification of the TRPV1 receptor, the first clinical trials with TRPV1 antagonists were started by several pharmaceutical companies for different treatment indications such as dental pain and migraine (Szallasi *et al.*, 2007). However, very few of them entered phase 3 due to side effects such as hyperthermia. At this moment, several thermally neutral TRPV1 antagonists are being investigated in different

stages of clinical trials including NEO6860 from NEOMED (Carnevale and Rohacs, 2016; Garami *et al.*, 2020). Also Mavatrep, a TRPV1 antagonist tested for its analgesic affects in patients with osteoarthritis has shown promising reduction in pain experience (Manitpisitkul *et al.*, 2016, 2018). Meanwhile the therapeutic use of capsaicin, the TRPV1 agonist, was proven efficient in many clinical trials. A brief excitation of TRPV1 seems to cause the neurons to become unresponsive for a period of time after topical application or injection either through desensitization or denervation (Chung and Campbell, 2016; Moran, 2018). Phase one clinical trials with developed TRPM8 antagonists so far have resulted in patients reporting to feel warm, confirming the recent study that found TRPM8 is required for warm perception but blocking the further use of them in phase 2 trials (Moran, 2018; Paricio-Montesinos *et al.*, 2020). Some TRPM8 agonists (i.e. menthol, icilin and eucalyptol) have been reported to clinically alleviate pain conditions (González-Muñiz *et al.*, 2019). Whether TRPM8 needs to be targeted by agonists or antagonists may depend on the type of pain occurring (Weyer and Lehto, 2017). More recently clinical trials with TRPA1 antagonists have started. Since TRPA1 is activated by a wide variety of stimuli, antagonizing the channel might have beneficial effects on many different painful conditions (Moran, 2018). Some candidates have shown promising results, but further research and clinical trials are necessary (Giorgi *et al.*, 2019). Regulation of TRPA1 is known to be dependent on oxygen after post-translational hydroxylation. A new strategy of blocking channel activity is therefore to target post-translational modification enzymes and then possibly bypassing TRP related side effects (Nagarajan, Rychkov and Peet, 2017).

1.1.5. ACID SENSING

Protons are able to activate nociceptors and cause nocifensive behavior in a variety of species including *C. elegans* (Sambongi *et al.*, 2000), fish (Sneddon, 2003), birds (Konnerth, Lux and Morad, 1987), rodents (Price *et al.*, 2001) and humans (Jones *et al.*, 2004) with few exceptions including the *Heterocephalus glaber* or naked mole-rat documented (Park *et al.*, 2008). In pathological conditions such as inflammation the proton concentration increases which could lead to tissue acidosis and subsequently to the activation of acid sensors. Four main groups of ion channels expressed in

nociceptors have been identified to be proton-sensitive: Acid Sensing Ion Channels (ASICs), TRP channels, Two-Pore-Domain Potassium channels (K2P) and Proton-Sensitive G Protein Coupled Receptors (PS-GPCRs).

ASICs are part of the bigger eNaC/DEG ion channel family. The six ASIC subunits are ASIC1a, ASIC1b, ASIC2a, ASIC2b, ASIC3 and ASIC4; which connect to each other to form a homo- or heterotrimer channels. Subunit composition determines the characteristic proton sensitivity of these channels (Wemmie, Taugher and Kreple, 2013). When activated by acid, cations (mostly Na^+) enter the cell and cause a depolarization which might lead to nociception. Using crystal structures, structure-function experiments and mutational studies, an acidic pocket was identified in ASICs in different animals such as chicken ASIC1a (Jasti *et al.*, 2007), zebrafish ASIC4 (Chen *et al.*, 2007) and mouse ASIC2a (Smith *et al.*, 2007). Several amino acids were found to be involved in proton sensitivity, for example the histidine residue H73 (mouse ASIC1a numbering) in the extracellular domain. A voltage clamp experiment with the deletion of H73 in mouse as well as in the very distant *Buccinum belcheri* (sea snail) ASIC1a showed a decrease in proton sensitivity compared to the wild-type channels (Lynagh *et al.*, 2018; Pattison *et al.*, 2019). Besides being activated by acid, ASICs are known to be regulated by peptides and other substances produced during inflammation, indicating these channels integrate inflammatory signals and have a crucial role in inflammatory pain. Studies in rats show that ASIC3 is regulated by slight acidification, hypertonicity and arachidonic acid, all signs of inflammation. The pain produced by acid injection in these rats could be blocked by an ASIC3 blocker, APETx2, which indicates this substance might have an analgesic effect on inflammatory pain (Deval *et al.*, 2008). However, targeting ASICs for pain treatments is more difficult, as the different channels also have roles in proprioception, mechanosensation and play a role in central neural plasticity (Pattison *et al.*, 2019). For example, genetic ablation of ASIC3, or DRASIC (Dorsal Root ASIC), in mice reduces the C-fiber sensitivity to acid- and noxious heat stimuli but increases the sensitivity to light touch, suggesting the channel has distinct roles in different cellular contexts (Price *et al.*, 2001).

In addition to ASICs, TRPV1 channels can also be either directly activated or potentiated by protons (Jordt, Tominaga and Julius, 2000; Leffler, Mönter and Koltzenburg, 2006; Tominaga *et al.*, 1998; Holzer, 2009). TRPV1 knock-out mice also have been shown to have an impaired proton sensitivity and less nocifensive behavior

upon acid administration (Caterina *et al.*, 2000; Davis *et al.*, 2000). Other TRP channels modulated or activated by an acidic extracellular pH are TRPV4, TRPM7, TRPP2, TRPP3, TRPC4, TRPC5 and TRPA1. While most of these channels are proton-sensitive in rodents, only the human TRPA1 has been found proton-sensitive. When compared to the amino acid sequence of the acid insensitive Rhesus monkey, researchers identified the beginning of the 6th TMD important for activation and sensitization by protons (De La Roche *et al.*, 2013). So far, we have considered nociception to be mediated by an increase of extracellular proton concentration, however intracellular acidity can also increase after weak acids (such as acetic acid and formic acid) penetrate the membrane and only dissociate after entering the cell causing nociception. For example, nociception after activation of TRPA1 was observed by intracellular acidification caused by weak acids in TG neurons from mice and in heterologously expressed rat TRPA1 (Wang *et al.*, 2011).

Two categories of proton sensitive channels have been less studied in relation to nociception: K2Ps and PS-GPCRs. Although widely expressed in many species from the Animalia kingdom, 15 different mammalian K2P channels are known, which can be further divided into 6 subfamilies: TREK, TRESK, TALK, TWIK, TASK and THIK. They are responsible for the background potassium efflux establishing the resting membrane potential of cells. Specifically in nociceptors they therefore contribute to the neuronal excitability (explained in more detail in Introduction section 1.1.6) (Pattison *et al.*, 2019). As extracellular acidity inhibits the channels, K+ cannot exit the cell effectively and depolarization with potential subsequent nociception happens. Similarly to ASICs, the channels integrate many inflammatory signals such as arachidonic acid and hypotonicity, proven in for example rat TRESK (Callejo, Giblin and Gasull, 2013). For the last category of channels, PS-GPCRs, the connection between acid sensing and nociception is less clear. Nevertheless, knock-outs of some of the proteins in pain model mice have shown significant effects on nocifensive behavior. Five conserved mammalian channels are identified: GPR68, GPR4, GPR65, GPR132 and GPR151. In a neuropathic pain model, GPR132−/− mice had less mechanical hypersensitivity (Hohmann *et al.*, 2017). The expression of GPR68, GPR4 and GPR65 is upregulated in an inflammatory mouse model (Chen *et al.*, 2009) and GPR4 activation by protons on its turn causes upregulation of pro-inflammatory genes and an increase in recruitment of immune cells

(Dong *et al.*, 2013). Very little is known about the exact link between PS-QPCRs and nociception (Pattison *et al.*, 2019).

The contribution from these 4 different channel types to the pain we feel after nociception caused by protons in different circumstances is being investigated and might be diverse and complex as is illustrated with the following example. A CFA injection in mice joints, leads to an arthritis model for acute and chronic pain related to this disease. While it has always been suggested that the synovial fluid is more acidic in these models, this was questioned in a recent paper measuring the tissue pH of the animals (Wright *et al.*, 2018). One study showed that knocking out GPR65, ASIC3 or TRPV1 proved only GPR65 was involved in acute pain of the rheumatoid arthritis model (Hsieh *et al.*, 2017), another study found evidence for the contribution of TRPV1 as they found that a systemic administration of a TRPV1 antagonist reduced acute pain in the same model (Chakrabarti *et al.*, 2018).

1.1.6. ION CHANNELS SET DRG NEURONAL EXCITABILITY

The resting membrane potential (RMP) of a cell is described as ”the electrical potential difference across the plasma membrane when that cell is in a non-excited state” (Chrysafides and Sharma, 2019). The RMP is established through two main parameters: 1) a large gradient for K^+ and Na^+ across the membrane (Ca^{2+} in excitable heart cells) which is a product of an active Na^+/K^+ pump constantly using ATP to pump K^+ inside the cell in exchange for transport of Na^+ to the outside and 2) the relative permeability of the membrane to these ions. This relative permeability is determined by ion channels open in the non-excited state. Many different channels are important for the resting K^+ conductance, leading to a high permeability for K^+. Na^+ and Ca^{2+} conductance is smaller and contribution of ion channels are less clear, but the majority of Na^+ ions have been suggested to “leak” through NALCN (Sodium Leak Channel Non-selective) (Ren, 2011). An ion flow between the intra-and extracellular compartments is induced by a chemical force (high $[K^+]$ in the cell, high $[Na^{2+}]$ outside of the cell) and an electrical force (inside of the cell more negative). Whenever they balance each other out, equilibrium is reached and a net flux is zero. At this point a resting membrane potential is established (Wright, 2004).

The transition from a resting to an excited state of a neuron is the result of a transient change in membrane potential generated upon activation of voltage gated ion channels (Purves *et al.*, 2001) and propagated along the cell axon, called an action potential (AP). When positive ions flow into the cell and depolarize the membrane to a certain threshold, voltage-gated sodium channels (NaVs) are activated and cause a rapid increase in membrane potential due to a sodium influx. This depolarization propagates along the axon by positively charged ions flowing to the more negative side and activating further voltage-gated sodium channels. Repolarization of the membrane occurs when NaVs are inactivated and voltage-gated potassium channels (KVs) open at +30mV so K^+ can flow out of the cell. Briefly, this will cause a hyperpolarization where the membrane potential is lower than the RMP, but after the KVs close the cell goes to the resting state again (Purves *et al.*, 2001; Basbaum *et al.*, 2009).

The importance of voltage-gated sodium and potassium channels in the perception of touch and pain has been shown by the numerous cases of channelopathies impairing these channels and their functions. Loss-of-function mutations in *SCN9A, SCN10A* or *SCNA11*, the genes encoding for NaV1.7, NaV1.8 and NaV1.9 respectively, cause congenital insensitivity to pain (CIP) while gain-of-function mutations cause diseases where patients feel an excess of pain such as primary erythromelalgia or small fiber neuropathy (Cregg *et al.*, 2010; Bennett and Woods, 2014; Waxman and Dib-Hajj, 2019). Mutations in KCNQ4, a type of voltage-gated potassium channel, have been linked to deafness by impairing the mechanosensitivity in cochlear hair cells and an increased touch sensitivity (Kubisch *et al.*, 1999; Heidenreich *et al.*, 2012).

As mentioned above, NALCN and other “leak” channels contribute to setting the RMP and therefore the excitability of the neuron. NALCN is a channel belonging to the voltage-gated calcium channels (CaVs) and NaVs superfamily which possess 24 transmembrane domains (TMDs). The pore forming subunit has 4 homologues domains with each six TMDs. It is distinct from CaVs and NaVs with an EEKE motif in the pore region, making it selective for monovalent cations with Na^+ being the most permeable (Lu *et al.*, 2007; Ren, 2011; Chua *et al.*, 2020). The channel was found to be voltage independent when expressed alone in a heterologous system (Lu *et al.*, 2007), but functional gating has been recently characterized and is suggested to depend on co-expression with UNC79, UNC80 and FAM155A. When co-expressed in a heterologous

system, currents were found to be voltage-sensitive despite carrying fewer voltage-sensitive residues and full closure was not observed suggested it is constitutively active (Chua *et al.*, 2020). Co-immunoprecipitation of these three proteins with NALCN identified an NALCN-UNC79-UNC80-FAM155A complex with the first one being the pore forming channel and the other three being transmembrane proteins important for trafficking as well as gating (Chua *et al.*, 2020) (*Figure 3*). Recently a protein-protein interaction between NALCN and FAM155A was discovered using size-exclusion chromatography and cryo-electromicroscopy, they suggest FAM155A is anchored with the pore via the extracellular residues the voltage sensing segment of domain IV (Kschonsak *et al.*, 2020). Gating could be pharmacologically blocked by Gd^{3+} and L-type calcium channel blocker Verapamil (Lu *et al.*, 2007; Chua *et al.*, 2020). Mutations in the channel have been linked to a few human neuronal diseases such as infantile neuroaxonal dystrophy (Köroğlu, Seven and Tolun, 2013), epilepsy (Al-Sayed *et al.*, 2013), cognitive delay and several psychiatric disorders (Cochet-Bissuel, Lory and Monteil, 2014). Also *UNC80* mutations have led to the human disease infantile hypotonia with psychomotor retardation and characteristic facies (IHPRF), a neurological disorder where patients show psychomotor regression at a very young age and often have characteristic facial dysmorphisms (Bramswig *et al.*, 2018). Knocking out *UNC79* in mice is lethal (Lu *et al.*, 2010).

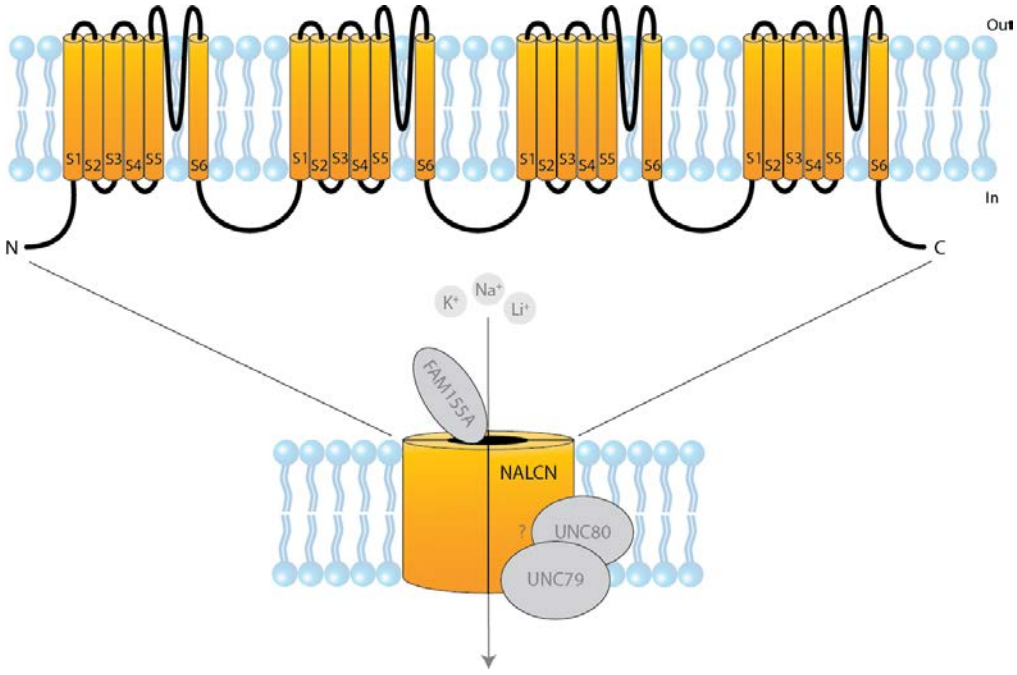

Figure 3: *Molecular structure of NALCN. FAM155 is indicated to interact with the pore. UNC79 and UNC80 are indicated on the image; however, their exact location remains unknown.*

1.2. THE AFRICAN MOLE-RAT FAMILY (*BATHYERGIDAE*) AND THE NAKED MOLE-RAT (*HETEROCEPHALIDAE*)

The species of the African mole-rat family (*Bathyergidae*) and the naked mole-rat (*Heterocephalus Glaber* from the family *Heterocephalidae*) are subterranean animals living over a wide area in sub-Saharan Africa. Phylogenetically, the families are part of the guinea pig-like sub-order (*Hystricomorpha*) within the order of Rodentia and diverged about 28-40 million years ago (Mya) from each other (*Figure 4*) (Kumar *et al.*, 2017). The 5 genera of *Bathyergidae* (*Cryptomys, Fukomys, Georychus, Heliophobius and Bathyergus*) encompass more than 30 different species. The areas in which they make their extensive underground burrow systems are geographically disparate and differ in soil type (ranging from compact clay to different types of sand), altitude, vegetation and climate, which has pushed divergence through adaptation to distinctive environmental stress factors. However the commonality between the habitats is the presence of geophytes, on which the animals mainly feed. (Bennett and Faulkes, 2000; Faulkes *et al.*, 2004; Eigenbrod *et al.*, 2019). Although the diet is thought to be mainly vegetarian, cases where African mole-rats eat worms, scarab larvae or termites have been described (Burda and Kawalika, 1993).

Evolutionary pressure in the African Mole-rat species has directed divergent social organizations. The *Georychus*, *Heliophobius* and *Bathyergus* genera are solitary species, while *Cryptomys* and *Fukomys* species are social animals with cooperative behaviors in small or big-sized colonies. One exception is the Damaraland mole-rat (*Fukomys damarensis*) which, together with the naked mole-rat, is eusocial, a hierarchic social organization where (reproductive) labor is divided amongst the colonies, with only a single breeding female (Bennett and Faulkes, 2000). As solitary species live in areas with more predictable rainfall than social species, the divergence of these social structures has been linked to the climatic differences and the distribution of geophyte food sources in their habitats, considering cooperative foraging is necessary for survival when food is more sparse (Burda and Kawalika, 1993; Faulkes and Bennett, 2013).

Many ecological constraints led to additional morphological and physiological specializations (Bennett and Faulkes, 2000). One of them is the hypoxia tolerance in naked mole-rats. Due to the large colony size living in a narrow underground tunnel system, the species adapted to living in an oxygen-deprived habitat by using fructose-

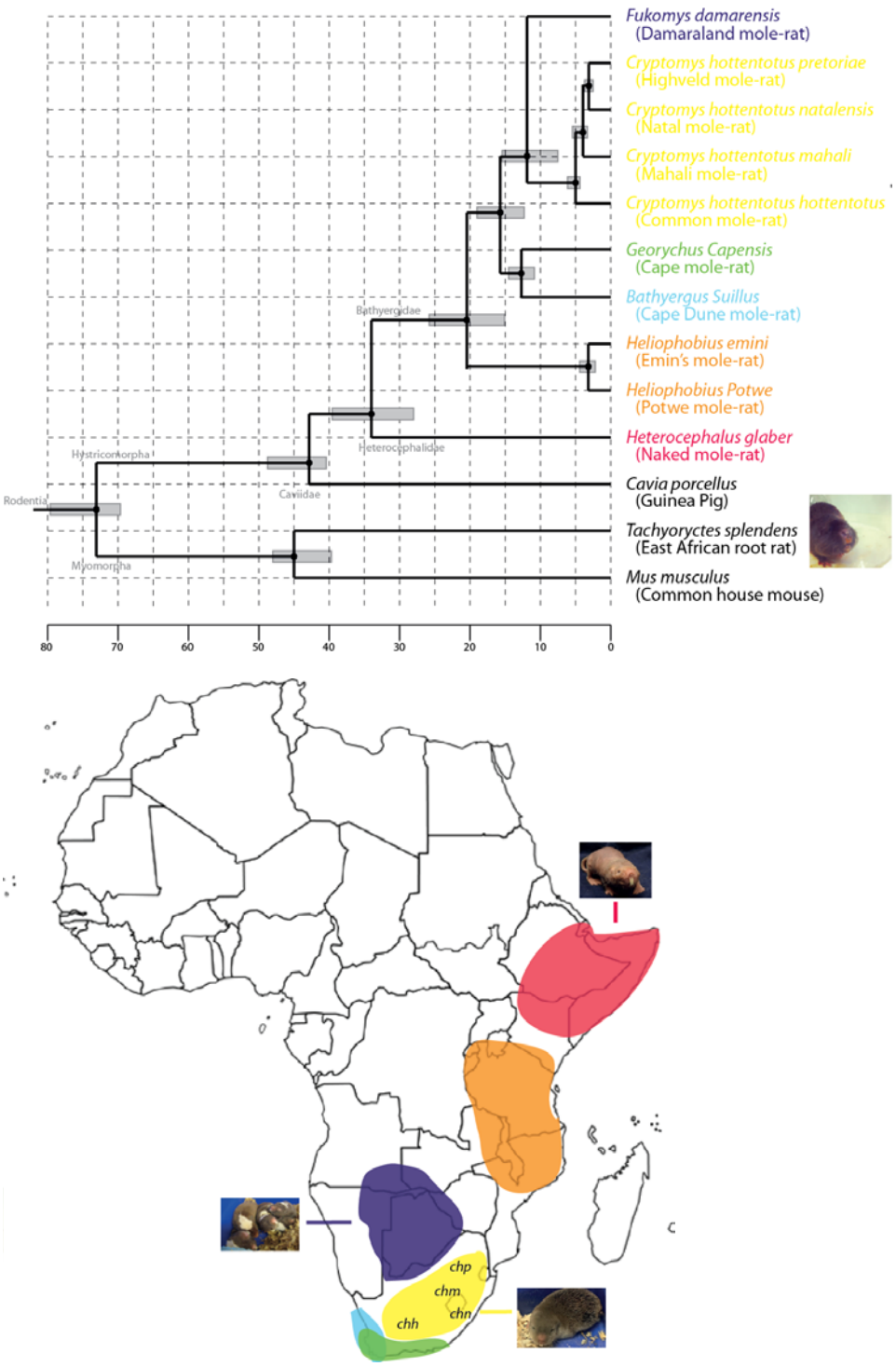

Figure 4: *A phylogenetic tree of rodents, including African mole-rats. Divergence times are indicated at the bottom (top). Below, a map of the African continent is shown with indications of the approximate habitats of each of the Bathyergidae and Heterocephalidae species ((chn: cryptomys hottentotus natalensis; chp:cryptomys hottentotus pretoriae; chh:cryptomys hottentotus hottentotus; chm:cryptomys hottentotus mahali)*

driven glycolysis (Park *et al.*, 2017). Furthermore, the naked mole-rat lost its thermoregulating abilities which are superfluous in a thermostable environment (Buffenstein and Yahav, 1991). Moreover, they can live up to 30 years and are therefore long-lived animals for their relatively small size (Kim *et al.*, 2011; Fang *et al.*, 2014). In the light of this thesis it is important to mention naked mole-rats show no behavioral responses upon stimulation with capsaicin and acid, something that will be discussed in more detail later.

1.3. GENERAL MECHANISM OF THE ABSENCE OF PAIN

Patients with congenital insensitivity to pain[1] do not perceive pain due to a genetic disease. Several different mutations have been characterized, such as in *SCN9A*, the gene coding for NaV1.7 (Cox *et al.*, 2006), *PRDM12*, coding for a transcriptional regulator influencing perception and sensation of pain (Zhang *et al.*, 2016) or in *NTRK1*, encoding TrkA, a receptor for NGF that sensitizes nociceptors (Indo, 2001). The loss of the ability to feel pain causes them to continuously harm themselves which has a detrimental impact on the individual's quality of life and even shortens life expectancy (Bennett and Woods, 2014). Although this illustrates the importance of pain, cases where insensitivity to a certain stimulus is beneficial for the survival of the species have been described. Smith, Park and Lewin, 2020, for example, recently reviewed the specific insensitivities to noxious stimuli from different African mole-rats.

1.3.1. ADAPTATION TO CHEMICAL NOCICEPTION

The ability for plants or insects to produce algogens that can cause chemical nociception is an advantageous evolutionary trait. One exception however is the insensitivity of the avian TRPV1 to capsaicin (Tewksbury and Nabhan, 2001; Jordt and Julius, 2002). Avian TRPV1 is insensitive to capsaicin stimulation although it is sensitive

[1] The term 'Congenital Insensitivity to Pain' is a generally accepted name despite the controversy about the pain terminology. Scientists have suggested that it is rather an insensitivity to a stimulus that causes the lack of a pain experience (Weisman, Quintner and Masharawi, 2019).

to heat and acid. In this way chili plants, normally discouraging predators, do not deter birds from consuming their fruits and therefore enabling them to disperse seeds effectively. By this 'directed deterrence', birds are able to eat the fruits and therefore widening their niche of food sources, causing an evolutionary advantage for both the bird and plant (Borges, 2001, 2009).

As mentioned earlier, the naked mole-rats are found to show no pain behavior upon stimulation with capsaicin or acid, although their pain responses after noxious mechanical, heat and other chemical stimuli are present (Park *et al.*, 2008; Eigenbrod *et al.*, 2019). An amino acid variant in the *SCNA9*, the gene encoding NaV1.7, is believed to be the cause of the molecular mechanism underlying the acid insensitivity. As a result of the negatively charged motif (EKE) in the normally positively charged (KKV) pore loop in domain IV, the channel becomes more sensitive to acid inhibition. Therefore, a depolarizing input from acid-sensitive channels cannot initiate an action potential. This adaptation is believed to protect the naked mole-rats against pain from tissue acidosis as they are exposed to a high CO_2 level in their underground and narrow burrows (Smith *et al.*, 2011; Smith, Park and Lewin, 2020).

The naked mole-rats' insensitivity to capsaicin is not completely understood. The TRPV1 channel is fully functional and C-fibers and isolated DRGs could to be excited after capsaicin application *ex vivo*. Interestingly, TRPV1-responsive neurons connect to deeper lamina of the dorsal horn instead of only the outer layers. This unusual connectivity has led to the hypothesis that the signal after capsaicin stimulation is not sufficient to activate pain circuits in the CNS (Park *et al.*, 2008). An evolutionary motivation for this adaptation has not yet been identified.

1.3.2. SPECIES-SPECIFIC INSENSITIVITIES IN THE AFRICAN RODENTS

Preliminary work, discussed in more detail in Results 3.1 (page 50) and published in Eigenbrod *et al.*, 2019 revealed several interesting chemical insensitivities in different African rodents. Injections of capsaicin, acid or AITC were given to 9 subterranean African rodents and C57Bl/6N mice. Four new species were found to completely lack a behavioral response to one or more of these algogens. The Natal mole-rat (*Cryptomys*

hottentotus natalensis) showed, just like naked mole-rats, no behavioral response to capsaicin. The Highveld mole-rat (*Cryptomys hottentotus pretoriae*), also a member of the *Cryptomys* genera, was identified as the sole species insensitive to AITC. Additionally, two new species were behaviorally insensitive to acid, the Cape mole-rat (*Georycus capensis*) and East African root rat (*Tachyorectes splendens*) (*Figure 5*) (Eigenbrod *et al.*, 2019).

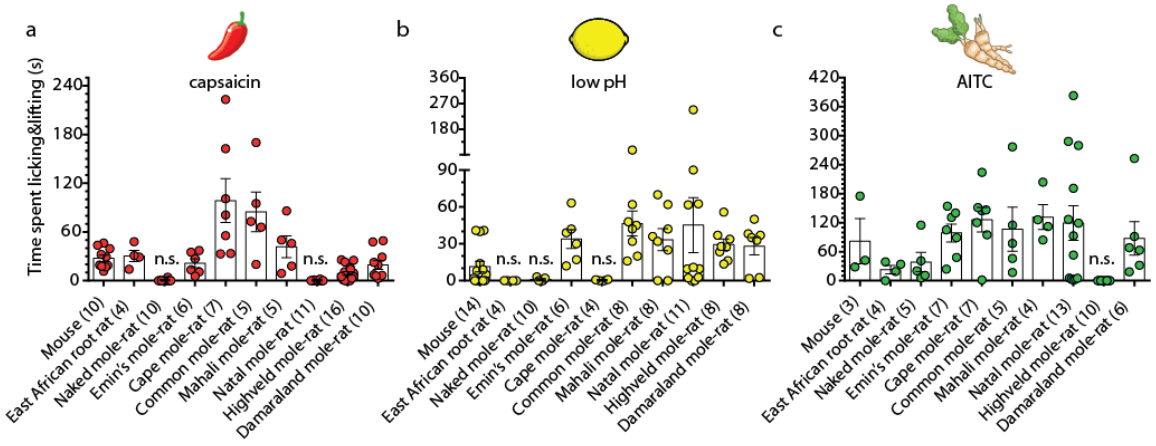

Figure 5: *Data figure from Eigenbrod et al., 2019 showing the cumulative responses after injection with capsaicin, acid or AITC. Animals whose response to the algogen was not different than the response to a vehicle injection is indicated with 'n.s.' (p>0.05) and is classified as insensitive to this algogen.*

1.4. OBJECTIVES OF THE STUDY

The aim of this thesis was to use the African mole-rat family as a model to investigate mechanisms of chemical nociception. This was done by elucidating the molecular mechanisms causing the absence of a behavioral response to a chemical irritant in one or more mole-rat species and by identifying the environmental triggers causing this divergence of phenotypes to occur. Firstly, to investigate the AITC insensitivity of the Highveld mole-rat,

- the function and sensitivity of the AITC sensor, TRPA1 was assessed as we hypothesized a lower sensitivity because of critical cysteine substitutions;
- the contribution of NALCN, a gene upregulated in Highveld mole-rats, was examined by looking at function and expression of the protein as well as in vivo experiments to block the channel;
- the species' response to more TRPA1 agonists was evaluated; and
- the natural habitat with natural food sources and predators was explored.

Secondly, the capsaicin sensitivity of the naked mole-rat and Natal mole-rat was investigated by

- testing TRPV1 function and sensitivity from different mole-rats; and
- comparing the TrkA amino acid sequences from the different mole-rats

The nociceptive mechanisms including, channel and receptor function and expression as well as peripheral signaling investigated in this thesis will provide valuable information for the discovery and development of next generation pain treatment.

2. MATERIALS AND METHODS

2.1. MATERIALS

2.1.1. CHEMICALS

Name	Supplier
Agar	Sigma-Aldrich Chemie GmbH, Munich, Germany
Agarose	Sigma-Aldrich Chemie GmbH, Munich, Germany
Allyl isothiocyanate	Santa Cruz Biotechnology, Heidelberg, Germany
Bovine serum albumin (BSA)	Sigma-Aldrich Chemie GmbH, Munich, Germany
CaCl2	Sigma-Aldrich Chemie GmbH, Munich, Germany
CAL520® AM	AAT Bioquest, Biomol GmbH, Hamburg, Germany
Capsaicin	Santa Cruz Biotechnology, Heidelberg, Germany
Carbenicillin	Carl Roth GmbH & Co. KG, Karlsruhe, Germany
Chloroform	Sigma-Aldrich Chemie GmbH, Munich, Germany
DEPC-treated water	Thermo Fisher Scientific GmbH, Dreieich, Germany
Diethylether	Carl Roth GmbH & Co. KG, Karlsruhe, Germany
DMSO	Sigma-Aldrich Chemie GmbH, Munich, Germany
Ethanol	Carl Roth GmbH & Co. KG, Karlsruhe, Germany
Ethidium Bromide	Carl Roth GmbH & Co. KG, Karlsruhe, Germany
Fetal calf serum (FCS)	PAN biotech, Aidenbach, Germany
Formalin	Merck Millipore, Darmstadt, Germany
Formic acid	Merck Millipore, Darmstadt, Germany
FuGENE	Promega GmbH, Mannheim, Germany
Glucose	Sigma-Aldrich Chemie GmbH, Munich, Germany
HCl	Carl Roth GmbH & Co. KG, Karlsruhe, Germany
HEPES	Carl Roth GmbH & Co. KG, Karlsruhe, Germany
HF or GC buffer	Thermo Fisher Scientific GmbH, Dreieich, Germany
Ionomyin, calcium salt	Thermo Fisher Scientific GmbH, Dreieich, Germany
Isoflurane	Sigma-Aldrich Chemie GmbH, Munich, Germany
Isopropanol	Sigma-Aldrich Chemie GmbH, Munich, Germany
KCl	Carl Roth GmbH & Co. KG, Karlsruhe, Germany

MgCl2	Sigma-Aldrich Chemie GmbH, Munich, Germany
NaCl	Sigma-Aldrich Chemie GmbH, Munich, Germany
NaOH	Sigma-Aldrich Chemie GmbH, Munich, Germany
NEB buffer 2	New England Biolabs GmbH, Frankfurt, Germany
O.C.T.TM Tissue Tek	Sakura Finetek, Zoeterwoude, Netherlands
PBS	Thermo Fisher Scientific GmbH, Dreieich, Germany
Penicillin/Streptomycin	Thermo Fisher Scientific GmbH, Dreieich, Germany
Paraformaldehyde	Sigma-Aldrich Chemie GmbH, Munich, Germany
ProLong Gold antifade reagent	Thermo Fisher Scientific GmbH, Dreieich, Germany
Poly L-lysine (PLL) 0.01%	Sigma-Aldrich Chemie GmbH, Munich, Germany
Pluronic acid	Thermo Fisher Scientific GmbH, Dreieich, Germany
Sodium acetate	Sigma-Aldrich Chemie GmbH, Munich, Germany
Sodium azide	Sigma-Aldrich Chemie GmbH, Munich, Germany
Sucrose	Sigma-Aldrich Chemie GmbH, Munich, Germany
TRIzol	Thermo Fisher Scientific GmbH, Dreieich, Germany
Trypsin	Thermo Fisher Scientific GmbH, Dreieich, Germany
Verapamil HCl	Sigma-Aldrich Chemie GmbH, Munich, Germany

2.1.2. LABWARE MATERIALS

Name	Supplier
Cornig 384 well microplates (CLS3683BC)	Sigma-Aldrich Chemie GmbH, Munich, Germany
6-/12-/24-/84-well plates	Sarstedt AG & Co. KG, Nümbrecht, Germany
Cell culture bottles	Sarstedt AG & Co. KG, Nümbrecht, Germany
Coverslips (round, 15mm)	Carl Roth GmbH & Co. KG, Karlsruhe, Germany
SuperFrost Plus cryosection slides	Thermo Fisher Scientific GmbH, Dreieich, Germany
Mounting slides (24x60mm)	Carl Roth GmbH & Co. KG, Karlsruhe, Germany
MicroAmp™ Optical 384-Well Reaction Plate with Barcode for qPCR	Thermo Fisher Scientific GmbH, Dreieich, Germany

2.1.3. BUFFERS, SOLUTIONS, MEDIA

Name	Composition
DMEM+glutaMAX™	- Dublecco's modified eagle medium - high glucose - GlutaMAX Suppl - pyruvate
LB medium	10g tryptone, 5g yeast extract, 10g NaCl in 1 L H_2O
LB Agar	LB-medium + 1.5% (w/v) agar
Paraformaldehyde solution (PFA 4%)	4% paraformaldehyde in 0.1 M PBS, adjusted to pH 7.2 – 7.4 with NaOH and HCl
SB buffer	50x stock: 20 g NaOH, pH to 8.0 with ±120 g H_3BO_3 to 1 L with dH_2O 1x working buffer: 20 ml of 50x stock 980 ml dH2O

2.1.4. KITS

Name	Supplier
FastStart universal Probe Master (Rox)	Roche, Mannheim, Germany
Fluo-4 Direct™ Calcium Assay Kit	Thermo Fisher Scientific GmbH, Dreieich, Germany
PureyieldTM plasmid Miniprep/Midiprep or Maxiprep system	Promega GmbH, Mannheim, Germany
Q5® site-directed mutagenesis kit	New England Biolabs GmbH, Frankfurt, Germany
RNAscope® multiplex fluorescent reagent kit v2	ACDbio, Bio-Techne GmbH, Wiesbaden-Nordenstadt, Germany
SuperScript®III First-Strand Synthesis kit	Thermo Fisher Scientific GmbH, Dreieich, Germany
Wizard® SV Gel and PCR clean-up system	Promega GmbH, Mannheim, Germany

2.1.5. MICROSCOPES AND EQUIPMENT

Name	Specifications	Supplier
Calcium imaging		
Fixed stage microscope	BX51WI	Olympus Europa GmbH, Hamburg, Germany
CCD camera	CoolSNAP HQ2	Visitron Systems GmbH, Puccheim, Germany
Illumination System	Lambda DG-4, Ultra-high-speed wavelength switching	Sutter Instruments by Science Products, Hofheim, Germany
Objective	UMPLFLN 10x/0.3W	Olympus Europa GmbH, Hamburg, Germany
Perfusion system	ValveLink 8.2	AutoMate Scientific by Science Products, Hofheim, Germany
Sucking Pump	Eheim Air200	Eheim GmbH 6 Co. KG., Deizisau, German
RNAscope imaging		
Confocal laser scanning Microscope	Inverted Axio Observer Z1 LSM 700	Carl Zeiss AG, Oberkochen, Germany
Stage controller	XY Step SMC 2009	Carl Zeiss AG, Oberkochen, Germany
Objective	40x/1.3Oil	Carl Zeiss AG, Oberkochen, Germany
Illumination System	HXP 120C and HAL 100 halogen illuminator	Carl Zeiss AG, Oberkochen, Germany

2.1.6. TECHNICAL EQUIPMENT

Name	Supplier
Cryostat: Cryostar nx70	Thermo Fisher Scientific GmbH, Dreieich, Germany
FLIPR Tetra system	Molecular Devices, Biberach an der Riss, Germany
GelDoc XR+ imager	Bio-Rad Laboratories GmbH, Münich, Germany
Hybez II oven	ACDbio, Bio-Techne GmbH, Wiesbaden-Nordenstadt, Germany
C1000 Touch^{TM} Thermal cycler	Bio-Rad Laboratories GmbH, Münich, Germany
TECAN plate reader Infinite 200 PRO	Tecan Group AG, Männedorf, Switzerland

2.1.7. SOFTWARE

Name	Developer
FIJI (Fiji is just ImageJ)	ImageJ, (Schindelin *et al.*, 2012)
GraphPad Prism 6	GraphPad Software Inc., La Jolla, CA, USA
Metafluor	Molecular Devices, Biberach an der Riss, Germany
Snapgene	GSL Biotech LLC, Chicago, IL, USA
Zen	Carl Zeiss AG, Oberkochen, Germany

2.1.8. ENZYMES

Name	Supplier
Hot start Phusion polymerase	Thermo Fisher Scientific GmbH, Dreieich, Germany
Restriction enzyme(s)	New England Biolabs GmbH, Frankfurt, Germany
T4 DNA ligase	Thermo Fisher Scientific GmbH, Dreieich, Germany
T4 DNA polymerase	Thermo Fisher Scientific GmbH, Dreieich, Germany

2.1.9. FLUOROPHORES

Name	Supplier
Opal 520	Perkin Elmer, Berlin, Germany
Opal 570	Perkin Elmer, Berlin, Germany
Opal 650	Perkin Elmer, Berlin, Germany

2.1.10. DNA

Name	Supplier
Designed primers	BioteZ, Berlin, Germany or Eurofins, Berlin, Germany
dNTPs	Thermo Fisher Scientific GmbH, Dreieich, Germany
Hydrolysis probe 83 for qPCR	Roche, Mannheim, Germany
Oligo(dT)20	Thermo Fisher Scientific GmbH, Dreieich, Germany
Random primers	Thermo Fisher Scientific GmbH, Dreieich, Germany
SmartLadder MW-1700-10	Eurogentec, Köln, Germany

2.1.11. CELL CULTURE MEDIA

Name	Supplier
HEK293(AD) cell growth media	DMEM (Dublecco's modified eagle medium) + GlutaMAX™, 100 units/mL penicillin, 100 µg/mL streptomycin, 10% fetal bovine serum

2.1.12. BACTERIAL STRAINS

Name	Supplier
NEB5alfa competent E. coli.	New England Biolabs GmbH, Frankfurt, Germany Genotype: *fhuA2 Δ(argF-lacZ)U169 phoA glnV44 Φ80Δ (lacZ)M15 gyrA96 recA1 relA1 endA1 thi-1 hsdR17*

2.1.13. PRIMERS

Name	Sequence (5'-3')
SLIC cloning	
mmTRPA1_F	CTGCACCTCGGTTCTGCCACCATGAAGCGCGGCTTGAGGAGGATTCTG
mmTRPA1_R	CAGAAGCTTAATTCACTAAAAGTCCGGGTGGCTAATAGAACAATGTG
nmrTRPA1_F	CTGCACCTCGGTTCTGCCACCATGAAGCGCAGCCTGAGGAAGATGCTG
nmrTRPA1_R	CAGAAGCTTAATTCACTAGTCCTTAGGACAGTGTGGTTTTGCTTTAAATGC
CryTRPA1_F	CTGCACCTCGGTTCTGCCACCATGAAGCGCAGCCTGGGGAAGATGC
CryTRPA1_R	CAGAAGCTTAATTCACTAGTGCTTAGGAGAGTGCGGTTTTGCCTTAAC
mNALCN_F	GCACCTCGGTTCTATGCCACCATGCTCAAAAGAAAGCAGAGTTCC
mNALCN_R	GAAGCTTAATTCAATCGAATATCCAGGAGGTCATCTCCACTCTCGTC
pNALCN_F	CTGCACCTCGGTTCTATGCCACCATGCTCAAAAGGAAGCAGAGTTCC
pNALCN_R	GAAGCTTAATTCAATCGAATATCTAAAAGGTCATCTCCACTCTCGTC
SLICNALCNqpcrF	CTGCACCTCGGTTCTATTTCCAACAAATGTGGGGGTC
SLICNALCNqpcrR	CAGAAGCTTAATTCAATTGCATCTTCGTGAAACATCTG
SLIC mutagenesis	
mm581QC_F	TCCTCCTGAACAAGAAGTGTGCTTCCTTTCTGCATATTGCCCTGC
mm581QC_R	GCAGGGCAATATGCAGAAAGGAAGCACACTTCTTGTTCAGGAGGA
mm622CF_F	CTCCAAGCAATCGATTTCCAATCATGGAGATGGTAGAATACCTCCC
mm622CF_R	GGGAGGTATTCTACCATCTCCATGATTGGAAATCGATTGCTTGGAG
mm976SC_F	GCTGAGGTCCAGAAGCATGCGTGTTTGAAGAGGATTGCTATGCAG
mm976SC_R	CTGCATAGCAATCCTCTTCAAACACGCATGCTTCTGGACCTCAGC
qPCR	
qPCR_NALCN_F	TTCCAACAAATGTGGGGGTCA
qPCR_NALCN_R	TGCATCTTCGTGAAACATCTG

2.1.14. ANIMALS

Animal species included in the scope of this work are listed below.

Family	Species	Common name
Bathyergidae	*Fukomys damarensis*	Damaraland mole-rat
	Cryptomys hottentotus pretoriae	Highveld mole-rat
	Cryptomys hottentotus natalensis	Natal mole-rat
	Cryptomys hottentotus mahali	Mahali mole-rat
	Cryptomys hottentotus hottentotus	Common mole-rat
	Georychus capensis	Cape mole-rat
	Bathyergus suillus	Cape Dune mole-rat
	Heliophobius emini	Emin's mole-rat
	Heliophobius potwe	Potwe mole-rat
Heterocephalidae	*Heterocephalus glaber*	Naked mole-rat
Spalacidae	*Tachyoryctes splendens*	East African root rat
Muridae	*Mus musculus*	House mouse

Mitochondrial DNA analysis by Dr. C. G. Faulkes from the University of London, confirmed one *Heliophobius* species to be 99.58% similar to the East Usamabara sample 3660 (*Heliophobius* clade 2b) described in his phylogeographical work (Faulkes *et al.*, 2011). We named the species *Heliophobius Potwe* or Potwe mole-rat, referring to the location it was found.

All animal protocols were approved by the University of Illinois at Chicago Institutional Animal Care and Use Committee, the German federal authorities (State of Berlin), or the Animal Use and Care Committee of the University of Pretoria, Republic of South Africa. Naked mole-rats used in this study were kept either at the Max-Delbrück Center for Molecular Medicine or at the University of Illinois at Chicago. All other Bathyergidae species and East African root rats were housed at the University of Pretoria.

2.2. METHODS

2.2.1. BEHAVIORAL EXPERIMENTS

2.2.1.1. PAIN BEHAVIOR ASSESSMENT

For the assessment of pain induced behavioral response, an injection of 1mM capsaicin, HCl solution (pH 3.5), 0.75% or 100% allyl-isothiocyanate (AITC), 10mM formic acid (pH 3.5) or a vehicle (PBS) was made into the ventral side of the hind paw. The time spent licking and lifting the injected paw were measured individually for each animal for 10 minutes and results for all animals combined.

For the formalin test, a 2% solution was made from a formalin stock solution (37wt% formaldehyde in water). The number of times the animal licked or lifted the paw was defined as the 'pain score' and was measured in 5-minute intervals for 120 minutes after injection or until the response was over.

The L-type calcium channel blocker, Verapamil was injected intraperitoneally (i.p.) to obtain a final concentration of 5 mg/kg. 1 hour and 24 hours post-injection, the animal's nocifensive behavior to AITC was tested as described above.

2.2.1.2. WHOLE BODY PERFUSION FIXATION AND DISSECTION

Whole body perfusion fixation and dissection of the animals was performed at the University of Pretoria in South-Africa. Animals were transcardially perfused as described in Gage, Kipke, & Shain, 2012. First, animals were anesthetized (using isoflurane), then the thoracic cavity was opened and while an incision was made in the right atrium, the perfusion needle was inserted into the left ventricle. Depending on the size of the animal 100-200mL of PBS was slowly injected in the circulatory system, subsequently the solution was switched to 4% paraformaldehyde (PFA) and an equal volume of fixative (100-200mL) was pumped through the body until all tissues were completely fixed.

Spinal cord and DRGs were collected and immersion fixed at 4°C in 4% PFA overnight. 24 hours later, the solution was changed to 30% sucrose with 0.01% azide and kept on 4°C until embedding for cryosectioning (See section RNAscope).

2.2.2. MOLECULAR BIOLOGY TECHNIQUES

2.2.2.1. TOTAL RNA EXTRACTION FROM ANIMAL TISSUES

Dorsal root ganglia (DRGs) and spinal cord tissue were dissected from mouse and several African rodents, from the African mole-rat family (*Bathyergidae*) and transferred to a tube containing 1 mL of TRIzol reagent per 100 mg of tissue sample. After homogenizing and incubating for 5 minutes, 0.2 mL of chloroform per 1 mL of TRIzol Reagent was added and mixed with the sample content. After an incubation of 3 minutes at room temperature, the samples where centrifuged for 10 minutes at 12,000 × g at 4°C in order to separate the RNA in the aqueous layer from the organic phase. For precipitation of the RNA, the aqueous layer was transferred to a new tube and 0.5 mL isopropanol (per 1 mL TRIzol reagent) was added. After an incubation time of 10 minutes at room temperature, the samples were centrifuged for 10 minutes at 12,000 × g at 4°C. The RNA pellet was first washed and air-dried with 75% ethanol, second with a mixture of ethanol, RNAse-free water and sodium acetate. Finally, the RNA was dissolved in 30 µL RNAse-free water.

2.2.2.2. FIRST-STRAND cDNA SYNTHESIS

First strand cDNA synthesis was performed according to the manufacturer's instructions.

In order to make cDNA, 1-3 µg of total RNA was mixed with oligo(dT)20, random primers, dNTP mix and RNAse-free water in a nuclease-free microcentrifuge tube. The mixture was heated to 65°C for 5 minutes and snap-cooled on ice to prevent RNA supercoiling. The First-Strand Buffer, dithiothreitol as a reducing agent and SuperScript™ III reverse transcriptase were added and a temperature protocol as follows was applied: 25°C for 5 minutes; 50°C for 60 minutes; 70°C for 15 minutes.

2.2.2.3. SEQUENCE- AND LIGATION-INDEPENDENT CLONING (SLIC)

cDNA was cloned into an expression vector using the sequence- and ligation-independent cloning (SLIC) method described in Jeong et al., 2012.

Fragment cloning: The cDNA created for the gene of interest was amplified by PCR using primers with homology extension to the linearized vector (see Materials section for sequences). An expression vector was linearized with restriction enzyme(s) overnight, separated by agarose gel electrophoresis and purified with a commercial gel purification kit (Promega).

Agarose gel electrophoresis: DNA samples were separated on 0.5-2% agarose gels with ethidium bromide. The SmartLadder MW-1700-10 (Eurogentec) was used as a DNA size marker and gels were imaged using a Biorad GelDoc XR+ imager with Image Lab™ Software.

Gel purification of DNA fragments: To extract the DNA bands of interest, they were cut out of the gel and purified using the Wizard® SV Gel and PCR clean-up system (Promega) as described below.

Ligation and transformation: The following mixture was made in which vector and insert were added at a molar ratio of 1:2.

	Stock concentration	Volume added	Final concentration
Linearized vector (6 kb)	100 ng/µL	1 µL	10 ng/µL
Insert (e.g. 3 kb)	40 ng/µL	1 µL	4 ng/µL
10x BSA	40 ng/µL	1 µL	4 ng/µL
10x NEB buffer 2		1 µL	1x
DPEC-treated H_2O		Up to 10 µL	1x
T4 DNA polymerase	3 U/µL	0.5 µL	1.5 U

Everything was incubated at room temperature for 2.5 minutes. After the reaction was put on ice for 10 minutes a standard heat shock transformation was done with NEB 5-alpha competent E. coli. An incubation time of 1 hour in SOC medium and 16 hours on agar plates with the required antibiotics for selection was performed to grow bacterial colonies containing an expression plasmid with the gene of interest inserted. Single colonies were picked for an overnight culture in LB medium.

2.2.2.4. PLASMID DNA EXTRACTION

A protocol provided with the PureyieldTM plasmid Miniprep/Midiprep or Maxiprep system (Promega) was used for plasmid DNA extraction. A bacterial pellet was obtained after centrifugation of the LB culture at 4000 rpm on 4°C. The cells were resuspended in water, lysed with a lysis buffer and subsequently the solution was neutralized with a second buffer. Centrifugation or vacuum and washing steps were performed in a DNA-binding column to separate DNA from the cell debris. The DNA was eluted with nuclease-free water by centrifugation or vacuum. DNA preparations were stored at a temperature of -20°C.

2.2.2.5. SANGER SEQUENCING

Samples were sent to LGC Genomics, Berlin and Source Bioscience, Berlin for Sanger DNA sequencing. The results were analyzed using the software Snapgene (GSL Biotech LLC).

2.2.2.6. MUTAGENESIS

For substitution of a single amino acid two different methods were used. One is based on the previous SLIC-method, the other one was performed using the Q5® site-directed mutagenesis kit (New England Biolabs® Inc.).

2.2.2.6.1. TWO FRAGMENT SLIC CLONING

Fragment cloning: Starting with the existing vector containing the DNA of the gene of interest, a PCR was performed to create 2 fragments. The primers (see in Materials 2.1.13, page 38) had homology extension to the linearized vector or were complementary with the gene sequence except for the base pairs that had to be substituted.

Furthers steps: Agarose gel electrophoresis, gel purification of DNA fragments, ligation and transformation were performed as described above. The linearized vector and inserts were mixed at a molar ratio of 1:2:2 (see above). Plasmid extraction and sequencing were performed as described above.

2.2.2.6.2. Q5® SITE-DIRECTED MUTAGENESIS

PCR: An expression vector containing the gene of interest was mixed with a Q5 Hot Start High-Fidelity 2X Master Mix, primers (described in the Material section) and nuclease free water. The following thermal cycles were performed:

Initial denaturation: 98°C, 30 seconds
Denaturation: 98°C, 10 sec
Annealing: primer dependent temperature, 20 sec
Extension: 72°C, 40 sec/kb
Repeat: 25 cycles
Final extension: 72°C, 2 min
Storage: 4-10°C

Kinase, Ligase, DPNI treatment: The KLD buffer mix was added to the PCR product for phosphorylation, intramolecular ligation/circularization and template removal in a 5-minute incubation step at room temperature

Transformation, plasmid extraction and sequencing were performed as described above.

2.2.2.7. QUANTITATIVE REAL-TIME PCR

A qPCR was performed as described in (Eigenbrod *et al.*, 2019). Total RNA was collected as described above (Methods 2.2.2.1, page 41) Total RNA extraction from animal tissues). For reverse transcription with the Superscript III reverse polymerase (Invitrogen) 0.5 µg of total RNA was used and cDNA was analyzed using the Universal Probe library (Roche) in a CFX384 Real Time PCR detection system. Primers to quantify Highveld and Natal mole-rat NALCN were designed using the transcript sequences determined by RNAseq and annotation and are listed in Methods 2.1.13, page 38. The standard curve method with known doses of a plasmid containing the cDNA amplicon from the primer pair was used to quantify mRNA transcripts by extrapolating a value by comparing unknowns to the standard curve of known transcript amounts.

2.2.3. CELL CULTURE

2.2.3.1. MAINTENANCE OF CULTURED CELLS

For all calcium imaging experiments HEK293AD cells were used and grown in a medium which consisted of Dulbecco's modified eagle medium (DMEM) supplemented with 10% fetal calf serum and an antibiotics mixture with penicillin (100 I.U./mL) and streptomycin (100 µg/mL). When necessary cells were passaged using trypsin for detachment and plated unto a new cell culture flask and stored in a 5% CO_2 incubator at 37°C.

For single cells calcium imaging, cells were plated onto PLL coated round glass coverslips with a diameter of 10mm two days before the experiment. For high throughput calcium imaging screens, cells were plated into the wells of a black 384-well microplate with a transparent bottom. Transfection was performed 24 hours after plating.

2.2.3.2. CELL TRANSFECTION

Twenty-four hours before the experiment, liposomal transfection was performed using FuGENE (Promega) and its supplied protocol. The transfection mixture contained

serum free medium, liposomes in a 3:1 ratio to the amount of DNA transfected (1µg per coverslip or 0.02µg per 384-well). Expression vectors contained a fluorescent marker for visual identification of transfected cells. TRPA1 and TRPV1 generally contained a dsRed marker, and NALCN contained EGFP. For single cell calcium imaging single coverslips were transfected, for the calcium imaging with the FLIPR, several transfection mixtures were made in different Eppendorf tubes to transfect each of the 64 wells in the 384-well plate. This means each 384-well plate contained 6 different transfection mixtures.

2.2.4. CALCIUM IMAGING

2.2.4.1. SINGLE CELL CALCIUM IMAGING

A single wavelength calcium indicator (CAL520® AM, AAT Bioquest, Inc.), was dissolved in DMSO and 0.02% pluronic acid. 2µL of a final 2.5mM mixture was loaded onto the cells one hour before the experiment. The coverslip containing the cells was then transferred to a custom-made chamber, and perfused with extracellular buffer (in mM: 140 NaCl, 4 glucose, 10 HEPES, 4 KCl, 2 CaCl2, 1 MgCl2, pH adjusted to 7.4 with NaOH, 5N) at room temperature for 10 – 20 minutes. Calcium imaging was carried out with an Olympus BX51WI microscope using a 20x water immersion objective, a 14-bit camera resolution and a sampling rate of 3 seconds. The cells were excited with a 520 nm laser to visualize red fluorescence from dsRed and a 480 nm laser for visualizing the Ca2+ indicator CAL520® AM. AITC was applied after 30 seconds of imaging for a period of 90 seconds. At the end of the experiment, 1µM ionomycin was applied until a maximum calcium response was reached. For analysis, single cells were manually selected and fluorescence over time was first normalized to the baseline and secondly to the ionomycin response.

2.2.4.2. FLUOROMETRIC IMAGING PLATE READER (FLIPR®)

As described in Eigenbrod *et al.*, 2019, transfection efficiency of the 384-well plate was tested one day after transection on a TECAN plate reader with 556 nm/586 nm wavelengths to measure the dsRed marker. The obtained values were used to calculate transfection outliers using the quartal method, which were excluded from further

analysis. Fluo-4 (Fluo-4 Direct™ Calcium Assay Kit Thermofisher) was prepared according to the manufacturer's instructions and added to the cells for one hour and washed off with extracellular buffer (in mM: 140 NaCl, 4 glucose, 10 HEPES, 4 KCl, 2 CaCl2, 1 MgCl2, NaOH 5N until pH 7.4) immediately before measurements were performed. Sampling rate was 1 second and AITC in several dilutions (0.1nM – 1mM final concentration) was added after 5 seconds. Ionomycin was added 180 seconds later (final concentration 1µM). Total fluorescence per well over time was first normalized to baseline and secondly to the maximal response of ionomycin. Per transfection mixture (64 wells), every dilution was applied on 8 wells. EC_{50} curves were calculated per transfection mixture.

2.2.5. PLANT EXTRACTION

Fresh plant samples were obtained by collaborators from the University of Pretoria in the direct environment. Only roots that grew in the burrows of the Highveld mole-rat were taken. The wasabi, *Wasabi Japonica*, was purchased from AgroDirect and originates from Japan. From each sample, 10 grams of root was homogenized and mixed with 25mL of ddH_2O until a paste was obtained. For hydrolysis, mixtures were incubated overnight at 25°C on shaker at 200rpm in sealed glass vessels. Twelve hours later 10ml of diethyl ether (Et_2O) was added to each sample. After shaking, 6 grams of NaCl was added and mixed to extract all the water from the organic layer. The ether layer was separated from the brine solution and filtered. Twice more 10mL diethyl ether was added, dried, separated and filtered. The organic solvent was evaporated and the remaining substances were re-dissolved in 1 ml DMSO. A diluted solution of 10%w/v in extracellular buffer was used during a single cell calcium imaging experiment (method described above).

2.2.6. PREPARATION OF ANT SUSPENSION

Ants were collected in areas surrounding the city of Pretoria where the Highveld mole-rats where caught by collaborators from the University of Pretoria. The abdominal

part of the ant was cut off and 60 abdomens were homogenized and suspended in 1mL PBS.

2.2.7. RNAscope

Animal tissue for RNAscope *in-situ* hybridization was collected as described in section '2.2.1.2 Whole body perfusion fixation and dissection', page 40. Tissue was shipped from Pretoria University to the MDC in Berlin in 4% sucrose with 0.01% azide. Upon arrival it was embedded in OTC and stored at -80°C until further use. Tissue was transferred to -20°C for 30 min prior to cryosectioning into 12 µm slices onto SuperFrost slides. After a brief drying at room temperature, slides were stored at -80°C.

RNAscope *in-situ* hybridization was performed according to manufacturer's instructions (ACDbio). Pretreatment of fixed frozen tissue was done by incubating the tissue for 10 minutes with hydrogen peroxide, 5 minutes with boiling target retrieval reagent and 15 minutes with Protease III. Subsequently, a combination of probes was added for 2 hours of hybridization at 42°C. After overnight storage in washing buffer, the pre-amplifiers, amplifiers and fluorophores were added in the correct order for signal amplification. DAPI was added as a nuclear marker. Finally, slides were mounted using the ProLong Gold antifade reagent (Thermo Fisher Scientific GmbH).

Imaging of the samples was performed with a Zeiss confocal laser scanning microscope using a 40x oil immersion objective and an 8-bit camera resolution. Analysis of the pictures was done using FIJI Software. The number of dots was calculated by defining the 'dot intensity' per picture and dividing the fluorescence intensity per cell by the dot intensity. For comparison, the number of dots was normalized for cell area.

2.2.8. Statistics and data analysis

All statistical analyses were performed using the GraphPad Prism software. Unless otherwise stated, a two-tailed unpaired t-test or Mann-Whitney test was employed, where * $p < 0.05$; ** $p < 0.01$; *** $p < 0.001$. All data are shown as mean ± S.E.M.

2.2.9. ADDITIONAL METHODS

The scientific work in the scope of this thesis was done in a collaborative manner; therefore, many other methods were performed by collaborators in and outside the research group of Prof. Dr. G.R. Lewin.

- RNA sequencing
    - RNA extraction was done with TRIzol as described above by Dr. Jane Reznick
    - Data processing and analysis of RNA sequencing data was done by Dr. Ole Eigenbrod
- Electrophysiological recordings of transfected HEK293 cells were done by Oscar Sánchez-Carranza as described in Eigenbrod et al
    - Whole cell patch clamp recordings were conducted on dsRed and/or EGFP-positive HEK293 cells 48-72 hours post transfection at room temperature. Patch pipettes were pulled from borosilicate glass capillaries and had a tip resistance of 3-6 MΩ. Recordings were made using EPC-9 amplifier (HEKA) and Patchmaster software (HEKA). A standard voltage-step protocol was used whereby cells were held at 0mV for 50 ms before stepping to the test potential -60mV – +60 mV in 20mV increments) for 1 sec, returning to the holding potential (0mV for 50 ms) between sweeps.
    - Performing current clamp, current pulses from -60pA to +20pA (20pA increments) were injected into the cell. The steady-state voltage responses were plotted against the amplitude of the current injection. The slope of the linear fit of this relationship was determined to calculate the input resistance.
- Additional statistical analyses were performed using the GraphPad Prism software. Unless otherwise stated, a two-tailed unpaired t-test or Mann-Whitney test was employed, where n.s. $p > 0.05$; * $p \leq 0.05$; ** $p \leq 0.01$; *** $p \leq 0.001$. All data are shown as mean ± SEM.

3. RESULTS

3.1. IDENTIFICATION OF ALGOGEN INSENSITIVITIES

3.1.1. CAPSAICIN, ACID AND MUSTARD OIL

As mentioned in Introduction 1.3.2 (page 29) and published in Eigenbrod *et al*., seven African mole-rats, the naked mole-rat, the East African root rat (a subterranean African rodent) and the C57Bl/6N mouse were tested for their behavioral response to a plantar injection of HCl (pH3.5), capsaicin (10mM) and AITC (0.75%). Two additional African mole-rats were added to the dataset later, revealing a total of 8 insensitivities. Behavioral responses were coded as time spent licking and lifting the injected paw in the first ten minutes following plantar injection of the algogen (*Figure 6* and *Table 3*). If the response time after an algogen injection was not significantly different from the response time after a vehicle injection using a Mann-Whitney U test, we concluded the animal was insensitive to this algogen (indicated with n.s.). Three species were found to be insensitive to capsaicin, namely the naked mole-rat, the Potwe mole-rat and the Natal mole-rat. The East African root rat, the naked mole-rat, the Potwe mole-rat and the Cape mole-rat were found to be insensitive to an acid injection. The Cape Dune mole-rat also showed a low response to acid, however, the mean response time was higher than the vehicle injection response time. The Highveld mole-rat was the only animal not responding to AITC. These experiments were carried out over a period of several years by Dr. J. Reznick, Dr. D. Omerbašic, Dr. A. Barker, Prof. Dr. T. Park, Prof. Dr. G.R. Lewin and K. Debus.

Focusing on the unique AITC insensitivity of the Highveld mole-rat, we tested the hypothesis that the animal is less sensitive than the other rodents and thus would respond to a higher concentration of AITC. Surprisingly, the response time of the animals to an injection of 100% AITC was not significantly different than the response after the injection of 0.75% AITC (p=0.083) (*Figure 7* and *Table 3*). However, in one animal a small response was observed after 7-8 minutes possibly caused by an inflammatory reaction at the injection site making it significantly higher than a vehicle injection (p=0.0385).

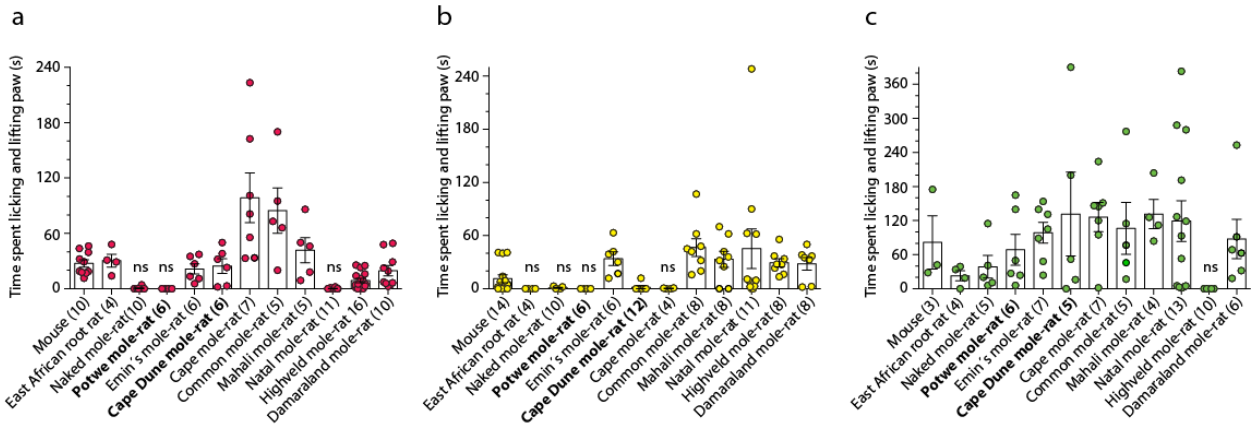

Figure 6: *Cumulative responses of selected rodents to 3 algogens. (a) Shows the cumulative responses to capsaicin, (b) to acid and (c) to AITC. The newly added and unpublished species Potwe mole-rat and Cape Dune mole-rat are highlighted. The graph shows mean ± SEM and single data points indicate single animals tested. The number of animals tested (n) is indicated behind the species names (Mann-Whitney U test (two-tailed), n.s (not significant) p<0.05). Modified from Eigenbrod et al., 2019.*

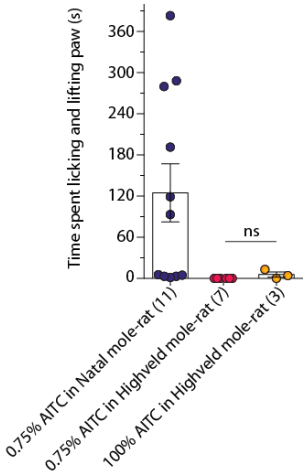

Figure 7*: Cumulative response after an injection of 100% AITC in the Highveld mole-rat. The response is not significantly different (ns) to the injection with 0.75% AITC. Single data points indicate single animals tested and the number of animals tested is indicated in parentheses (Mann-Whitney U test (two-tailed), n.s p<0.05).Reproduced from Eigenbrod et al. 2019*

3.1.2. FORMIC ACID AND CITRIC ACID

With four species insensitive to an injection of HCl, we tested the response of several mole-rats and mice to weaker acids such as citric acid and formic acid. Fewer animals were tested based on the availability of wild animals at the University of Pretoria. Weaker acids dissociate only partially, causing the proton concentration to be

lower in comparison to strong acids (such as HCl). Furthermore, the undissociated form is able to cross the membrane and dissociate inside the cell, acidifying the intracellular environment and so activating TRPA1 and initiating nociception (Wang *et al.*, 2011). We hypothesized that the Highveld mole-rat might have an impaired TRPA1 functionality and therefore be insensitive to citric acid. Confirming this hypothesis, we found additionally that the naked mole-rat was insensitive to citric acid. This was presumably because even at a slightly increased proton concentration, the naked mole-rat NaV1.7 channel gets blocked, a mechanism previously described by Smith *et al.*, 2011. The HCl-insensitive Cape mole-rat showed a small pain response to citric acid compared to other sensitive animals, although significantly higher than a vehicle injection (p=0.0095) (*Figure 8* and *Table 3*).

An injection of formic acid was given to the Highveld mole-rat as well as the Mahali mole-rat and Damaraland mole-rat; the latter two species were responsive to every algogen tested thus far. While the Mahali mole-rat and the Damaraland mole-rat showed nocifensive behavior after the injection, again the response time of the Highveld mole-rat was not significantly different from the response time after a vehicle injection (Mann-Whitney U test (two-tailed). This result confirmed the hypothesis that weaker acids do not cause measurable pain responses in this specific *Cryptomys* species (*Figure 9* and *Table 3*).

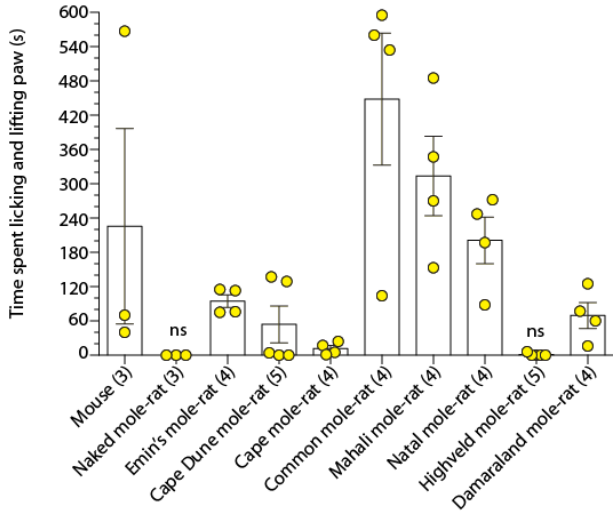

Figure 8: *Cumulative responses of mice and several mole-rat species to a citric acid injection. The naked mole-rat as well as the Highveld mole-rat were insensitive, meaning the response is not significantly different from a vehicle injection. Single data points indicate single animals tested and the number of animals tested is indicated in parentheses (Mann-Whitney U test (two-tailed), n.s. p<0.05).*

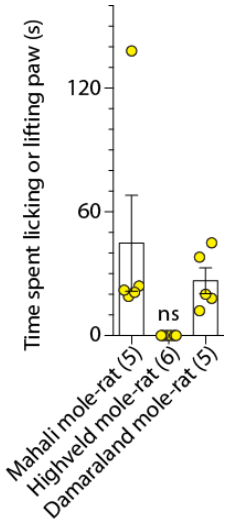

Figure 9: *Cumulative responses of three mole-rat species to a formic acid injection. The Highveld mole-rat was insensitive, meaning the response was not significantly different from a vehicle injection. Single data points indicate single animals tested and the number of animals tested is indicated in parentheses (Mann-Whitney U test (two-tailed), n.s. p<0.05).*

	Vehicle	**Capsaicin**	**Acid (HCl)**	**AITC (0.75%)**	**AITC (100%)**	**Citric acid**	**Formic acid**
Mouse	0.20 s (±0.13)	27.52 s (±3.93)	11.43 s (±4.39)	81.87 s (±46.78)	x	225.7 s (±170.90)	x
East African root rat	0.28 s (±0.18)	30.50 s (±6.96)	0.0 s (±0.0) p>0.9999	23.00 s (±8.765)	x	x	x
Naked mole-rat	0.75 s (±0.45)	0.43 s (±0.43) p=0.9323	1.06 s (±0.66) p=0.0721	36.68 s (±20.01)	x	0.00 s (±0.00) p>0.9999	x
Potwe mole-rat	0.00 (±0.00)	0.00 s (±0.00) p>0.9999	0.00 s (±0.00) p>0.9999	68.67 s (±27.31)	x	x	x
Emin's mole-rat	1.50 s (±1.50)	21.55 s (±5.44)	33.90 s (±7.58)	98.76 s (±18.30)	x	94.75 s (±11.12)	x
Cape Dune mole-rat	0.28 s (±0.18)	24.67 s (±7.87)	1.714 s (±1.71)	131.6 s (±73.64)	x	54.00 s (±32.28)	x
Cape mole-rat	0.17 s (±0.12)	98.56 s (±26.88)	0.425 s (±0.25) p=4286	126.2 s (±25.59)	x	11.75 s (±5.31)	x
Common mole-rat	0.11 s (±0.11)	84.80 s (±24.55)	46.50 s (±10.15)	106.4 s (±45.65)	x	448.3 s (±115.40)	x
Mahali mole-rat	0.60 s (±0.60)	41.80 s (±13.57)	33.38 s (±9.01)	131.5 s (±25.70)	x	313.8 s (±69.63)	44.80 s (±23.31)
Natal mole-rat	0.25 s (±0.25)	0.30 s (±0.21) p>0.9999	45.27 s (±22.41)	119.4 s (±35.91)	x	201.0 s (±40.77)	x
Highveld mole-rat	0.10 s (±0.10)	8.906 s (±2.32)	29.39 s (±4.70)	0.0 s (±0.0) p>0.9999	5.67 s (±3.84)	1.20 s (±1.20) p=0.7619	0.0 s (±0.0) p>0.9999
Damaraland mole-rat	0.08 s (±0.08)	19.45 s (±5.59)	28.20 s (±7.02)	87.73 s (±43.75)	x	69.50 s (±22.53)	26.60 s (±6.32)

Table 3: *Cumulative responses of tested rodents to different algogens. Mean ± SEM. Results that were not significantly different from a vehicle injected tested are highlighted in gray where also the p-value when compared to vehicle is indicated (Mann-Whitney U test (two-tailed), n.s. p<0.05). X denotes test not performed.*

3.1.3. FORMALIN

By employing the formalin test (Dubuisson and Dennis, 1977; Abbott, Franklin and Westbrook, 1995), we measured the biphasic nocifensive behavior usually observed after an injection of 2% formalin in the plantar side of an animals' hind paw. The first responsive phase indicates the direct activation of chemoreceptors (acute pain), whereas the second responsive phase is thought to provide information about central sensitization. The number of times the animal lifted or licked the injected paw was counted in five-minute intervals and the sum of these events was defined as the pain score. The mean traces per animal are given in *Figure 10a*, a cumulative pain score per animal per species is shown in *Figure 10b*. While all animals tested showed a response higher than a response to a vehicle injection in both the first and the second phases of the formalin test, the cumulative pain score of the Highveld mole-rats during the first 15 minutes after the formalin injection (pain score of 0.8000 (±0.5831)) was not significantly different from a pain score measured 15 minutes after a vehicle injection (pain score of 0.1 (±0.1), Mann-Whitney U test, p=0.1685), suggesting nocifensive behavior in the first responsive phase was completely absent in these animals. The second responsive phase showed a pain score of 498.6 (±146.8) in the Highveld mole-rat which is significantly higher than after a vehicle injection (pain score 0.7 (±0.7)) and not significantly higher than the other tested mole-rat species (244.0 (±47.01), 267.2 (±79.26), 255.8 (± 43.06) and 363.6 (± 64.44) for the naked mole-rat, the Cape Dune mole-rat, the Natal mole-rat and the Damaraland mole-rat respectively) using a Kruskal-Wallis multiple comparison test (p>0.9999 in all cases). These results suggest that acute nociceptive activation by formalin in Highveld mole-rats were blunted.

3.2. RNA SEQUENCING OF AFRICAN RODENT SENSORY TISSUE

In order to understand the cellular basis of aberrant algogen sensitivity in the African mole-rat family, sensory tissue was collected from behaviorally characterized animals to perform RNA sequencing. In this way, a database was created to obtain access to annotated gene sequences and RNA expression levels from DRG and spinal cord (SC) from the different African rodents for comparative phylogenetic analysis. This

analysis allowed us to identify amino acid variants and differentially expressed genes from animals insensitive to specific algogens when compared to those that are sensitive. This experiment was carried out by Dr. J. Reznick and Dr. O. Eigenbrod and published in Eigenbrod *et al.*, 2019.

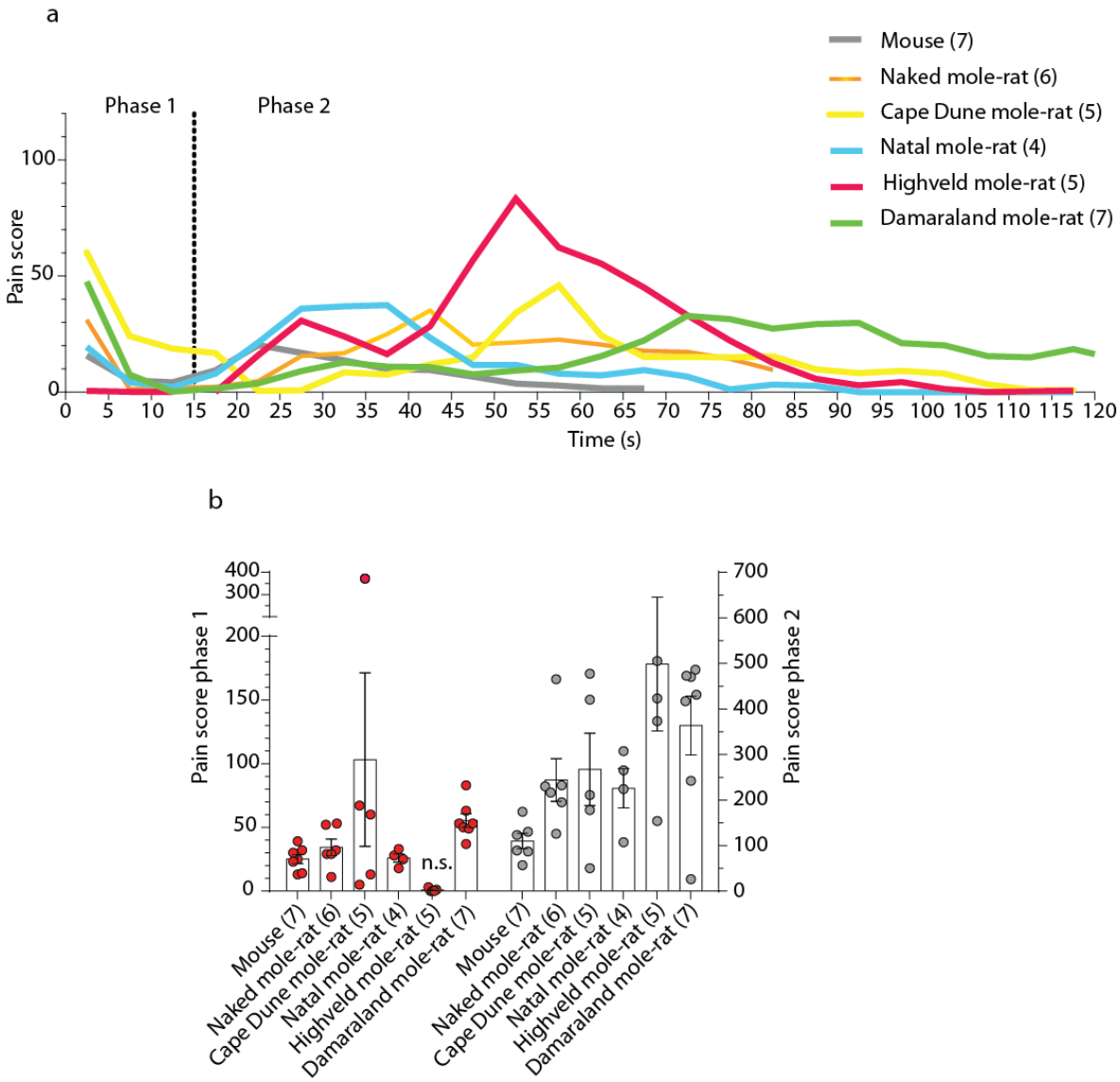

***Figure 10**: The formalin test. (a) Shows mean traces per species showing the pain score over time. (b) Shows cumulative pain score per species in first (first 15 minutes) and second responsive phases (after 15 minutes). Error bars are mean ± SEM. Single data points indicate single animals tested and n numbers are written behind the species names. The Highveld mole-rat was insensitive to formalin during the first phase. The pain score in phase I was not significantly (n.s.) different from a response to a vehicle injection (Mann-Whitney U test (two-tailed), n.s p<0.05). Reproduced from Eigenbrod et al. 2019.*

3.2.1. PROTEIN SEQUENCE ALIGNMENTS

De novo assembly and annotation of the RNA reads made it possible to analyze predicted amino acid sequences from thousands of genes expressed in the DRG or SC. In total 6878 genes were annotated and for genes that were not reconstructed with the de novo assembly approach due to technical errors, the transcript was retrieved by assembly with the naked mole-rat sequences from RefSeq (e.g. for *SCNA9*, the coding gene for NaV1.7). The ratio of non-synonymous (d_N) to synonymous substitutions (d_S) was used to define the strength of divergent selection in amino acid variation. Using this method, we evaluated candidate protein sequences, known to be involved in observed phenotypes, for substitutions.

Interesting candidates related to this thesis are listed in *Table 4*. For acid insensitivity, ASICs, TRPV1 and NaV1.7 were examined. TRPV1 and TRPA1 were investigated closely as they are receptor proteins for capsaicin and AITC, respectively. Interspecies alignments of ASIC3 showed no evidence of changes in sequence that could influence the channels' function in insensitive species (Eigenbrod, 2018). Similar to naked mole-rats in which TRPV1 has already been identified to be functional and sensitive to capsaicin (Park *et al.*, 2008), the Natal mole-rat did not show a clear pathological variants. In the amino acid sequences of TRPA1, however, the cysteine at position 622 (human numbering 621) known to be involved in the channel activation by AITC was substituted to a phenylalanine in all *Cryptomys* species suggesting this might lead to a decrease in TRPA1 sensitivity (Macpherson, Dubin, *et al.*, 2007; Bahia *et al.*, 2016). In two other positions near the AITC binding site, 581 and 975, the *Cryptomys* species displayed an introduction of a cysteine (*Figure 11*). One substitution, H1086N, was found to be unique to the AITC insensitive Highveld mole-rat.

As the naked mole-rats' EKE mutation in domain IV of NaV1.7 is suggested to inhibit the action potential initiation by acid block, the sequences of the *SCNA9* gene were aligned and investigated (Park *et al.*, 2008; Smith *et al.*, 2011). This analysis revealed that all African mole-rat species contain a negatively charged motif in domain IV instead of a positively charged motif as found in many other species including humans, fish, birds, rodents, reptilians, etc. However, while all species show an EKD (-+-) motif, the acid insensitive species, the naked mole-rat and the Cape mole-rat have

the same EKE (-+-) mutations. In domain III another variation was found where only the naked mole-rat and Cape mole-rat show a negatively charged NED motif. In the behavioral tests, the East African root rat also showed no pain response after acid injection. This species, not a member of the African mole-rat family (*Bathyergidae*), shows the EKD motif in domain IV and no variants in domain III (Eigenbrod, 2018; Eigenbrod *et al.*, 2019). However, another adaptation might have led to the insensitivity to acid. Looking at the RNA expression data or sequences from the East African root rat, could help us identify other candidates to investigate.

In conclusion, a database was established by Dr. Eigenbrod with single transcript sequences identified after RNA sequencing of sensory tissue. Key proteins related to algogen insensitivity were investigated and we identified several variations in *trpa1* and *SCN9A* that could potentially give rise to the sensory phenotypes in African mole-rats.

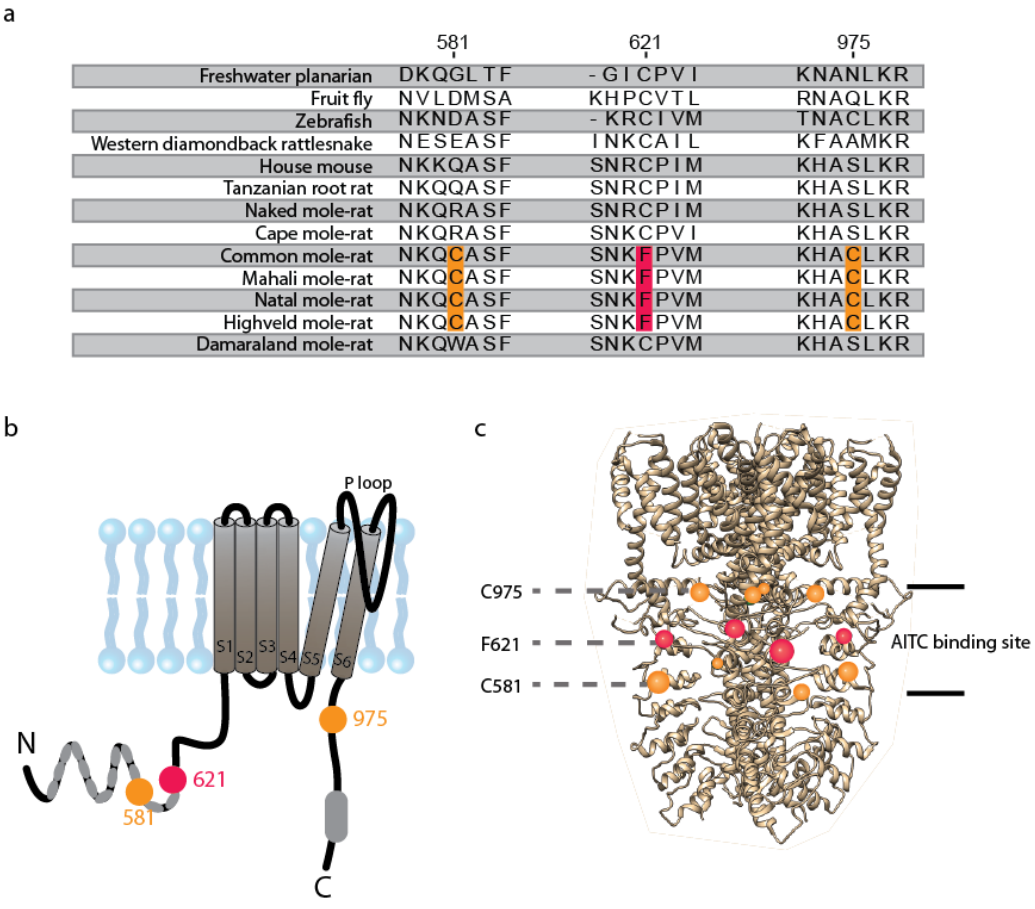

***Figure 11**: Cryptomys specific amino acid changes in TRPA1. (a) Amino acid sequences from a range of species including Cryptomys species indicating a gain of cysteine (orange) or a loss of cysteine (red). (b) and (c) show the molecular structure and the crystal structure of TRPA1 respectively with the position of the cysteine changes indicated. Adapted from Eigenbrod et al 2019.*

Insensitivity	Target proteins	Amino acid variation
Acid	NaV1.7	EKE mutation in domain IV in Cape and Naked mole-rat NED mutation in domain III in Cape and Naked mole-rat
	ASICs	No apparent changes
	TRPV1	No apparent changes
Capsaicin	TRPV1	No apparent changes
AITC	TRPA1	Cysteine 621 substituted in *Cryptomys* species Introduction of cysteine in position 581 and 975 in *Cryptomys* species

Table 4: *Interesting protein candidates related to the observed algogen insensitivities in the African mole-rat family.*

3.2.2. RNA QUANTIFICATION

Expression levels of 6878 annotated transcripts were quantified, allowing a comparison across species and tissues. Of particular interest after the outcome of the behavioral testing (1.3.2, page 29), is the differential expression of genes in insensitive species compared to sensitive species tested (Eigenbrod, 2018; Eigenbrod *et al.*, 2019). To do this Dr. Eigenbrod used a phylogenetic generalized least squares (pGLS) model to control for the phylogenetic distance between the animals. Performing ANOVA, a gene was identified as differentially expressed when the p-value (statistical significance) was smaller than 0.05 and log2FC (log magnitude of change) was larger than 1 (Eigenbrod, 2018).

For the capsaicin insensitive species, the naked mole-rat and the Natal mole-rat, only *BMPER* was found to be upregulated in DRGs. This gene codes for a protein regulating the differentiation of osteoblasts. It is however unclear whether it could be involved in the observed algogen insensitivity (Eigenbrod, 2018; Eigenbrod *et al.*, 2019). Differential expression analysis of the acid-insensitive species the naked mole-rat, the Cape mole-rat and the East African root rat showed many down- and upregulated genes

(20 and 21, respectively). Interestingly, a downregulation of *ACCN3* (which codes for the acid sensing channel ASIC3), *KCNK1* (which codes for an acid sensitive potassium channel TWIK1) and *SLC50A1* (which codes for SWEET1, a sugar transporter) was observed. SLC49A (which codes for a proton coupled folate transporter) was one of the genes found to be upregulated in the spinal cord and DRG (Eigenbrod, 2018; Eigenbrod *et al.*, 2019). In the only AITC insensitive species, the Highveld mole-rat, differential expression analysis revealed only one single gene upregulation in both spinal cord and DRG. *Nalcn*, the gene coding for the sodium leak channel largely responsible for the background sodium leak conductance and therefore regulating the resting membrane potential (Ren, 2011; Eigenbrod, 2018; Eigenbrod *et al.*, 2019).

3.3. MUSTARD OIL INSENSITIVITY IN THE HIGHVELD MOLE-RAT

3.3.1. COMPARING TRPA1 SENSITIVITY AMONG DIFFERENT SPECIES

3.3.1.1. CLONING THE TRPA1 CHANNEL FROM DIFFERENT MOLE-RAT SPECIES

Plasmids carrying the TRPA1 gene from the mouse, Highveld mole-rat, Natal mole-rat and naked mole-rat were made using RNA from sensory tissue from the respective animals. After reverse transcription to cDNA, a PCR with primers based on the predicted sequences was done and the product was inserted into a vector plasmid (see Methods 2.2.2, page 41). The similarity of the amino acid sequences was 100% for all four animals. Afterwards relevant amino acid substitutions were made described in Methods 2.2.2.6, page 43.

3.3.1.2. SINGLE CELL CALCIUM IMAGING

The activity of TRPA1 from mouse, Highveld mole-rat and Natal mole-rat was tested using calcium imaging on HEK293 cells transfected with the respective DNA constructs, mTRPA1, HvTRPA1 and nTRPA1, respectively. An increasing concentration

of AITC ranging from 0.1nM to 10mM was applied to the cells to which a calcium dye was added before. The fluorescence intensity reflecting the concentration of intracellular calcium was used as a proxy for channel activity. The maximal increase in intracellular calcium was measured after an application of ionomycin. This maximal response was used to normalize the AITC responses and the dose-response curve was calculated with nonlinear regression analysis. An increase in intracellular calcium was observed after AITC was applied to the transfected cells suggesting that all three proteins were responsive to AITC when compared to mock-transfected HEK cells. However, the sensitivity from the HvTRPA1 was significantly decreased when compared to mTRPA1. The EC_{50}, the concentration at which a half-maximal response of the channel is detected, was 0.52µM (or $10^{-6.290} \pm 10^{0.2220}$), 4.20µM (or $10^{-5.377} \pm 10^{0.2810}$) and 0.30µM ($10^{-6.518} \pm 10^{0.2832}$) for mTRPA1, HvTRPA1 and nTRPA1, respectively. The HvTRPA1 EC_{50} was significantly higher than that of mTRPA1 and nTRPA1 (one-way ANOVA, p=0.0377 and p=0.0081) (*Figure 12* and *Figure 13*). From this experiment we concluded that the TRPA1 channel from the AITC-insensitive Highveld mole-rat is functional but less sensitive.

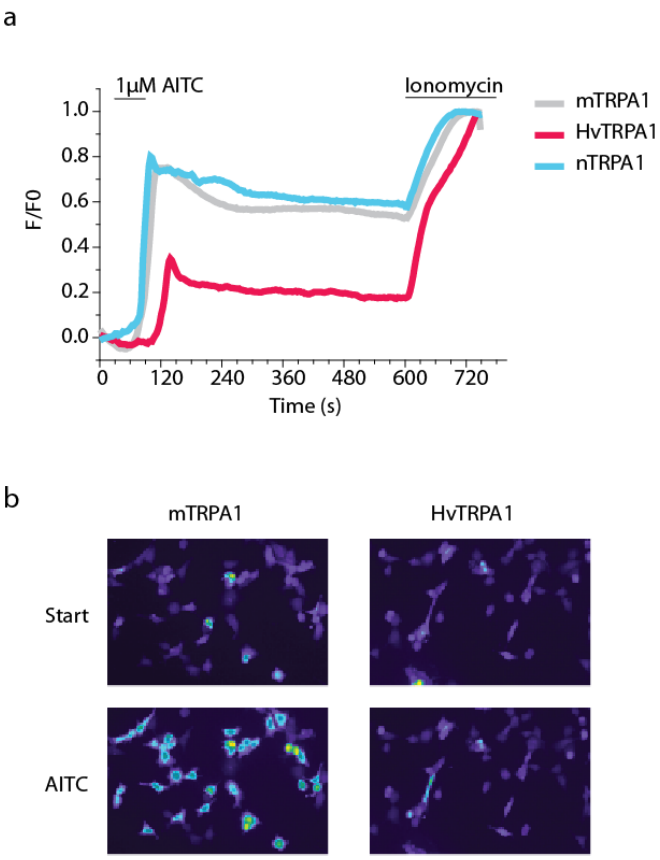

Figure 12: *(a) Sample traces of intracellular calcium over time in HEK293 cells transfected with TRPA1 constructs from mouse, Highveld mole-rat and Natal mole-rat. (b) Imaging pictures of HEK293 cells transfected with mTRPA1 or HvTRPA1 before and during AITC application.*

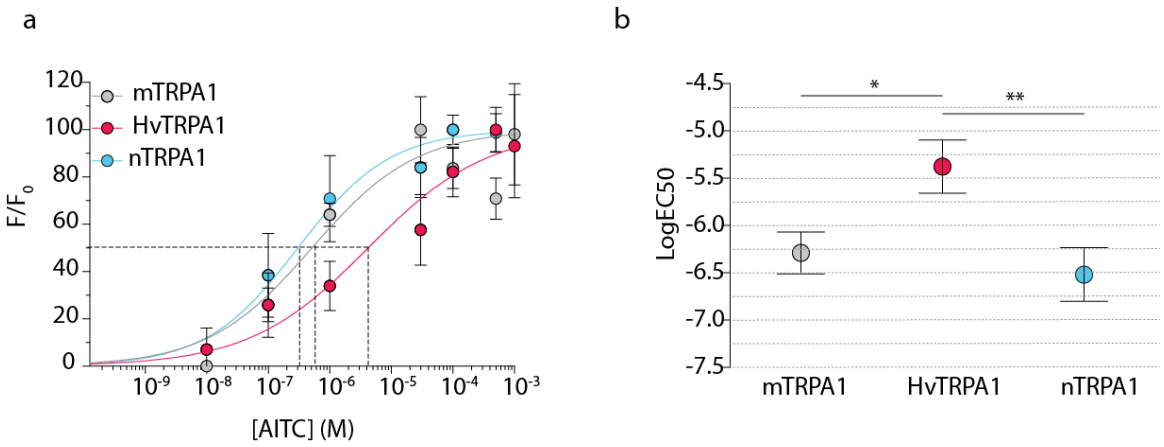

Figure 13: *EC_{50} calculation for mTRPA1, HvTRPA1 and nTRPA1 to AITC. (a) EC_{50} curves of the three constructs. Dotted line indicates the half maximal response. (b) EC_{50} values of the different constructs are plotted on a log scale (One-way ANOVA, * p≤0.05; ** p≤0.01). For each construct a minimum of six transfected cover slips were tested with minimal 20 cells chosen to analyze. Modified from Eigenbrod et al., 2019*

3.3.1.3. CALCIUM IMAGING USING FLIPR

Several mutant versions of the TRPA1 channels were made to evaluate the contribution of amino acid variations in the Highveld mole-rat TRPA1. We substituted cysteine 621 with a phenylalanine in the mouse TRPA1 ($mTRPA1_{F621C}$). Another construct was made with two additional substitutions of amino acids 581 and 975 with a cysteine ($mTRPA1_{Q581C/C621F/S975C}$) (see *Figure 13*). The Highveld mole-rat TRPA1 construct was mutated to change the phenylalanine at position 621 back into a cysteine ($HvTRPA1_{C621F}$). Given the increased number of different DNA constructs to test, we switched to a high-throughput system for performing the calcium imaging experiments where we transfected HEK293 cells in a 384-well plate format. This change in experimental setup required us to repeat the initial experiment with mTRPA1, HvTRPA1 and nTRPA1 in addition to experiments performed with the newly generated mutant constructs. In the high-throughput system, the fluorescence intensity reflecting the intracellular calcium was measured from a whole well of a mixture of transfected and non-transfected cells as opposed to from the individually selected transfected cells in the previous method (in Results 3.3.1.1). Differences EC_{50} values measured between the

two methods can therefore be attributed to this difference in data collection as well as in normalization of the data. Dose response relationships and curves could be calculated by nonlinear regression analysis after an application of AITC with concentrations ranging from 0.1nM to 10mM followed by ionomycin. We confirmed a significantly lower sensitivity of the HvTRPA1 channel (EC_{50}: 119µM or $10^{-3.925}$ ($\pm10^{0.08184}$)) in comparison to mTRPA1 (EC_{50}: 11µM or $10^{-4.967}$ ($\pm10^{0.2508}$)) (Mann-Whitney U test, p=0.0013). Surprisingly, the EC_{50} of the nTRPA1 (EC_{50}: 125µM or $10^{-3.904}$ ($\pm10^{0.02806}$)) was not different from the HvTRPA1 (p=0.9551). We considered the high-throughput screening (with n numbers much higher than the single cell method) a more reliable experimental setup and therefore we continued to test the remaining constructs. The EC_{50} curves, as well as the exact values can be found in (*Figure 14*). The constructs for expressing TRPA1 channels from mouse and naked mole-rat (EC_{50}: 34µM or $10^{-4.474}$ ($\pm10^{0.1069}$)) had a similar sensitivity to AITC (p=0.2486). Removing the cysteine in position 621 in mTRPA1 confirmed a significant decrease in sensitivity as was found previously in the literature (Hinman *et al.*, 2006; Macpherson, Dubin, *et al.*, 2007) ($mTRPA1_{C621F}$ EC_{50}: 129µM or $10^{-3.891}$ ($\pm10^{0.04807}$)) and was not different from HvTRPA1 or nTRPA1 (Mann-Whitney U test, p=0.9626 and 0.2463 respectively). Introducing the two cysteines found in the *Cryptomys* species to this construct did not change the decreased sensitivity significantly ($mTRPA1_{Q581C/C621F/S975C}$ EC_{50}: 90µM or $10^{-4.046}$ ($\pm10^{0.07741}$), Mann-Whitney U test, p=0.0589 when compared to $mTRPA1_{C621F}$). By introducing the cysteine at position 621 in the HvTRPA1, we found again an increase in sensitivity, although not to the level of mTRPA1 ($HvTRPA1_{F621C}$ EC_{50}: 46µM or $10^{-4.337}$ ($\pm10^{0.06056}$), Mann-Whitney U test, p=0.0025 when compared to HvTRPA1). Taken together, we can conclude that the sensitivity of the Highveld TRPA1 channel is decreased and that the amino acid substitution on position 621 from a cysteine to a phenylalanine is most likely a contributing factor to this phenomenon.

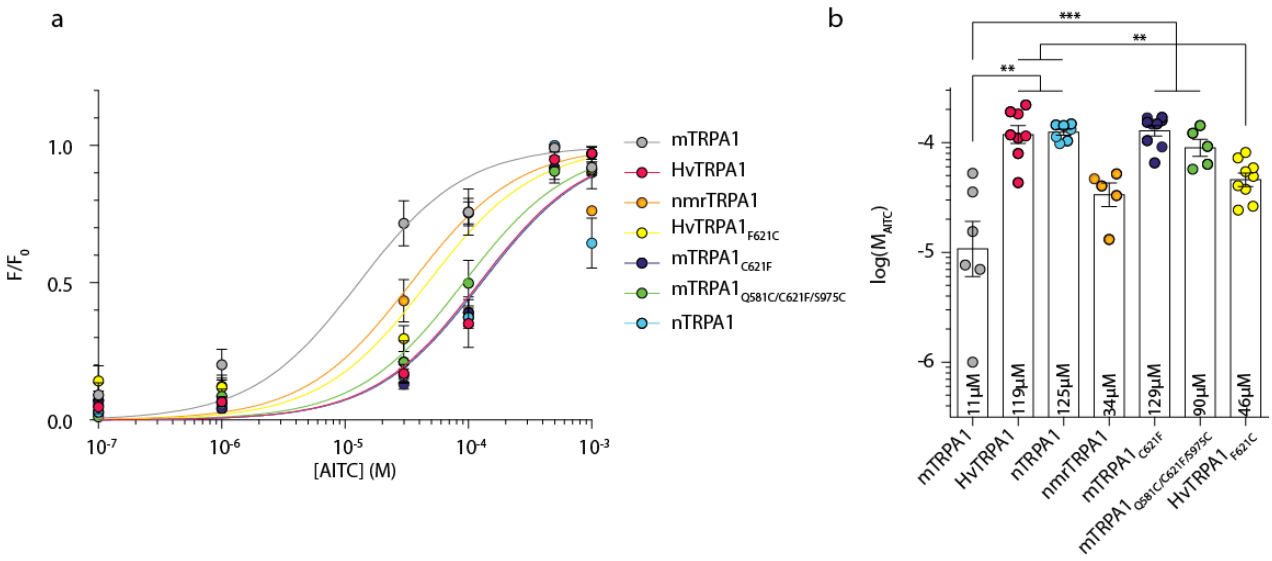

***Figure 14**: Results from calcium imaging using FLIPR. (a) EC_{50} curves for the different constructs tested. (b) EC_{50} values for the different constructs with significant differences indicated. (Mann-Whitney U test, ** p≤0.01 and *** p≤0.001). Each data point indicates a new transfection in HEK393 cells that was tested with all AITC concentrations (for details look in Methods 2.2.4, page 46). Reproduced from Eigenbrod et al., 2019.*

3.3.2. Investigation of the upregulated NALCN leak channel

3.3.2.1. NALCN expression levels in mole-rat DRGs and TGs by qPCR

Performing RNA sequencing on DRG and spinal cord tissues from the species tested with the three algogens, allowed us to identify upregulated genes. For the AITC-insensitive Highveld mole-rat, the gene for NALCN was upregulated in comparison to the other animals studied (Eigenbrod, 2018; Eigenbrod *et al.*, 2019). We confirmed this by qPCR on DRGs and TGs from the Natal and the Highveld mole-rat. As we only had two TGs from Highveld mole-rats, we cannot perform statistics on this data, however in the DRG tissue a significant increase in RNA transcripts of *nalcn* was found ($517.40*10^3$ per 10ng RNA ($\pm 150.8*10^3$) from Highveld mole-rat versus $12.68*10^3$ per 10ng RNA ($\pm 8.753*10^3$) from Natal mole-rat, Mann-Whitney U test, p=0.0238) *(Figure 15*).

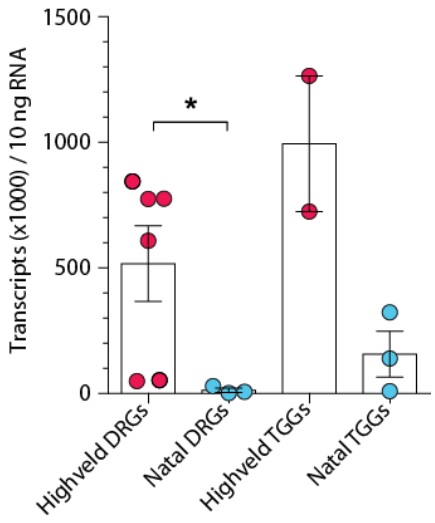

Figure 15: *RNA expression of NALCN. qPCR data on DRG and TG tissues from the Natal and Highveld mole-rat (Mann-Whitney U test, * p≤0.05). Single data points represent tissue samples from different animals.*

3.3.2.2. Molecular cloning of Highveld NALCN for electrophysiological analysis

We investigated a possible role of NALCN in causing insensitivity to AITC in the Highveld mole-rat. Our hypothesis was that an overexpression of NALCN in neurons leads them to be more 'leaky' and therefore have a higher resting membrane potential, causing some of the voltage-gated sodium channels to be in an inactivated state (see Introduction 1.1.6, page 23). This state would cause the neuron to be less likely to fire and thus be less likely to transmit nociceptive information flowing exposure to AITC.

We expressed the Highveld NALCN channel alone or together with HvTRPA1 in HEK293 cells and performed whole cell patch clamp recordings. A leak current was observed when stepping the voltage from -60mV to +60mV in 20mV increments in HEK293 cells transfected with HvNALCN (-5.602 pA/pF (±1.02), -3.789 pA/pF (±0.7113), -1.931 pA/pF (±0.3635), 2.016 pA/pF (±0.403), 4.287 pA/pF (±0.9463), 7.334 pA/pF (±1.87) at -60mV, -40mV, -20mV, +20mv, +40mV and +60mV respectively) alone or together with HvTRPA1 (-8.262 pA/pF (±2.354), -5.496 pA/pF (±1.625), -2.485 pA/pF (±0.8658), 2.991 pA/pF (±0.9233), 6.689 pA/pF (±2.018), 11.07 pA/pF (±3.587)) in comparison with untransfected cells (-1.353 pA/pF (±0.3923), -0.7739 pA/pF (±0.2945), -

0.4081 pA/pF (±0.1579), 0.5757 pA/pF (±0.1087), 1.066 pA/pF (±0.2238), 1.640 pA/pF (±0.3191)) *(Figure 16a*). The current voltage relationship was linear, different from voltage dependent currents seen in voltage sensitive channels which are more bell-shaped. Input resistance was measured by injecting current into the cell and analyzing the resulting voltage change (R=ΔV/ΔI). Large changes in membrane potential mean that not much current leaked which gives high input resistances; small changes indicate a larger leak and results in a lower input resistance. Indeed, a significantly lower input resistance was measured in HEK293 with HvNALCN (0.9625 GΩ (±0.1657)) alone or together with HvTRPA1 (0.6855 GΩ (±0.1346)), reflecting a higher number of open ion channels than in untransfected cells (2.080 GΩ (±0.2033)) (one-way ANOVA, p=0.0003 and p<0.0001) (*Figure 16b*). This indicates that NALCN is constitutively active as described in the literature. Furthermore, we calculated the resting membrane potential in the same cells and found an increase in the presence of HvNALCN (-17.26mV (±3.626)) alone or together with HvTRPA1 (-11.53mV (±2.949)) when compared to untransfected cells (-61.66mV (±3.974) (Kruskal-Wallis test, p=0.0007 and p<0.0001) (*Figure 16c*). These results support the hypothesis that the membrane potential is increased to a value where important voltage gated channels such as NaV1.7 are in an inactivated state. These experiments were performed by O. Sánchez-Carranza and K. Debus.

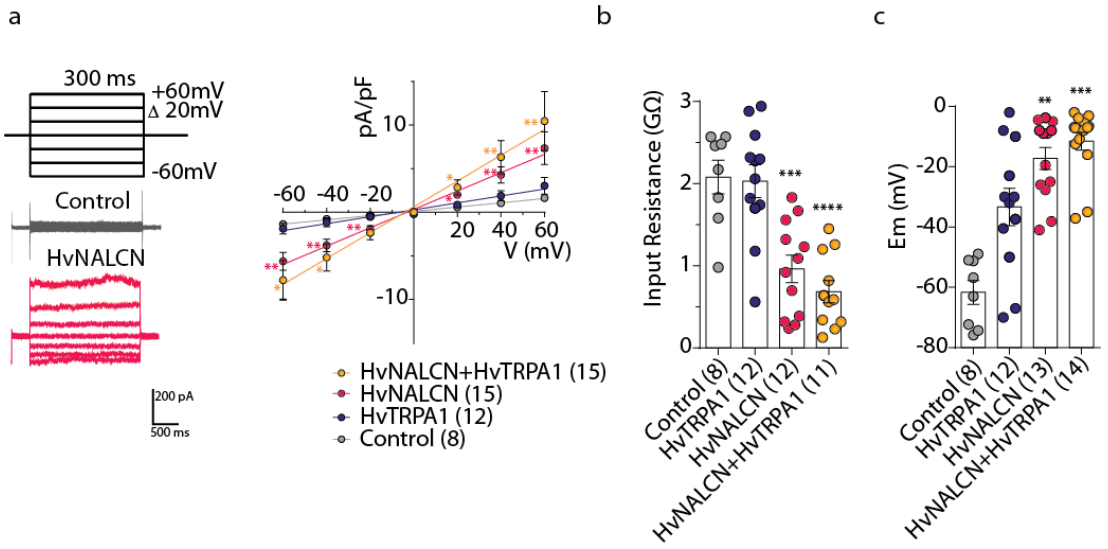

Figure 16*: Patch clamp recordings of NALCN transfected HEK293 cells. (a) Shows a significant increase in leak conductance in HEK293 cells transfected with HvNALCN alone or together with HvTRPA1. (b) The input resistance in NALCN transfected HEK293 cells was decreased and (c) the membrane potential was depolarized. The number of cells patched (n) are indicated behind the transfection plasmid. Error bars are mean ± SEM. (Kruskal-Wallis tests, Dunn's multiple comparison tests and one-way ANOVA, n.s. p>0.05, * p≤0.05 ** p≤0.01, *** p≤0.001 and **** p≤0.0001). Reproduced from Eigenbrod et al., 2019.*

3.3.2.3. NALCN EXPRESSION AND LOCALIZATION IN DRGS BY RNASCOPE

The question remains as to why the animals respond to other algogens such as capsaicin. Therefore, we hypothesized that *nalcn* is only overexpressed in a subset of DRG neurons, namely TRPA1-positive cells. In this way only the neurons expressing the TRPA1 channels would be unable to transduce the nociceptive signals. Information on stimuli activating other receptors expressed in the remainder neurons would reach the central nervous system. To assess this, we performed RNA scope, a novel *in situ* hybridization technique to visualize RNA in intact cells. Individual probes that bind mRNA molecules can be visualized by fluorescence microscopy which gives a punctate pattern representing single RNA molecules in the cell. The advantage of this technique over protein staining is that the probes are designed for the specific species being investigated and therefore are more precise than using antibodies with reactivity against only known mice proteins, although we acknowledge that RNA expression does not always correspond to protein levels. We collected DRGs from three Highveld mole-rats and three Natal mole-rats and stained for *nalcn* and trpa1. In *Figure 17*, example images are shown. For every image, the number of puncta, each representing a single RNA molecule stained by the RNAscope probes was calculated. We found that *nalcn* is not overexpressed in trpa1 positive cells compared to cells negative for trpa1. The number of puncta was similar in trpa1 positive (1308.3 puncta (±54.73) per cell) and in trpa1 negative cells (1266.1 puncta (±29.46) per cell) in the Highveld mole-rat DRGs (Mann-Whitney U test, $p=0.2831$). Therefore, our hypothesis was not supported by this experiment and further work needs to be done to understand NALCN regulation of TRPA1. The overall number of puncta from *nalcn* in the whole image, normalized by the DRG area was significantly higher in Highveld mole-rat (1279.4 puncta (±26.38) per cell) than in Natal mole-rat (272.9 puncta (±16.24) per cell) (Mann-Whitney U test, $p<0.0001$), confirming the overexpression of *nalcn* in these animals and the results obtained in the RNA sequencing and qPCR experiment (*Figure 18*).

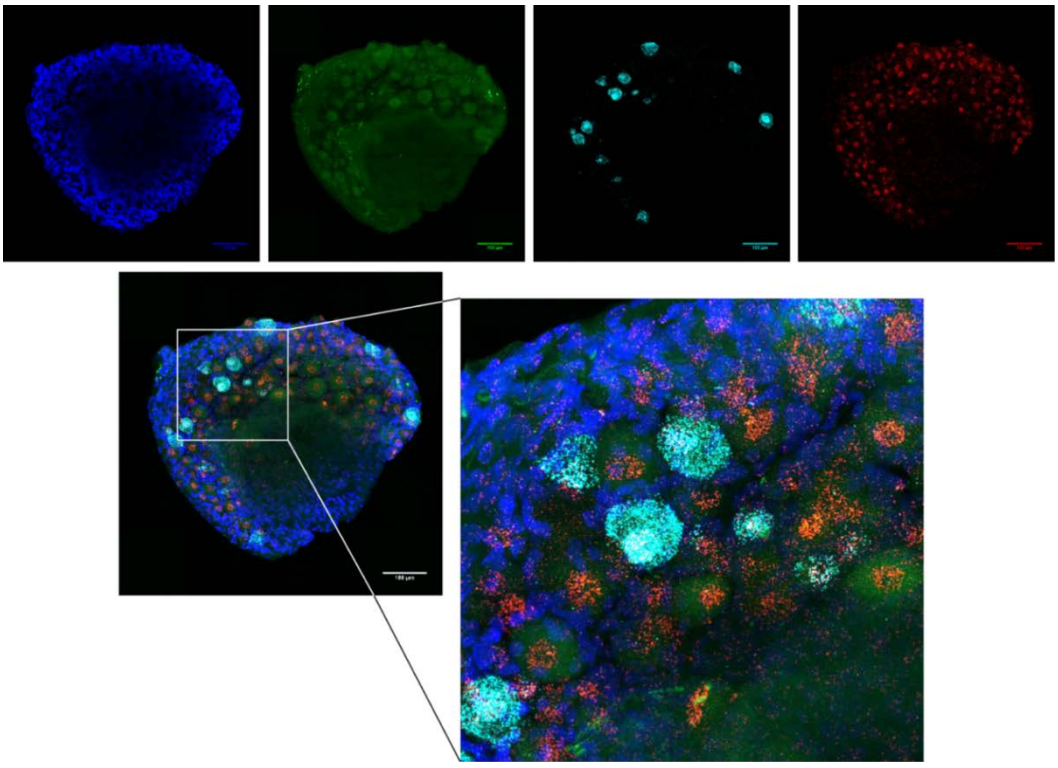

Figure 17: *RNAscope images of Highveld mole-rat DRGs. Nuclei are stained with DAPI (blue). RNA coding for NALCN is indicated in red and TRPA1 in cyan. A neuron marker NeuN is indicated in green. Each puncta indicates one RNA molecule bound to the probe.*

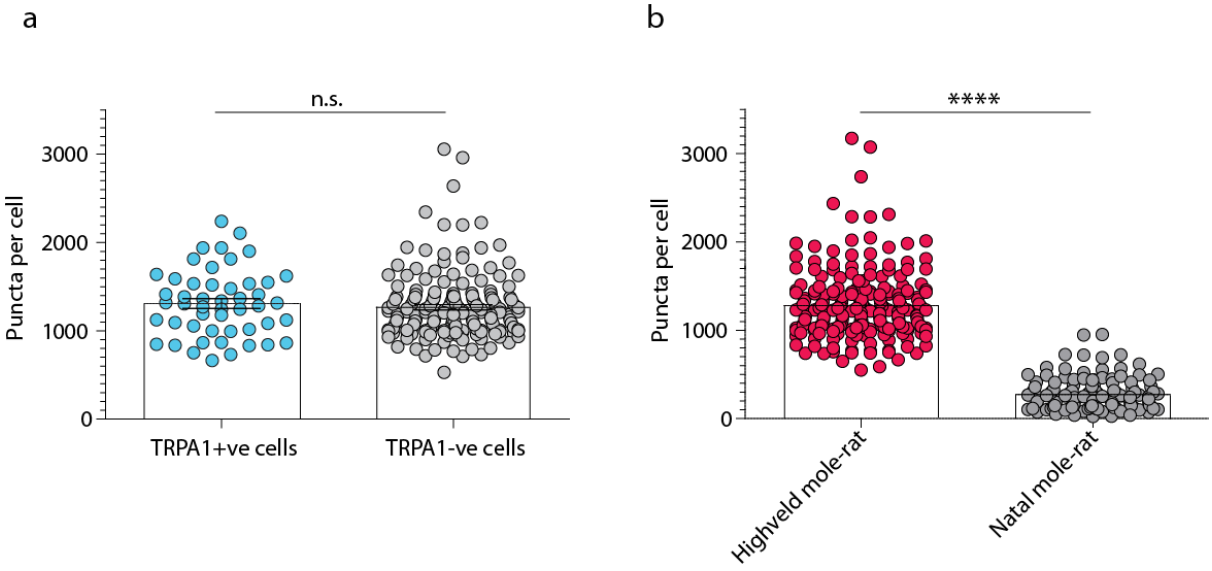

Figure 18: *Analysis of RNAscope data. The graphs show the number of puncta representing nalcn per cell. N corresponds to the number of cells analyzed from DRGs from 3 different animals. (a) The difference between TRPA1 positive and negative cells is not significant. (b) The overall nalcn expression in three Highveld mole-rats is higher than in three Natal mole-rats. Error bars are mean ± SEM (Mann Whitney U test, n.s. p>0.05; **** p≤0.0001).*

3.3.2.4. EXPRESSION AND SEQUENCE VARIATION OF PROTEINS FROM THE NALCN COMPLEX

The expression levels of *UNC79*, *UNC80* and *FAM155A* could not be retrieved from our RNA sequencing database. Differential expression of these transcripts could therefore not be calculated. However, as single amino acid transcripts were available from the RNA sequencing data, a comparative alignment of the different protein sequences of the NALCN complex from human (*Homo sapiens,* Uniprot references Q9P2D8 (UNC79), Q8N2C7 (UNC80) and B1AL88 (FAM155A)), mouse (*Mus musculus* Q0KK59, Q8BLN6 and Q8CCS2), rat (*Rattus norvegicus* D3ZSV8, D3ZXX3), guinea pig (*Cavia* porcellus H0VMV8, H0VCT4, H0VN86) and the available transcript from the tested African rodents was made. For FAM155A, The Highveld mole-rat and the East-African mole-rat sequences were aligned with the above-mentioned species. Performing pairwise alignment, a similarity percentage of 81.82% was found between Highveld mole-rat and mouse FAM155A, 88.45% between Highveld mole-rat and guinea pig and 80.06% between Highveld mole-rat and East African root rat (as a reference, the amino acid similarity between human and mouse FAM155A is 87.2%). Many unique variations were found in the Highveld mole-rat due to the lack of sequences from close-related species. It is difficult to make predictions about the effects of the variations on functionality, but we know that amino acids thought to be involved in the interaction with NALCN are conserved (K287, E290, K307, G3644) (Kang, Wu and Chen, 2020). We conclude that these calculations don't give enough information about potential significant variations for the functioning of the protein complex NALCN-FAM155A. A high similarity was found between the sequences from UNC79 and UNC80. The Highveld mole-rat UNC79 sequence was compared to the above-mentioned species as well as to all African rodents sequenced and analyzed by Dr. O. Eigenbrod. 91.17% Amino acid similarity was found between guinea pig and Highveld mole-rat UNC79, and 99.04% similarity between Natal and Highveld mole-rat. Also for UNC80 few variations were detected. Amino acid similarity between mouse and Highveld mole-rat was 93.66% and between Natal and Highveld mole-rat was 99.82% with no single unique variation in the latter one. Whether the UNC79 and UNC80 are involved in the observed insensitivity to AITC in the Highveld mole-rat cannot be concluded from these alignments. An additional

qPCR experiment could be performed in order to detect differential expression of UNC79 and UNC80 across different species.

3.3.2.5. BEHAVIORAL ANALYSIS AFTER NALCN BLOCKING IN VIVO

If overexpression of NALCN contributes to the insensitivity of the Highveld mole-rat to AITC, blocking the channel *in vivo* could reverse the phenotype and possibly recover nocifensive behavior in response to a painful sensation. A completely specific blocker for NALCN was not available, but verapamil, an L-type calcium channel blocker currently used to treat high blood pressure has been shown to block the channel (Lu *et al*., 2017). We therefore hypothesized that an intraperitoneal (i.p.) injection of verapamil (5mg/kg) could make the Highveld mole-rat newly sensitive to AITC.

Remarkably, one hour after a verapamil injection was administered, the Highveld mole-rat showed nocifensive behavior following an injection of 0.75% AITC. A significant increase in response time was observed to on average 201.1 seconds (±81.88) compared to 0.667 seconds (±0.667) before the injection (Mann-Whitney U test, p=0.0121). After 24 hours, this effect disappeared again (6.667 s (± 3.528)). The same experiment was done with Damaraland mole-rats were no significant differences in response times to an AITC injection were observed after verapamil administration (53.40 seconds (±12.08), 78.00 seconds (±17.06), 86.20 seconds (±16.26) before, 1 and 24 hours after respectively, Mann-Whitney U test, p= 0.5476 and 0.4020) (*Figure 19*).

The effect of verapamil administration on the response of Highveld mole-rats to formic acid and formalin was tested as well. Animals responded 1 hour after the verapamil administration significantly longer to an injection of formic acid in the paw (38.25 seconds (± 27.76), Mann-Whitney U test, p=0.0286). The response was still present in one animal after 24 hours which we think was caused by an inflammation of the paw (*Figure 20*). Compared to the results without verapamil (Results 3.1.3, page 54), the animals responded now to a formalin injection in the first responsive phase (pain score of 68.0 (±21.79) compared to 0.8 (±0.5831) without verapamil, Mann-Whitney U test, p=0.0325). The pain score measured in the second responsive phase was not found significantly different (pain score of 464.7 (±106) with verapamil and 498.6

(±146.8) without, Mann-Whitney U test, p=1) (*Figure 21*). These results confirmed that NALCN in an important contributor to algogen insensitivity in the Highveld mole-rat.

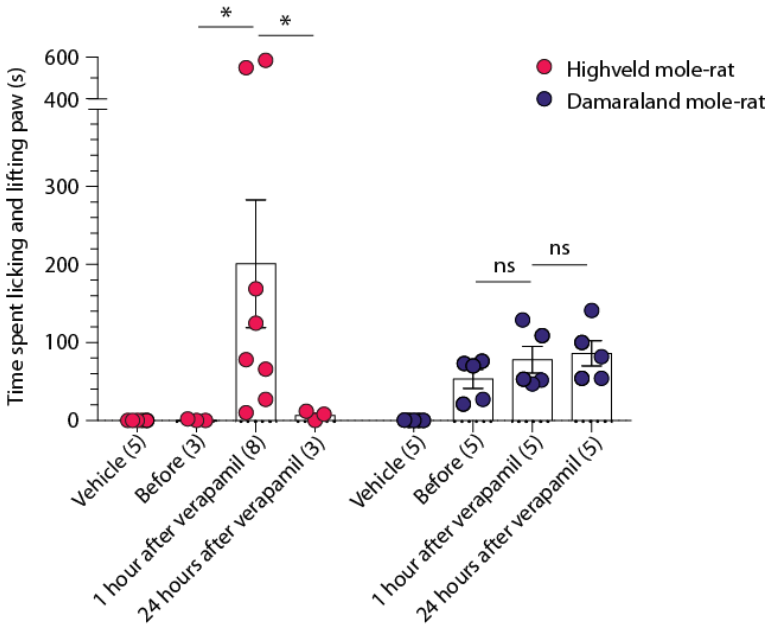

Figure 19: *Cumulative responses to an AITC injection following verapamil administration. A significant increase in cumulative response rate was observed 1 hour after verapamil injection. It disappeared 24 hours later. For the Damaraland mole-rat, no effect was observed. Error bars are mean ± SEM. Single data points indicate single animals tested and n numbers are written in parentheses (Mann-Whitney U test, * p≤0.05, n.s p>0.05). Reproduced from Eigenbrod et al., 2019.*

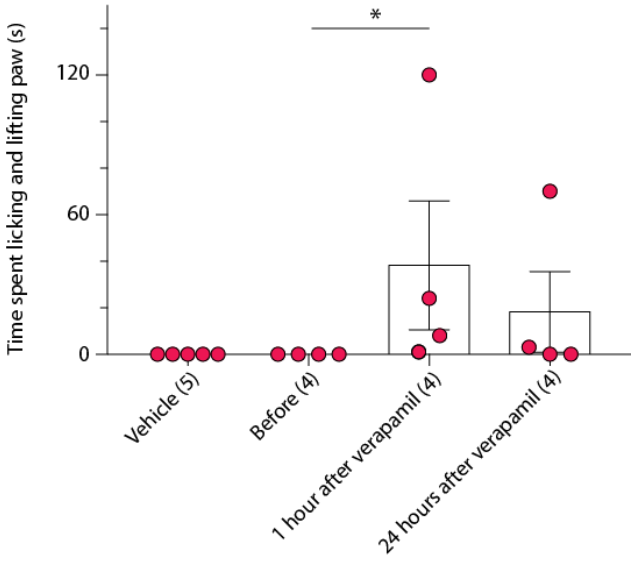

Figure 20: *Cumulative response to formic acid after verapamil administration. The Highveld mole-rats responded significantly higher than before. Error bars are mean ± SEM. Single data points indicate single animals (n in parentheses) (Mann-Whitney U test, * p≤0.05). Reproduced from Eigenbrod et al., 2019.*

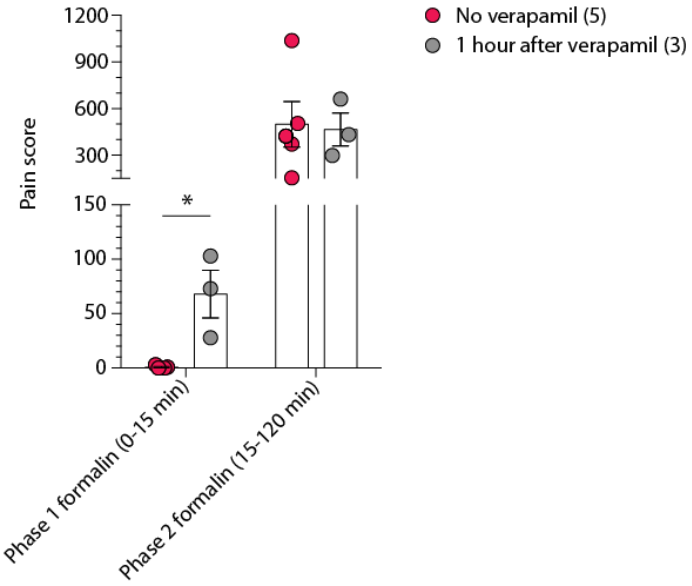

Figure 21: *Formalin test after verapamil administration. A significant increase in nocifensive behavior in phase 1 of the formalin test was observed one hour after verapamil was injected. Error bars are mean ± SEM. Single data points indicate single animals tested and n numbers are written in parentheses (Mann-Whitney U test, * p≤0.05). Reproduced from Eigenbrod et al., 2019.*

3.3.3. INVESTIGATION OF THE NATURAL ENVIRONMENT OF THE HIGHVELD MOLE-RAT

So far, the Highveld mole-rat is the only known animal that shows complete insensitivity to an AITC-mediated pain response. The lack of nocifensive behavior made us wonder why this species lost a trait highly conserved in the kingdom Animalia. We therefore investigated their natural habitat and found two potential answers – their food source and their co-habitation with poisonous ants.

3.3.3.1. EXAMINATION OF FOOD SOURCES

Highveld mole-rats, like other African mole-rats, feed on geophytes. For this reason, we collected bulbs, tubers and rhizomes found around and in their burrows and hypothesized that they might contain a TRPA1 activating algogen. Considering that the

Highveld mole-rat is insensitive to this algogen, we speculated it would gain an evolutionary advantage by broadening its food source niche.

The Small Matweed or *Guilleminea densa* was almost always abundantly present in the tunnels of the Highveld mole-rats. After an ether extraction was done as described in Methods 2.2.5 (page 47), and a diluted solution of 10%w/v was applied to HEK293 cells transfected with mTRPA1 or HvTRPA1. Using calcium imaging, a significant intracellular calcium increase was observed in mouse and Highveld mole-rat TRPA1 transfected cells when the extraction was applied to the cells compared to mock transfected cells (for values see *Table 5*, Mann-Whitney U test, $p<0.0001$ for both mTRPA1 and HvTRPA1). We concluded that the root system of the Small Matweed contains a TRPA1 activating substance. A control experiment was done with the very pungent wasabi root, known to contain AITC. Results were similar with no significant differences found between the increase in intracellular calcium caused by wasabi and small matweed and neither between mTRPA1 and HvTRPA1. For results, see *Table 5* (*Figure 22).*

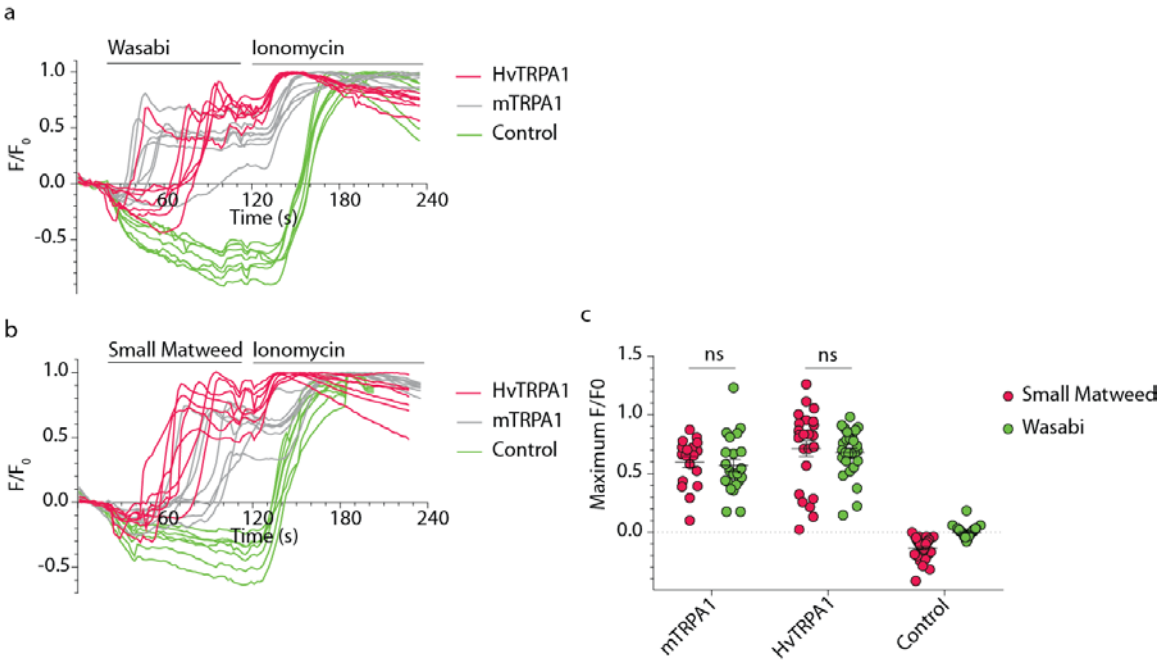

Figure 22*: Single cell calcium imaging with root extraction application. (a) Shows the response of TRPA1-transfected and mock-transfected cells to a wasabi stimulation followed by ionomycin, (b) shows the same for Small Matweed. (c) Shows that no difference could be found in a maximal response to both of the extracts. At least 20 cells were taken from three experiments per extract and transfection condition (Mann-Whitney U test, n.s. p>0.05).*

	mTRPA1	HvTRPA1	Mock
Wasabi	0.571 ±0.0528	0.680 ±0.0387	-0.001 ±0.0057
Small Matweed	0.598 ±0.0478	0.714 ±0.0683	-0.134 ±0.0151

Table 5: *Normalized maximal fluorescence calcium imaging response after the plant extract application. Mean ± SEM*

3.3.3.2. ROLE OF CO-HABITATING ANTS IN AITC INSENSITIVITY

Visiting the tunnel systems of the Highveld mole-rat frequently, our collaborator Dr. D. Hart observed another interesting phenomenon: some of the burrows seemed to be inhabited by mole-rats as well as by ants while other burrows were in close proximity to ant nests. Further investigation by the Social Insects Research Group (SIRG) from the University of Pretoria identified these ants as Natal droptail ants or *Myrmicaria natalensis*, ants known for their painful stings *(Figure 23*). The pain experience from their bites is caused by the release of a poisonous mix of limonene and several alkaloids (e.g. Mymicarin derivates) after biting (Slingsby, 2017). The insects use these compounds as a communication system as well as a protective algogen against predators (Brand *et al*., 1974; Kaib *et al*., 1990; Francke *et al*., 1995; Movassaghi *et al*. 2005). As the Highveld mole-rats are frequently seen in proximity of these ants, we hypothesize they might have adapted to the painful stings through evolution, perhaps the reason why they are insensitive to AITC and other algogens.

Figure 23: *The Natal droptail ant*

We collected the ants from the common burrow system of Highveld mole-rats and blended the abdomen containing the poisonous gland as described in Methods 2.2.6, page 47. An injection of this mixture was given to the Highveld mole-rat as well as to Mahali and Damaraland mole-rats, the latter two species were sensitive to all algogens tested. Confirming our hypothesis, we observed no response in the Highveld mole-rat (2.0 s (±1.683)) when compared to the response time after a vehicle injection (0.1 s (±0.1), Mann-Whitney U test, p=0.1209). The Mahali mole-rat (95.20 s (±50.42)) as well as the Damaraland mole-rat (208.5 s (±75.59)) both had a large response time after the mixture was injected, significantly higher than after a after a vehicle injection (0.6 s (±0.6) and 0.8 s (±0.8) for Mahali and Damaraland mole-rat respectively, Mann-Whitney U test, p=0.0476 and 0.0159). Amazingly and in line with our hypothesis about the role of NALCN, the Highveld mole-rat showed *de novo* nocifensive behavior to the mixture after a verapamil injection. The difference was statistically significant (145.0s (±58.87), Mann-Whintey U test, p= 0.0294) *(Figure 24*).

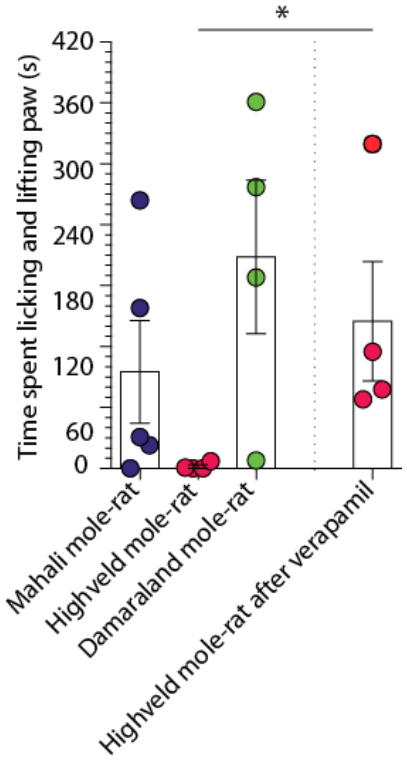

***Figure 24**: Cumulative behavioral responses to an ant mixture injection. The response of the Highveld mole-rat one hour after verapamil injection was significantly higher than before (Mann-Whitney U test, * p≤0.05). Reproduced from Eigenbrod et al., 2019.*

3.4. CAPSAICIN INSENSITIVITY IN THREE MOLE-RAT SPECIES

Three species were identified as insensitive to capsaicin, namely the naked mole-rat, the Potwe mole-rat and the Natal mole-rat (Results 3.1, page 50) (Park *et al*., 2008; Omerbašic *et al*., 2016; Eigenbrod *et al*., 2019). Park *et al*. and Omerbašic *et al*. found that the TRPV1 channel in naked mole-rats is completely functional and sensitive to capsaicin by performing *ex vivo* skin nerve experiments and *in vitro* patch clamp recordings on mouse and naked mole-rat TRPV1. Park *et al.* suggested an anatomical change in central connectivity of capsaicin-sensitive nociceptors could be the reason for the unique insensitivity. The driving force for this evolutionary change remains unknown.

3.4.1. COMPARING TRPV1 SENSITIVITY AMONG DIFFERENT SPECIES

As we know the homology of the *trpv1* gene among the African mole-rats included in the RNA sequencing database is high (Results 3.2.1, page 56), we hypothesized that the insensitivity of the Natal mole-rat is not due to a dysfunctional or hyposensitive TRPV1 channel. The Potwe mole-rat is not included in the database as behavioral data was obtained only recently.

3.4.1.1. SINGLE CELL CALCIUM IMAGING

We tested this hypothesis by performing calcium imaging in HEK293 cells transfected with either mouse TRPV1 (mTRPV1), the capsaicin-insensitive Natal mole-rat (nTRPV1) or the capsaicin-sensitive and close-related Highveld mole-rat (HvTRPV1). We identified three functional TRPV1 channels with EC_{50} values 52.4nM or $10^{-7.281}$ ($\pm 10^{0.1791}$), 49.6nM or $10^{-7.305}$ ($\pm 10^{0.1344}$) and 99.7nM or $10^{-7.001}$ ($\pm 10^{0.2201}$) for mTRPV1, nTRPV1 and HvTRPV1 respectively. The EC_{50} values were not significantly different from each other (one-way ANOVA, p=0.4629) (*Figure 25* and *Figure 26*).

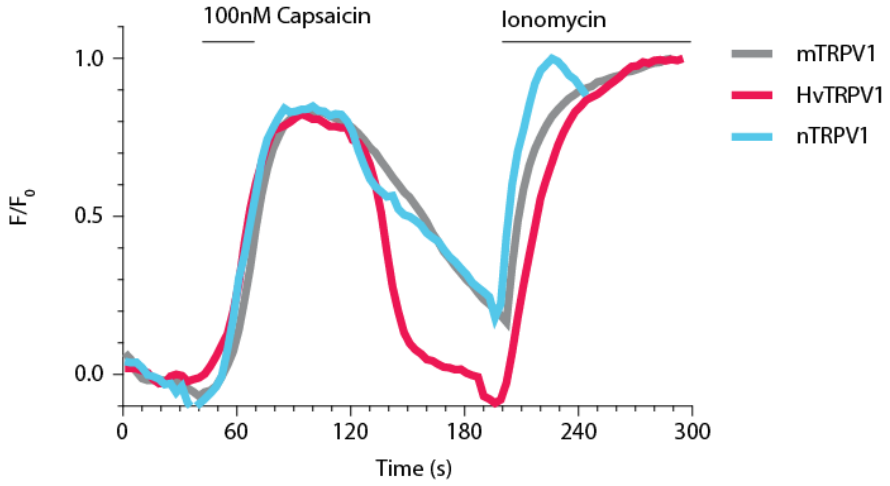

Figure 25: *Sample traces of intracellular calcium response over time in HEK293 cells transfected with TRPV1 from mouse, Highveld mole-rat and Natal mole-rat.*

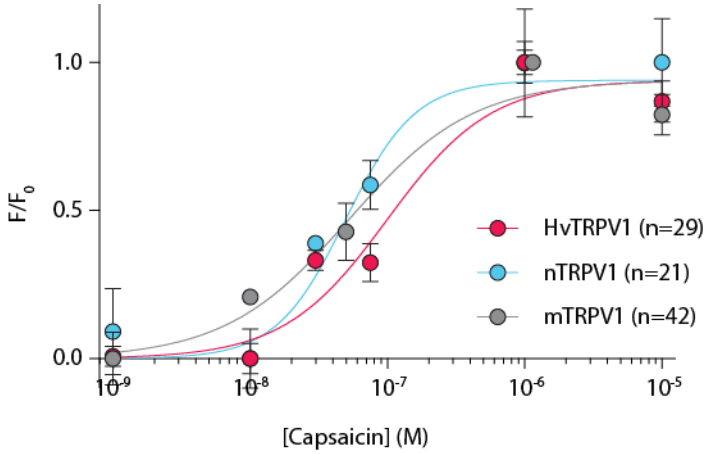

Figure 26*: EC_{50} curves of mTRPV1, nTRPV1 and HvTRPV1 to capsaicin. No significant difference was found between the EC_{50} values (unpaired t-test, n.s. p>0.05). N denotes the total number of coverslips tested. Figure published in Eigenbrod et al., 2019.*

3.4.2. TRKA SEQUENCE COMPARISON AMONG AFRICAN MOLE-RATS

Omerbašić *et al.*, 2016 showed that the naked mole-rat TrkA amino acid sequence caries a few variations in the N-terminus which are thought to contribute to the impaired function of the receptor. It is not known whether this contributes to the observed capsaicin insensitivity in the species, but with the Natal mole-rat identified with the same phenotype, we considered it necessary to look at the Natal mole-rat TrkA amino acid sequence. As done in the research thesis from Dr. Omerbašić, 2014, the TrkA amino acid sequences where compared among each other as well as to the sequences from mouse (*Mus musculus,* UniProt Entry Q3UFB7), rat (*Rattus norvegicus,* P35739), guinea pig (*Cavia porcellus,* H0V0A7), European rabbit (*Oryctolagus cuniculus,* G1SZT9), cow (*Bos taurus*, A0A3Q1MJ18), dog (*Canis lupus familiaris*, F6XBZ5), rhesus macaque (*Macaca mulatta*, F7DJ84), human (*Homo sapiens*, P04629), sperm whale (*Physeter catodon*, A0A2Y9EWI1), pig (*Sus scrofa*, F1RHK6), Cape golden mole (*Chrysochloris asiatica*, NCBI reference XP_006861670.1), Cape elephant shrew (*Elephantulus edwardii*, ncbi reference XP_006895805.1), the Tasmanian Devil (*Sarcophilus harrissii*, ncbi reference XP_003768150.1) and the Naked mole-rat (*Heterocephalus glaber,* ncbi ref XP_004871305.1). However, when aligning the sequence from the capsaicin insensitive Natal mole-rat with the other capsaicin sensitive species, no unique variation was found. All tyrosine residues known to be important for phosphorylation and autophosphorylation were conserved and therefore the function of the receptor as well as activation of downstream pathways are predicted to be intact. Also, no other variations were identified that could affect protein functionality. The TrkA amino acid similarity between mouse and Natal mole-rat was 83.85%, between naked mole-rat and Natal mole-rat was 94.94% and between Highveld and Natal mole-rat was 99.37%. Therefore, we think the TrkA protein of the Natal mole-rat is functional and probably does not contribute to the observed capsaicin insensitivity, however electrophysiological recordings with heterologous expression of TrkA with TRPV1 or other *in vitro* or *ex vivo* experiments as in Omerbašić *et al.*, 2016 could rule this out.

The TrkA amino acid sequence from the Potwe mole-rat is not available at this moment and could therefore not be aligned with the multiple species mentioned above.

4. DISCUSSION

The finding that several African rodents possess a unique insensitivity to algogens (such as capsaicin, acid and/or AITC), led us to investigate some of their unique evolutionary adaptations. The Highveld mole-rat was identified as the sole species unresponsive to an injection of AITC and displayed diminished pain behaviors to weak acids and formalin. TRPA1, a receptor activated by these algogens was found to carry amino acid variations that make the channel less sensitive to AITC activation. This mutation however, is not unique to the Highveld mole-rat and therefore it is likely that an additional adaptation contributes to the observed AITC insensitivity. RNAseq data from several African rodents led us to identify one upregulated gene in the Highveld mole-rats, *nalcn*. This gene codes for a sodium leak channel, known to contribute to setting the resting membrane potential (RMP) in neurons and an upregulation of this protein could potentially result in nociceptors that are less responsive to noxious stimuli. The contribution of this channel was evaluated *in vivo* by administration of verapamil, an NALCN blocker. Following i.p. administration of verapamil, we observed a remarkable rescue of pain responses upon injection of algogens the animal was originally insensitive to. We examined the natural habitat of the Highveld mole-rat to find evolutionary stressors leading to these adaptations. We suggest that the insensitivity of the species could be a result of food sources containing TRPA1 activating substances as well as living in close proximity with aggressive stinging ants to which the Highveld mole-rat was impervious. Additionally, three African subterranean rodents were behaviorally insensitive to acid and capsaicin: the well-known naked mole-rat, the Natal mole-rat and the Potwe mole-rat. The TRPV1 channel from the Natal mole-rat was, just like the naked mole-rat, functional and sensitive. More work is needed to dissect the mechanism behind the capsaicin insensitivity in these three mole-rat species as well as the evolutionary origins of the adaptation.

4.1. AITC INSENSITIVITY OF THE HIGHVELD MOLE-RAT

We found that the TRPA1 channel from the Highveld mole-rat had a lower sensitivity to AITC compared to the mouse channel by monitoring channel activation with calcium imaging. Patch clamp recordings revealed that an overexpression of Highveld NALCN in HEK293 cells increases their RMP and *in vivo* administration of verapamil in Highveld mole-rats rescued pain responses to all algogens tested including the ant alkaloid mixture which is thought to have contributed to the evolutionary adaptation towards AITC insensitivity. A few unanswered questions remain. During calcium imaging experiments, the functional characterization of the Highveld TRPA1 did not show an altered sensitivity when compared to the Natal TRPA1 channel. Furthermore, as NALCN was not selectively overexpressed in a subset of neurons, we could question why the Highveld mole-rat is responsive to capsaicin and acid. The results from the formalin test showed the second responsive phase is still present in Highveld mole-rats. This suggests a central sensitization is taking place without a first acute response. Additionally, the Natal mole-rat and the Highveld mole-rat diverged less than 7 mya (Eigenbrod *et al.*, 2019). An evolutionary response, happening this rapidly usually happens after an environmental change in their habitat (Turcotte, Reznick and Hare, 2011; Burke and Long, 2012). This made us wonder how and at what rate their natural habitats had changed. The following discussion will highlight the different mechanisms of AITC insensitivity with these considerations in mind.

4.1.1. MOLECULAR CHANGES IN THE *CRYPTOMYS* TRPA1

In chemical nociception, the activation of TRP channels at peripheral sensory terminals by algogens triggers neuronal firing by depolarizing the membrane to the threshold potential for action potential generation. Changes in the kinetics of the channel might therefore affect the initiation and propagation of these action potentials and subsequently inhibit nociceptive signaling. Protein sequence alignment and RNA quantification uncovered substitutions of important cysteines in the TRPA1 channel of several *Cryptomys* species that might alter the activation mechanism. A substitution of

cysteine at position 621 to an alanine has been shown to decrease the sensitivity of the channel significantly (Bahia *et al.*, 2016). Several cysteines in mouse TRPA1 have been identified to form disulfide bridges which are involved in conformational changes during activation or desensitization of the channel (Wang *et al.*, 2012). In line with these findings, the additional cysteines in the *Cryptomys* species could alter the number of disulfide bridges, which could in turn change the protein conformation and render the channel less or more sensitive to AITC activation.

Two different sets of experiments were carried out to define and compare the sensitivity of different TRPA1 proteins. Both experiments confirmed that the EC_{50} of Highveld mole-rat TRPA1 was approximately 8-10 times higher than the EC_{50} of mouse TRPA1. However, the two experiments showed contradictory results for the Natal TRPA1. Only the high-throughput screening showed a similar reduction in sensitivity as seen in the Highveld mole-rat. As the n number in this screening with FLIPR was much higher, we consider the results from this experiment to be more reliable. The further experiments with several mutated constructs confirmed the influence of the important cysteine in position 621 on the sensitivity. The Natal TRPA1 also possesses this mutation thus confirming the lower sensitivity result. But as only the Highveld mole-rat lacks a behavioral response upon AITC injection, the mutation at C621 fails to explain the complete AITC insensitivity in the Highveld mole-rat. An additional mutation H1068N found in the Highveld mole-rat was not investigated as both the location (the C-terminus) and the similarity of the amino acids (both positively charged) did not suggest a major impact on channel functionality. However, for a more complete investigation, calcium imaging experiments and electrophysiological recordings would be required. Besides, the question remains as to why all *Cryptomys* species have acquired this amino acid variation that seems to impact the sensitivity of the channel without demonstrating a phenotype similar to the Highveld mole-rats. Potentially the different species are subjected to a similar ecological pressure rendering them less sensitive to cysteine-binding TRPA1 agonists; only in the Highveld mole-rat did an additional mechanism cause complete AITC insensitivity.

4.1.2. CONTRIBUTION OF OVEREXPRESSED NALCN TO PERIPHERAL SENSITIVITY

Because the mutation in TRPA1 failed to explain insensitivity to AITC in Highveld mole-rats, we turned to a comparison of other differentially regulated genes within the African mole-rat family. The only overexpressed gene in the Highveld mole-rat was *nalcn*, which codes for a protein we confirmed increases the membrane potential in a heterologous system. Overexpression of *nalcn* mRNA was observed in the CNS and PNS, the heart and the pancreas. *In vitro* studies have shown that neurons from *nalcn* knock-out mice are hyperpolarized and overexpression of NALCN depolarizes neurons, providing evidence for its contribution in setting the RMP (Lu *et al.*, 2007). In mice, the channel was shown to be important in the regulation of respiratory rhythm (Lu *et al.*, 2007), osmoregulation (Sinke *et al.*, 2011) and intestinal pacemaker activity (Kim *et al.*, 2012). We hypothesized that the overexpression seen in the Highveld mole-rat might contribute to the observed behavioral insensitivity by depolarizing the neuron and bringing voltage-sensitive channels such as NaV1.7 to an inactivated state and therefore rendering sensory neurons less excitable.

RNA sequencing of several Highveld mole-rat tissues revealed an overexpression of NALCN in peripheral and central sensory tissue as well as in other tissues such as the heart. The question arises whether this impairs the respiratory system, heart rhythm and other vital functions of the animals. Further investigation would be necessary to identify effects on other organs as well as potential compensatory mechanisms.

That the combination of a less sensitive TRPA1 and an overexpression of NALCN is necessary for a complete absence of AITC sensitivity was supported by the fact that Highveld mole-rats still show nocifensive behavior after an injection with capsaicin or HCl. However, the response to capsaicin is lower than in the closely-related *Cryptomys* species when we compare the cumulative responses (*Table 6)*. This could be explained by the overexpression of NALCN which makes it more difficult to trigger action potentials after TRPV1 activation. The behavior after an acid injection is similar in all four animals, potentially because protons have many target receptors in nociceptors.

	Highveld - AITC	**Highveld - Capsaicin**	**Highveld - Acid**
Common	*** (lower) p=0.003	** (lower) p=0.0025	n.s. p=0.1949
Mahali	*** (lower) p=0.001	* (lower) p=0.0145	n.s. p=0.6363
Natal	****(lower) p<0.0001	** (Higher- Natal insensitive) p=0.0027	n.s. p=0.3421

Table 6: *Differences in cumulative responses between Highveld mole-rats and other Cryptomys species to AITC, capsaicin and acid. Mann-Whitney U test, n.s. when p>0.05; *p≤0.05, **p≤0.01 ***p≤0.001, ****p≤0.0001*

If an abundance of NALCN channels causes the neurons to be more depolarized, we hypothesized that blocking the channel, might return the membrane potential to a level were voltage-sensitive channels are functional. Our approach to block the channel, was to use verapamil in vivo, as it was identified as an NALCN inhibitor (Lu *et al.*, 2007). Using this pharmacological approach, we anticipated a reversal of the effect caused by the overexpression in the Highveld mole-rat. Since 1962, verapamil is a commonly used drug in humans with heart rhythm problems, chest pain or hypertension (Singh, Ellrodt and Peter, 1978). As an L-type calcium channel blocker, it inhibits calcium from entering the cells of vascular smooth muscles and myocardium and therefore diminishes the likelihood of action potentials being generated and propagated. In this way it delays heart rhythm, reduces contraction force of the myocardium and relaxes coronary arteries and peripheral vessels (Norris and Bradford, 1985; Fahie and Cassagnol, 2020). At higher concentrations, verapamil is also known to block Na+ channels (Norris and Bradford, 1985). When overdosing verapamil in humans, hypotension, myocardial depression and disturbances in cardiac conduction can be lethal (Barrow, Houston and Wong, 1994). In therapeutic doses, the drug is known to be safe and with few side effects. However, rare adverse symptoms such as joint and muscle pain have been reported by people who receive verapamil either via injection or orally. The mechanism behind this is not reported, but it is in line with our finding that it increases sensitivity to noxious stimuli. The effect of verapamil on pain perception in rats has been tested by several investigators. Kumar, Mehra and Ray, 2010 showed an increased first and second phase of the formalin response in rats when given an L-type calcium channel blocker including verapamil, while others reported nociceptive effects as a result of the potentiation of opioid receptor agonists such as morphine (Bongianni *et al.*, 1986;

Tamaddonfard *et al.*, 2014; Feliks and Wrońska, 2017). The mechanism of this potentiation remains unknown, but is thought to be a peripheral mechanism as the administration of naloxone-methiodide (an opioid antagonist that does not cross the blood-brain barrier) abolished the affect (Shimizu *et al.*, 2004). An anti-nociceptive effect of verapamil alone was observed in sheep undergoing duodenal distension, a model for visceral pain (Kania, Brytan and Tomaszewska, 2009).

A single systemic dose of verapamil in the Highveld mole-rat caused a complete reversal of the Highveld mole-rats' pain response to AITC and other algogens. The animal responded substantially by lifting and licking its injected paw as opposed to being unresponsive to these algogen injections without verapamil administration. Effects on other vital organs, such as heart rate and respiratory rhythm were not tested, but animals displayed no major side effects and were healthy after the experiment.

4.1.2.1. THE NALCN COMPLEX

As mentioned above, no amino acid variations that indicated an altered function of the NALCN complex proteins were identified when making an interspecies alignment of UNC79, UNC80 and FAM155A. Gene expression comparison from the RNA sequencing data could only be done when sufficient mRNA levels from the gene of interest were detected in all species. A comparison of the expression levels of *UNC79, UNC80* or *FAM155A* between the different African mole-rats could not be made as the RNAseq data did not find enough transcript levels of these genes in the sensory tissue or the other tissue including heart, liver and adipose tissue in one or more species. Therefore, a quantitative PCR could verify these results. A selective overexpression of one of the proteins in specific neurons from the Highveld mole-rat could explain a selective insensitivity to certain substances, a hypothesis that could be validated by performing RNAscope on DRG sections.

4.1.3. BEHAVIORAL INSENSITIVITIES RELATED TO TRPA1

In addition to AITC-insensitivity in the Highveld mole-rat, we found other unique behavioral insensitivities to formic acid, citric acid, ant alkaloids and the first responsive phase following a formalin injection. The behavioral insensitivities to these different compounds have one thing in common: they all activate TRPA1. While AITC activates TRPA1 through covalent modification of intracellular cysteines (Macpherson, Dubin, *et al.*, 2007), the activation by intracellular acidification is thought to be mechanistically different, however the exact mechanism remains unknown (Wang *et al.*, 2011). Moreover, formalin has similarly been shown to directly activate TRPA1 in humans and rodents (McNamara *et al.*, 2007). Whilst neurons from TRPA1 knock-out mice are unresponsive to formalin, pain responses during the formalin test are reduced in both phases, but were not absent (McNamara *et al.*, 2007). This means TRPA1 is involved in the formalin response, but is not the only receptor responsible for formalin-driven nocifensive behavior.

These findings strongly suggested that the TRPA1 channel in Highveld mole-rats is structurally or functionally unique compared to other species. Possibly the overexpression of NALCN contributes to the complete absence of the first phase of nocifensive behavior in the formalin test. However, the presence of the second responsive phase in the behavior of the Highveld mole-rat without this initial phase is unusual. It is generally thought that the direct activation of C-fibers in the first responsive phase of the formalin test produces central sensitization causing the second responsive phase (Dickenson and Sullivan, 1987; Lebrun, Manil and Colin, 2000). This hypothesis is based on observed effects such as hyperalgesia and allodynia in rats outside of the injection site. Electrical recordings on rat nociceptors revealed that in the second phase Aδ- and C-fibers around and outside of the injection site are still firing at low levels (McCall, Tanner and Levine, 1996; Puig and Sorkin, 1996). However, lidocaine was found to block phase two activity, indicating ongoing nociceptor activity during phase two is more involved than is generally thought (Puig and Sorkin, 1996). Observing a clear nocifensive behavior in the Highveld mole-rat during the second phase indicates that certain pain circuits where activated. We speculate that formalin in Highveld mole-rats causes a local inflammation or damage of nociceptive fibers leading either directly and/or

through central sensitization to a second, more persistent responsive phase during the formalin test.

4.1.4. RAPID MOLECULAR EVOLUTION

A species' survival can be challenged by drastic environmental changes requiring rapid adaptation. Therefore, rapid evolution is hypothesized to be driven by rapid ecological and geographical change (Thompson, 1998; Hairston *et al.*, 2005). For this to happen, there are two requirements: (1) the degree of the divergence from the ancestor is correlated with the degree of environmental difference and (2) there is a positive relationship between the acquired trait and the change the animal undergoes (Losos, Warheit and Schoener, 1997). This means that a rapid and drastic change in environment can cause an accelerated and specific change in phenotype. For example, it was found that when lizards were moved from their habitat to another with a very different vegetation or other competitive lizard species, the animals' legs and toepads grew over the course of just 20 generations thanks to their 'phenotypic plasticity' (Losos, Warheit and Schoener, 1997; Stuart *et al.*, 2014). In the case of bats, it was found that vampire bats (*Desmotontinae*) have an accelerated evolutionary rate of mutational changes when compared to other subfamilies of the leaf-nosed bat family (*Phylostomidae*). It was suggested this is due to their very specific shift towards feeding on blood which needed a drastic change in metabolism and predation strategies (Botero-Castro *et al.*, 2018). Evidence also shows that evolution occurs more rapidly when interspecies competition dynamics are weakened, meaning that species' co-existence would be promoted by the adaptive change (Turcotte, Reznick and Hare, 2011; Kopp and Matuszewski, 2014; Hart, Turcotte and Levine, 2019).

On a molecular level, the frequency at which a DNA mutation is fixed (shared by most individuals of a population) can be measured. However, these calculations can be complicated by many factors, such as generation times, location of the genome in the cell, species, type of genetic adaptation, etc. (Cordero and Janzen, 2013). This makes it especially difficult to speculate about a standard molecular evolutionary rate and therefore the evolutionary rate of genetic or phenotypic adaptations always needs to be put in perspective of similar animals or adaptations.

4.1.4.1. RAPID EVOLUTION IN MAMMALS

Looking at mutational rates across mammals, we see a wide variation (Kumar and Subramanian, 2002). For example, mutation rates in primates are lower than in rodents (Gu and Li, 1992). And within the primate order, humans have the slowest mutation rate per generation (Besenbacher *et al.*, 2019). The time of divergence between mouse and rat is approximately 33 mya, but it is unclear at which rate the speciation process took place (Nei, Xu and Glazko, 2001). Within the *Cryptomys* species of the African mole-rat family, only recently a distinction was made between the subspecies Highveld mole-rat, Natal mole-rat, Common mole-rat and Mahali mole-rat (Faulkes *et al.*, 2004). Besides the fact they are optically and behaviorally very similar, they have short divergence times between them. The AITC-insensitive Highveld and sensitive Natal mole-rat diverged less than 7 mya, meaning the speciation process happened within this short timeframe. For the Highveld mole-rats, poisonous stinging ants might have been a stressor that contributed to this rapid adaptation towards AITC insensitivity. So far we observed that the Natal mole-rat does not burrow in areas with (many of) these ants. To promote survival of the Highveld mole-rat (and/or Natal droptail ant), an adaptation of TRPA1 activation and NALCN overexpression might have been beneficial.

4.1.4.2. THE SMALL MATWEED

The Small Matweed is a plant from the *Amaranthaceae* family. It grows in the Central and North America, eastern Australia and southern Africa such as Zimbabwe and the eastern part of South-Africa (Bromilow, 2001). We know this area overlaps with the burrows of many of the *Cryptomys* and *Fukomys* species found in southern Africa but not with the *Georychus* or *Bathyergus* species. Other than the *Brassicaceae* family (including wasabi and horseradish plants), which is known to produce TRPA1-activating substances (Ramirez *et al.*, 2020), it is not known for its algogen production. Phytochemical studies have shown some plants of the *Amaranthaceae* contain alkaloids that have rather analgesic effects (Ashok Kumar *et al.*, 2010), but no substance has previously been described in the Small Matweed with direct effect on nociceptive

receptors. However, after performing our calcium-imaging experiments with extracts from the plant on TRPA1 expressing HEK293 cells (3.3.3.1, page 71), we believe that a TRPA1-activating substance is present in the roots of the plant. However, we do not know the molecular nature of such an AITC like substance.

Capsaicin, the TRPV1-activating substance native to chili plants, was identified as the presumed driver for the evolutionary altered sensitivity of avian TRPV1 channels. A single mutation on amino acid position 578 (S4-S5 Helix) of the receptor was recently identified to account for the lower TRPV1 sensitivity and therefore the behavioral insensitivity of the bird towards capsaicin and chili plants (Chu, Cohen and Chuang, 2020). This evolution of the avian lineage allows birds to disperse the seeds of the plant and widens the niche of food sources, an evolutionary advantage for both the bird and plant (Borges, 2001, 2009). The cysteine changes observed in the four *Cryptomys* species are unique. So far no other animals were identified with similar amino acid changes. An abundance of the Small Matweed in their natural habitats might have contributed the evolution of a less sensitive TRPA1 channel to enable them to eat the roots of the plant. Although we do not know what the precise diet of these animals encompasses, having inspected the burrow areas of the Highveld mole-rats, we observed the plant is the most abundant and often exclusive plant growing where they live. We therefore speculate that the Highveld mole-rat consumes the Small Matweed as its main food sources and therefore benefited from an additional adaptation that made its consumption possible.

4.2. CAPSAICIN INSENSITIVITY IN SEVERAL AFRICAN MOLE-RATS AND THE NAKED MOLE-RAT

Behavioral testing of the different African rodents revealed a lack of nocifensive behavior to capsaicin in three species. Besides the known naked mole-rat (Park *et al.*, 2008), the Natal mole-rat and the Potwe mole-rat showed no paw flicking/licking after a capsaicin injection. The TRPV1 channel from naked mole-rats was found to be functional and sensitive to capsaicin and it can activate C-fibers. A previous study found a lack of neuropeptides Substance P and GCRP in C-fibers from naked mole-rats (Park *et al.*, 2008). An intrathecal infusion of Substance P could “rescue” the capsaicin evoked

response. However, mice lacking these neuropeptide are known to have a reduced behavior to noxious stimuli, but not absent (Cao *et al.*, 1998; Salmon *et al.*, 2001). Additionally, in naked mole-rats, the nociceptors connect not only to superficial dorsal horn neurons as in mice but also to deeper layers. Therefore the researchers suggested that superficial layers of the dorsal horn are insufficiently activated to result in a pain experience or hyperalgesia (Park *et al.*, 2008; Smith, Park and Lewin, 2020).

In order to investigate the insensitivity of the Natal mole-rat, sensory tissue was collected to include in our RNA sequencing database. We hypothesized that the capsaicin insensitive species might have specific and unique genetic changes in common that explain the behavioral adaptation. After analysis, we investigated key proteins connected to capsaicin nociception (such as TRPV1) as well as differential expression in the insensitive species compared to sensitive ones. We found the amino acid sequence of TRPV1 was conserved with no apparent changes important for the channel functionality (Eigenbrod, 2018). One gene was found to be downregulated in the Natal mole-rat sensory tissue as well as in the naked mole-rats, BMPER. BMPER or 'BMP (Bone morphogenetic protein) endothelial cell precursor-derived regulator' is a protein regulating the differentiation of osteoblasts. The transcript levels of *BMPER* mRNA are found to be downregulated in mice endothelial cells *in vitro* and retina cells *in vivo* under hypoxic conditions (Moreno-Miralles *et al.*, 2011). The mole-rats are known to live in burrows with very low oxygen levels and it would be interesting to investigate the effect of these conditions on the RNA and protein expression levels of BMPER. We hypothesize subjecting Natal mole-rat cells to a hypoxic environment will decrease transcript levels. However, it is unclear how this protein could contribute to capsaicin insensitivity. Further experiments with a downregulation of *BMPER* in neurons would be required to examine its potential role in nociception.

To compare functionality and sensitivity of the TRPV1 channel we performed calcium imaging in HEK293 cells. These experiments helped demonstrate that the TRPV1 channel from the Natal mole-rat is also activated by capsaicin. The sensitivity of the channel is similar to that of the mouse TRPV1 and closely-related Highveld mole-rat TRPV1. This confirms that the insensitivity of the Natal mole-rat, just like the naked mole-rat is most likely not caused by impaired function of TRPV1 and further investigation into an evolutionary adaptive mechanism is necessary.

Another receptor worth examining is TrkA. After activation by NGF, the protein auto-phosphorylates at important tyrosine residues which makes it able to sensitize TRPV1 and cause thermal hyperalgesia in mice and rats (Lewin, Ritter and Mendell, 1993; Hirose, Kuroda and Murata, 2016). It was found that the naked mole-rat has a hypofunctional TrkA caused by mutation(s) near the phosphorylation site. As a consequence, TRPV1 sensitization is absent and the naked mole-rat does not experience thermal hyperalgesia (Omerbašić *et al.*, 2016). The Natal mole-rats do not have the same mutation in the kinase domain and multiple sequence alignment of Natal TrkA with a variety of species does not suggest an impaired function. Additionally the TRPV1 channel, also required for heat hyperalgesia, is functional in the Natal mole-rat. Therefore, we expect there is no absence of heat hyperalgesia in the Natal mole-rat as in the naked mole-rat. However, electrophysiological analysis of heterologous expressed TrkA together with TRPV1 and behavioral experiments could give us more information on this.

The Potwe mole-rat tissue was not included in the RNA sequencing database as the behavioral data was only collected after the database was established. The species, officially not named yet, is thought to be a close relative to the naked mole-rat based on geographical location and (intra-generic) phylogenetic studies (Faulkes *et al.*, 2011). The animal is part of the *Heliophobius* genus, which are found in a large area spanning over Kenya, Tanzania, the eastern part of the Democratic Republic of Congo, Zambia, Malawi and Mozambique. This area is right in between the natural habitat of the naked mole-rat (more to the north, in the Horn of Africa) and the Southern Africa living *Bathyergus* and *Georychus* species. Phylogenetic data of the African mole-rats and the naked mole-rats, showed that the *Heliophobius* genus is the oldest one from the *Bathyergidae* and it diverged 34 mya (±28-39) from the naked mole-rats (Kumar *et al.*, 2017). Analysis of mitochondrial DNA from 62 collected *Heliophobius* species revealed the genus can be divided into five clades with a clear geographical division (Faulkes *et al.*, 2011). DNA analysis of the tested Potwe mole-rats by the Faulkes group showed that the animals showed 99.58% similarity with Clade 2b, the second oldest clade of the *Heliophobius* genus. The animals were named Potwe mole-rat, referring to the location they were captured, a small town in the Usambara Mountains of Tanzania. Interestingly, it exhibits acid insensitivity, just like the naked mole-rat and thus it would be very valuable to analyze RNA sequences and expression levels. In this way, we might be able to narrow

down the number of interesting proteins in light of the acid insensitivity phenotype and amino acid sequences of key proteins could be evaluated.

Another way of investigating the capsaicin-induced nociceptive pathway in different mole-rats is to look at central activation of immediate early genes (IEGs), genes that are known to be activated by neuronal activity (Hunt, Pini and Evan, 1987). An animal could be injected with capsaicin in one paw and a vehicle in the other after which the whole body could be perfused to collect the spinal cord. Using RNAscope, IEGs such as *cFos* and *Arc* could be visualized and could indicate whether a neuronal signal reached the central nervous system after capsaicin injection. Such experiments were planned, but the pandemic situation (2020) has prevented access to specimens to carry out a full study.

4.3. CONCLUSION

In this thesis I have gathered evidence for the molecular adaptations in the Highveld mole-rat in the light of its AITC insensitivity. An amino acid variation in TRPA1 and a change in the expression level of NALCN suppress nociceptive signaling caused by several chemicals including AITC. We identified pungent food sources and cohabiting poisonous ants as two ecological factors that might have driven the divergence of this phenotype. In the light of the capsaicin insensitivity of the naked mole-rat, the Natal mole-rat and the Potwe mole-rat, more research is needed to unravel this phenomenon.

The findings of this work show that identifying diversity in non-model organisms can provide a great insight in the molecular mechanisms and evolution of chemical nociception. Elucidating these evolutionary processes is not only relevant in the characterization of individual proteins or phenotypes; it also provides a new perspective for pain research and the development of novel analgesics for humans.

5. REFERENCES

Abbott, F. V., Franklin, K. B. J. and Westbrook, R. F. (1995) 'The formalin test: scoring properties of the first and second phases of the pain response in rats', *Pain*. No longer published by Elsevier, 60(1), pp. 91–102. doi: 10.1016/0304-3959(94)00095-V.

Abdo, H. *et al.* (2019) 'Specialized cutaneous schwann cells initiate pain sensation', *Science*. American Association for the Advancement of Science, 365(6454), pp. 695–699. doi: 10.1126/science.aax6452.

Akbarzadeh, A. *et al.* (2007) 'Induction of diabetes by Streptozotocin in rats', *Indian Journal of Clinical Biochemistry*. Indian J Clin Biochem, 22(2), pp. 60–64. doi: 10.1007/BF02913315.

Al-Sayed, M. D. *et al.* (2013) 'Mutations in NALCN cause an autosomal-recessive syndrome with severe hypotonia, speech impairment, and cognitive delay', *American Journal of Human Genetics*. Elsevier, 93(4), pp. 721–726. doi: 10.1016/j.ajhg.2013.08.001.

Almaraz, L. *et al.* (2014) 'TRPM8', *Handbook of Experimental Pharmacology*. Springer New York LLC, 222, pp. 547–579. doi: 10.1007/978-3-642-54215-2_22.

Alpizar, Y. A. *et al.* (2014) 'Allyl isothiocyanate sensitizes TRPV1 to heat stimulation', *Pflugers Archiv European Journal of Physiology*, 566(3), pp. 507–515. doi: 10.1007/s00424-013-1334-9.

Andersson, D. A. *et al.* (2008) 'Transient Receptor Potential A1 Is a Sensory Receptor for Multiple Products of Oxidative Stress', *The Journal of Neuroscience*, 28(10), pp. 2485 LP – 2494. doi: 10.1523/JNEUROSCI.5369-07.2008.

Andersson, D. A., Chase, H. W. N. and Bevan, S. (2004) 'TRPM8 activation by menthol, icilin, and cold is differentially modulated by intracellular pH', *Journal of Neuroscience*. Society for Neuroscience, 24(23), pp. 5364–5369. doi: 10.1523/JNEUROSCI.0890-04.2004.

Andrè, E. *et al.* (2008) 'Cigarette smoke–induced neurogenic inflammation is mediated by α,β-unsaturated aldehydes and the TRPA1 receptor in rodents', *Journal of Clinical Investigation*. doi: 10.1172/JCI34886.

Arenas, O. M. *et al.* (2017) 'Activation of planarian TRPA1 by reactive oxygen species reveals a conserved mechanism for animal nociception', *Nature Neuroscience*. 2017/12/01, 20(12), pp. 1686–1693. doi: 10.1038/s41593-017-0005-0.

Ashok Kumar, B. S. *et al.* (2010) 'Pain management in mice using methanol extracts of three plants belongs to family Amaranthaceae', *Asian Pacific Journal of Tropical Medicine*. No longer published by Elsevier, 3(7), pp. 527–530. doi: 10.1016/S1995-7645(10)60127-7.

Bahia, P. K. *et al.* (2016) 'The exceptionally high reactivity of Cys 621 is critical for electrophilic activation of the sensory nerve ion channel TRPA1', *J Gen Physiol*. 2016/06/01, 147(6), pp. 451–465. doi: 10.1085/jgp.201611581.

Baliki, M. N. and Apkarian, A. V. (2015) 'Nociception, Pain, Negative Moods, and Behavior Selection', *Neuron*. Cell Press, pp. 474–491. doi: 10.1016/j.neuron.2015.06.005.

Bandell, M. *et al.* (2004) 'Noxious cold ion channel TRPA1 is activated by pungent compounds

and bradykinin', *Neuron*. Cell Press, 41(6), pp. 849–857. doi: 10.1016/S0896-6273(04)00150-3.

Bang, S. *et al.* (2007) 'Transient receptor potential A1 mediates acetaldehyde-evoked pain sensation', *European Journal of Neuroscience*. John Wiley & Sons, Ltd, 26(9), pp. 2516–2523. doi: 10.1111/j.1460-9568.2007.05882.x.

Barik, A. *et al.* (2018) 'A Brainstem-Spinal Circuit Controlling Nocifensive Behavior', *Neuron*. Cell Press, 100(6), pp. 1491-1503.e3. doi: 10.1016/j.neuron.2018.10.037.

Barrow, P. M., Houston, P. L. and Wong, D. T. (1994) *Overdose of sustained-release verapamil*, *British Journal of Anaesthesia*. doi: 10.1093/bja/72.3.361.

Basbaum, A. I. (1999) 'Distinct neurochemical features of acute and persistent pain', *Proceedings of the National Academy of Sciences of the United States of America*. National Academy of Sciences, 96(14), pp. 7739–7743. doi: 10.1073/pnas.96.14.7739.

Basbaum, A. I. *et al.* (2009) 'Cellular and molecular mechanisms of pain', *Cell*. 2009/10/20, 139(2), pp. 267–284. doi: 10.1016/j.cell.2009.09.028.

Bautista, D. M. *et al.* (2005) 'Pungent products from garlic activate the sensory ion channel TRPA1', *Proceedings of the National Academy of Sciences of the United States of America*, 102(34), pp. 12248 LP – 12252. doi: 10.1073/pnas.0505356102.

Bautista, D. M. *et al.* (2006) 'TRPA1 Mediates the Inflammatory Actions of Environmental Irritants and Proalgesic Agents', *Cell*. Cell Press, 124(6), pp. 1269–1282. doi: 10.1016/J.CELL.2006.02.023.

Bautista, D. M. *et al.* (2007) 'The menthol receptor TRPM8 is the principal detector of environmental cold', *Nature*. Nature Publishing Group, 448(7150), pp. 204–208. doi: 10.1038/nature05910.

Belrose, J. C. and Jackson, M. F. (2018) 'TRPM2: a candidate therapeutic target for treating neurological diseases', *Acta Pharmacologica Sinica*, 39, pp. 722–732. doi: 10.1038/aps.2018.31.

Bennett, D. L. H. and Woods, C. G. (2014) 'Painful and painless channelopathies', *The Lancet Neurology*. Lancet Publishing Group, pp. 587–599. doi: 10.1016/S1474-4422(14)70024-9.

Bennett, G. J. and Xie, Y. K. (1988) 'A peripheral mononeuropathy in rat that produces disorders of pain sensation like those seen in man', *Pain*. Pain, 33(1), pp. 87–107. doi: 10.1016/0304-3959(88)90209-6.

Bennett, N. C. and Faulkes, C. G. (2000) *African mole-rats : ecology and eusociality*. Cambridge University Press.

Besenbacher, S. *et al.* (2019) 'Direct estimation of mutations in great apes reconciles phylogenetic dating', *Nature Ecology and Evolution*. Nature Publishing Group, 3(2), pp. 286–292. doi: 10.1038/s41559-018-0778-x.

Bessac, B. F. *et al.* (2008) 'TRPA1 is a major oxidant sensor in murine airway sensory neurons', *The Journal of Clinical Investigation*. The American Society for Clinical Investigation, 118(5), pp. 1899–1910. doi: 10.1172/JCI34192.

Bessou, P. and Perl, E. R. (1969) 'Response of cutaneous sensory units with unmyelinated

fibers to noxious stimuli.', *Journal of neurophysiology*, 32(6), pp. 1025–43. doi: 10.1152/jn.1969.32.6.1025.

Bishop, T. *et al.* (2007) 'Characterisation of ultraviolet-B-induced inflammation as a model of hyperalgesia in the rat', *Pain*. Pain, 131(1–2), pp. 70–82. doi: 10.1016/j.pain.2006.12.014.

Blair, N. T. *et al.* (2019) 'Transient Receptor Potential channels (version 2019.4) in the IUPHAR/BPS Guide to Pharmacology Database', *IUPHAR/BPS Guide to Pharmacology CITE*, 2019(4). doi: 10.2218/gtopdb/f78/2019.4.

Bongianni, F. *et al.* (1986) 'Calcium channel inhibitors suppress the morphine-withdrawal syndrome in rats', *British Journal of Pharmacology*. Br J Pharmacol, 88(3), pp. 561–567. doi: 10.1111/j.1476-5381.1986.tb10236.x.

Borges, R. M. (2001) 'Why are chillies pungent?', *Journal of Biosciences*. Indian Academy of Sciences, pp. 289–291. doi: 10.1007/BF02703736.

Borges, R. M. (2009) 'Of pungency, pain, and naked mole rats: chili peppers revisited', *J Biosci*, 34(3), pp. 349–351. Available at: https://www.ncbi.nlm.nih.gov/pubmed/19805895.

Botero-Castro, F. *et al.* (2018) 'In cold blood: Compositional bias and positive selection drive the high evolutionary rate of vampire bats mitochondrial genomes', *Genome Biology and Evolution*. Oxford University Press, 10(9), pp. 2218–2239. doi: 10.1093/gbe/evy120.

Boukalova, S. *et al.* (2014) 'Gain-of-Function Mutations in the Transient Receptor Potential Channels TRPV1 and TRPA1: How Painful?', *Physiol. Res*, 63, pp. 205–213. Available at: www.biomed.cas.cz/physiolres (Accessed: 27 February 2020).

Bradman, M. J. G. *et al.* (2015) 'Practical mechanical threshold estimation in rodents using von Frey hairs/Semmes–Weinstein monofilaments: Towards a rational method', *Journal of Neuroscience Methods*, 255, pp. 92–103.

Bramswig, N. C. *et al.* (2018) 'Genetic variants in components of the NALCN–UNC80–UNC79 ion channel complex cause a broad clinical phenotype (NALCN channelopathies)', *Human Genetics*. Springer Verlag, 137(9), pp. 753–768. doi: 10.1007/s00439-018-1929-5.

Brauchi, S. *et al.* (2006) 'A hot-sensing cold receptor: C-terminal domain determines thermosensation in transient receptor potential channels', *Journal of Neuroscience*. Society for Neuroscience, 26(18), pp. 4835–4840. doi: 10.1523/JNEUROSCI.5080-05.2006.

Bromilow, C. (2001) *Problem plants of South Africa*.

Brône, B. *et al.* (2008) 'Tear gasses CN, CR, and CS are potent activators of the human TRPA1 receptor', *Toxicology and Applied Pharmacology*, 231(2), pp. 150–156. doi: https://doi.org/10.1016/j.taap.2008.04.005.

Buffenstein, R. and Yahav, S. (1991) 'Is the naked mole-rat Hererocephalus glaber an endothermic yet poikilothermic mammal?', *Journal of Thermal Biology*. doi: 10.1016/0306-4565(91)90030-6.

Burda, H. and Kawalika, M. (1993) 'Evolution of eusociality in the Bathyergidae. The case of the giant mole rats (Cryptomys mechowi).', *Die Naturwissenschaften*, 80(5), pp. 235–7. doi: 10.1007/bf01175742.

Burgess, G. M. *et al.* (1989) ‘Second messengers involved in the mechanism of action of bradykinin in sensory neurons in culture’, *Journal of Neuroscience*. Society for Neuroscience, 9(9), pp. 3314–3325. doi: 10.1523/jneurosci.09-09-03314.1989.

Burke, M. K. and Long, A. D. (2012) ‘What paths do advantageous alleles take during short-term evolutionary change?’, *Molecular Ecology*. John Wiley & Sons, Ltd, 21(20), pp. 4913–4916. doi: 10.1111/j.1365-294X.2012.05745.x.

Burke, R. E. (2006) ‘Sir Charles Sherrington’s The integrative action of the nervous system: a centenary appreciation’, *Brain*. Oxford University Press, 130(4), pp. 887–894. doi: 10.1093/brain/awm022.

Cain, D. M., Khasabov, S. G. and Simone, D. A. (2001) ‘Response Properties of Mechanoreceptors and Nociceptors in Mouse Glabrous Skin: An In Vivo Study’, *Journal of Neurophysiology*. American Physiological SocietyBethesda, MD, 85(4), pp. 1561–1574. doi: 10.1152/jn.2001.85.4.1561.

Callejo, G., Giblin, J. P. and Gasull, X. (2013) ‘Modulation of TRESK Background K+ Channel by Membrane Stretch’, *PLoS ONE*. Edited by V. Ceña. Public Library of Science, 8(5), p. e64471. doi: 10.1371/journal.pone.0064471.

Cao, Y. Q. *et al.* (1998) ‘Primary afferent tachykinins are required to experience moderate to intense pain’, *Nature*. Nature Publishing Group, 392(6674), pp. 390–394. doi: 10.1038/32897.

Carnevale, V. and Rohacs, T. (2016) ‘TRPV1: A Target for Rational Drug Design’, *Pharmaceuticals*. MDPI AG, 9(3), p. 52. doi: 10.3390/ph9030052.

Caterina, M. J. *et al.* (1997) ‘The capsaicin receptor: a heat-activated ion channel in the pain pathway’, *Nature*. Nature Publishing Group, 389(6653), pp. 816–824. doi: 10.1038/39807.

Caterina, M. J. *et al.* (2000) ‘Impaired nociception and pain sensation in mice lacking the capsaicin receptor’, *Science*. American Association for the Advancement of Science, 288(5464), pp. 306–313. doi: 10.1126/science.288.5464.306.

Caterina, M. J. and Julius, D. (2000) *THE VANILLOID RECEPTOR: A Molecular Gateway to the Pain Pathway*. Available at: www.annualreviews.org (Accessed: 18 February 2019).

Cesare, P. and Mcnaughton, P. (1996) ‘A novel heat-activated current in nociceptive neurons and its sensitization by bradykinin’, *Proceedings of the National Academy of Sciences of the United States of America*. National Academy of Sciences, 93(26), pp. 15435–15439. doi: 10.1073/pnas.93.26.15435.

Chakrabarti, S. *et al.* (2018) ‘Acute inflammation sensitizes knee-innervating sensory neurons and decreases mouse digging behavior in a TRPV1-dependent manner’, *Neuropharmacology*. Elsevier Ltd, 143, pp. 49–62. doi: 10.1016/j.neuropharm.2018.09.014.

Charles Scott Sherrington (1906) *The integrative action of the nervous system*. New Haven: Yale University press. Available at: https://archive.org/details/integrativeactio00sheruoft/page/n8 (Accessed: 9 April 2019).

Chen, J. and Hackos, D. H. (2015) ‘TRPA1 as a drug target--promise and challenges’, *Naunyn Schmiedebergs Arch Pharmacol*, 388(4), pp. 451–463. doi: 10.1007/s00210-015-1088-3.

Chen, J. and Lariviere, W. R. (2010) ‘The nociceptive and anti-nociceptive effects of bee venom

injection and therapy: a double-edged sword.', *Progress in neurobiology*. NIH Public Access, 92(2), pp. 151–83. doi: 10.1016/j.pneurobio.2010.06.006.

Chen, X. *et al.* (2007) 'Zebrafish acid-sensing ion channel (ASIC) 4, characterization of homo- and heteromeric channels, and identification of regions important for activation by H+', *Journal of Biological Chemistry*. American Society for Biochemistry and Molecular Biology, 282(42), pp. 30406–30413. doi: 10.1074/jbc.M702229200.

Chen, Y.-J. *et al.* (2009) 'Expression and Function of Proton-Sensing G-Protein-Coupled Receptors in Inflammatory Pain', *Molecular Pain*. SAGE PublicationsSage CA: Los Angeles, CA, 5, pp. 1744-8069-5–39. doi: 10.1186/1744-8069-5-39.

Christensen, A. P., Akyuz, N. and Corey, D. P. (2016) 'The Outer Pore and Selectivity Filter of TRPA1', *PLOS ONE*, 11(11), p. e0166167. doi: 10.1371/journal.pone.0166167.

Chrysafides, S. M. and Sharma, S. (2019) *Physiology, Resting Potential*, *StatPearls*. StatPearls Publishing. Available at: http://www.ncbi.nlm.nih.gov/pubmed/30855922 (Accessed: 17 February 2020).

Chu, Y., Cohen, B. E. and Chuang, H. hu (2020) 'A single TRPV1 amino acid controls species sensitivity to capsaicin', *Scientific Reports*. Nature Research, 10(1), pp. 1–12. doi: 10.1038/s41598-020-64584-2.

Chua, H. C. *et al.* (2020) *The NALCN channel complex is voltage sensitive and directly modulated by extracellular calcium*.

Chuang, H. H. *et al.* (2001) 'Bradykinin and nerve growth factor release the capsaicin receptor from PtdIns(4,5)P2-mediated inhibition', *Nature*. Nature Publishing Group, 411(6840), pp. 957–962. doi: 10.1038/35082088.

Chung, M.-K. and Campbell, J. (2016) 'Use of Capsaicin to Treat Pain: Mechanistic and Therapeutic Considerations', *Pharmaceuticals*. MDPI AG, 9(4), p. 66. doi: 10.3390/ph9040066.

Clapham, D. E. (2015) 'Pain-sensing TRPA1 channel resolved', *Nature*, 520, pp. 439–441.

Cochet-Bissuel, M., Lory, P. and Monteil, A. (2014) 'The sodium leak channel, NALCN, in health and disease', *Front Cell Neurosci*. 2014/06/07, 8, p. 132. doi: 10.3389/fncel.2014.00132.

Cohen, M. R. and Moiseenkova-Bell, V. Y. (2014) 'Structure of Thermally Activated TRP Channels', in *Current Topics in Membranes*. doi: 10.1016/B978-0-12-800181-3.00007-5.

Cordero, G. A. and Janzen, F. (2013) 'Does life history affect molecular evolutionary rates?', *Nature Education Knowledge*, 4(4), p. 1.

Cortelli, P. *et al.* (2013) 'Nociception and autonomic nervous system', *Neurological Sciences*. Springer, 34(SUPPL. 1), pp. 41–46. doi: 10.1007/s10072-013-1391-z.

Cox, J. J. *et al.* (2006) 'An SCN9A channelopathy causes congenital inability to experience pain', *Nature*. Nature Publishing Group, 444(7121), pp. 894–898. doi: 10.1038/nature05413.

Cregg, R. *et al.* (2010) 'Pain channelopathies', *The Journal of Physiology*. John Wiley & Sons, Ltd, 588(11), pp. 1897–1904. doi: 10.1113/jphysiol.2010.187807.

Davis, J. B. *et al.* (2000) 'Vanilloid receptor-1 is essential for inflammatory thermal hyperalgesia',

Nature. Nature Publishing Group, 405(6783), pp. 183–187. doi: 10.1038/35012076.

Davoody, L. *et al.* (2011) 'Conditioned place preference reveals tonic pain in an animal model of central pain', *Journal of Pain*. NIH Public Access, 12(8), pp. 868–874. doi: 10.1016/j.jpain.2011.01.010.

Decosterd, I. and Woolf, C. J. (2000) 'Spared nerve injury: An animal model of persistent peripheral neuropathic pain', *Pain*. Pain, 87(2), pp. 149–158. doi: 10.1016/S0304-3959(00)00276-1.

Deuis, J. R., Dvorakova, L. S. and Vetter, I. (2017) 'Methods used to evaluate pain behaviors in rodents', *Frontiers in Molecular Neuroscience*. Frontiers Media S.A., p. 284. doi: 10.3389/fnmol.2017.00284.

Deval, E. *et al.* (2008) 'ASIC3, a sensor of acidic and primary inflammatory pain', *The EMBO Journal*. John Wiley & Sons, Ltd, 27(22), pp. 3047–3055. doi: 10.1038/emboj.2008.213.

Dhaka, A. *et al.* (2009) 'TRPV1 senses both acidic and basic pH', *J. Neurosci.*, 29(1), pp. 153–158. doi: 10.1016/j.pestbp.2011.02.012.Investigations.

Dickenson, A. H. and Sullivan, A. F. (1987) 'Peripheral origins and central modulation of subcutaneous formalin-induced activity of rat dorsal horn neurones', *Neuroscience Letters*. Elsevier, 83(1–2), pp. 207–211. doi: 10.1016/0304-3940(87)90242-4.

Diver, M. M., Cheng, Y. and Julius, D. (2019) 'Structural insights into TRPM8 inhibition and desensitization', *Science*. American Association for the Advancement of Science, 365(6460), pp. 1434–1440. doi: 10.1126/science.aax6672.

Dong, L. *et al.* (2013) 'Acidosis Activation of the Proton-Sensing GPR4 Receptor Stimulates Vascular Endothelial Cell Inflammatory Responses Revealed by Transcriptome Analysis', *PLoS ONE*. Edited by N. Signoret. Public Library of Science, 8(4), p. e61991. doi: 10.1371/journal.pone.0061991.

Dubin, A. E. and Patapoutian, A. (2010) 'Nociceptors: the sensors of the pain pathway.', *The Journal of clinical investigation*. American Society for Clinical Investigation, 120(11), pp. 3760–72. doi: 10.1172/JCI42843.

Dubuisson, D. and Dennis, S. G. (1977) 'The formalin test: A quantitative study of the analgesic effects of morphine, meperidine, and brain stem stimulation in rats and cats', *Pain*, 4(Supp C), pp. 161–174. doi: 10.1016/0304-3959(77)90130-0.

Duo, L. *et al.* (2018) 'TRPV1 gain-of-function mutation impairs pain and itch sensations in mice', *Molecular Pain*. SAGE Publications Inc., 14. doi: 10.1177/1744806918762031.

Eddy, N. B. and Leimbach, D. (1953) 'Synthetic analgesics II Dithienylbutenyl- and diethylbutylamines', *Journal of Pharmacology and Experimental Therapeutics*. American Society for Pharmacology and Experimental Therapeutics, 107(3), pp. 385–393. Available at: http://jpet.aspetjournals.org/content/107/3/385.

Eigenbrod, O. (2018) *Dissecting genetic signatures of extreme physiology using African mole-rats*.

Eigenbrod, O. *et al.* (2019) 'Rapid molecular evolution of pain insensitivity in multiple African rodents.', *Science (New York, N.Y.)*. American Association for the Advancement of Science,

364(6443), pp. 852–859. doi: 10.1126/science.aau0236.

Escalera, J. *et al.* (2008) 'TRPA1 Mediates the Noxious Effects of Natural Sesquiterpene Deterrents', *Journal of Biological Chemistry* , 283(35), pp. 24136–24144. doi: 10.1074/jbc.M710280200.

Everaerts, W. *et al.* (2011) 'The capsaicin receptor TRPV1 is a crucial mediator of the noxious effects of mustard oil', *Curr Biol*. 2011/02/15. Cell Press, 21(4), pp. 316–321. doi: 10.1016/j.cub.2011.01.031.

Fahie, S. and Cassagnol, M. (2020) 'Verapamil.', in. Treasure Island (FL).

Fajardo, O. *et al.* (2008) 'TRPA1 channels: Novel targets of 1,4-dihydropyridines', *Channels*. Taylor & Francis, 2(6), pp. 429–438. doi: 10.4161/chan.2.6.7126.

Fang, X. *et al.* (2014) 'Adaptations to a Subterranean Environment and Longevity Revealed by the Analysis of Mole Rat Genomes', *Cell Reports*. Elsevier B.V., 8(5), pp. 1354–1364. doi: 10.1016/j.celrep.2014.07.030.

Faulkes, C. G. *et al.* (2004) 'Phylogeographical patterns of genetic divergence and speciation in African mole-rats (Family: Bathyergidae)', *Molecular Ecology*. 2004/02/12. John Wiley & Sons, Ltd, 13(3), pp. 613–629. doi: 10.1046/j.1365-294X.2004.02099.x.

Faulkes, C. G. *et al.* (2011) 'Phylogeography and cryptic diversity of the solitary-dwelling silvery mole-rat, genus Heliophobius (family: Bathyergidae)', *Journal of Zoology*. Edited by A. Kitchener. John Wiley & Sons, Ltd, 285(4), pp. 324–338. doi: 10.1111/j.1469-7998.2011.00863.x.

Faulkes, C. G. and Bennett, N. C. (2013) 'Plasticity and constraints on social evolution in African mole-rats: ultimate and proximate factors', *Philos Trans R Soc Lond B Biol Sci*, 368(1618), p. 20120347. doi: 10.1098/rstb.2012.0347.

Feliks, K. B. and Wrońska, D. (2017) 'Voltage-Gated Calcium Channel Antagonists: Potential Analgesics for Jejunal Pains', in *Pain Relief - From Analgesics to Alternative Therapies*. InTech. doi: 10.5772/66597.

Fleig, A. and Penner, R. (2004) 'The TRPM ion channel subfamily: Molecular, biophysical and functional features', *Trends in Pharmacological Sciences*. doi: 10.1016/j.tips.2004.10.004.

Fleischer, E., Handwerker, H. O. and Joukhadar, S. (1983) 'Unmyelinated nociceptive units in two skin areas of the rat', *Brain Research*, 267(1), pp. 81–92. doi: https://doi.org/10.1016/0006-8993(83)91041-7.

Fujita, F. *et al.* (2007) 'Methyl p-hydroxybenzoate causes pain sensation through activation of TRPA1 channels', *British Journal of Pharmacology*. John Wiley & Sons, Ltd, 151(1), pp. 134–141. doi: 10.1038/sj.bjp.0707219.

Gage, G. J., Kipke, D. R. and Shain, W. (2012) 'Whole Animal Perfusion Fixation for Rodents', *Journal of Visualized Experiments : JoVE*. MyJoVE Corporation, (65). doi: 10.3791/3564.

Garami, A. *et al.* (2020) 'Hyperthermia induced by transient receptor potential vanilloid-1 (TRPV1) antagonists in human clinical trials: Insights from mathematical modeling and meta-analysis', *Pharmacology and Therapeutics*. Elsevier Inc., p. 107474. doi: 10.1016/j.pharmthera.2020.107474.

García-Sanz, N. *et al.* (2004) ‘Identification of a tetramerization domain in the C terminus of the vanilloid receptor’, *Journal of Neuroscience*. Society for Neuroscience, 24(23), pp. 5307–5314. doi: 10.1523/JNEUROSCI.0202-04.2004.

Gaudet, R. (2006) ‘Structural Insights into the Function of TRP Channels’, in. CRC Press/Taylor & Francis, pp. 349–360. doi: 10.1201/9781420005844.ch25.

Gaudet, R. (2008) ‘A primer on ankyrin repeat function in TRP channels and beyond’, *Molecular BioSystems*. Royal Society of Chemistry, 4(5), pp. 372–379. doi: 10.1039/b801481g.

Gauriau, C. and Bernard, J.-F. (2002) ‘Pain Pathways and Parabrachial Circuits in the Rat’, *Experimental Physiology*. Cambridge University Press, 87(2), pp. 251–258. doi: 10.1113/eph8702357.

Gees, M. *et al.* (2013) ‘Mechanisms of transient receptor potential vanilloid 1 activation and sensitization by allyl isothiocyanate.’, *Molecular pharmacology*, 84(3), pp. 325–34. doi: 10.1124/mol.113.085548.

Giorgi, S. *et al.* (2019) ‘Is TRPA1 burning down TRPV1 as druggable target for the treatment of chronic pain?’, *International Journal of Molecular Sciences*. MDPI AG. doi: 10.3390/ijms20122906.

Glatte, P. *et al.* (2019) ‘Architecture of the Cutaneous Autonomic Nervous System’, *Frontiers in Neurology*. Frontiers Media S.A. doi: 10.3389/fneur.2019.00970.

González-Muñiz, R. *et al.* (2019) ‘Recent progress in TRPM8 modulation: an update’, *International Journal of Molecular Sciences*. MDPI AG. doi: 10.3390/ijms20112618.

Gregory, N. S. *et al.* (2013) ‘An overview of animal models of pain: disease models and outcome measures.’, *The journal of pain : official journal of the American Pain Society*, 14(11), pp. 1255–1269. doi: 10.1016/j.jpain.2013.06.008.

Gu, X. and Li, W. H. (1992) ‘Higher rates of amino acid substitution in rodents than in humans’, *Molecular Phylogenetics and Evolution*. Mol Phylogenet Evol, 1(3), pp. 211–214. doi: 10.1016/1055-7903(92)90017-B.

Hairston, N. G. *et al.* (2005) ‘Rapid evolution and the convergence of ecological and evolutionary time’, *Ecology Letters*. John Wiley & Sons, Ltd, 8(10), pp. 1114–1127. doi: 10.1111/j.1461-0248.2005.00812.x.

Han, S. *et al.* (2015) ‘Elucidating an Affective Pain Circuit that Creates a Threat Memory’, *Cell*. Cell Press, 162(2), pp. 363–374. doi: 10.1016/j.cell.2015.05.057.

Haraguchi, K. *et al.* (2012) ‘TRPM2 contributes to inflammatory and neuropathic pain through the aggravation of pronociceptive inflammatory responses in mice’, *Journal of Neuroscience*. Society for Neuroscience, 32(11), pp. 3931–3941. doi: 10.1523/JNEUROSCI.4703-11.2012.

Hargreaves, K. *et al.* (1988) ‘A new and sensitive method for measuring thermal nociception in cutaneous hyperalgesia’, *Pain*, 32(1), pp. 77–88. doi: 10.1016/0304-3959(88)90026-7.

Hart, S. P., Turcotte, M. M. and Levine, J. M. (2019) ‘Effects of rapid evolution on species coexistence’, *Proceedings of the National Academy of Sciences of the United States of America*. National Academy of Sciences, 116(6), pp. 2112–2117. doi: 10.1073/pnas.1816298116.

Heidenreich, M. *et al.* (2012) 'KCNQ4 K + channels tune mechanoreceptors for normal touch sensation in mouse and man', *Nature Neuroscience*. Nature Publishing Group, 15(1), pp. 138–145. doi: 10.1038/nn.2985.

Hill, K. and Schaefer, M. (2007) 'TRPA1 is differentially modulated by the amphipathic molecules trinitrophenol and chlorpromazine', *J Biol Chem*. 2007/01/16, 282(10), pp. 7145–7153. doi: 10.1074/jbc.M609600200.

Hinman, A. *et al.* (2006) 'TRP channel activation by reversible covalent modification', *Proceedings of the National Academy of Sciences*, 103(51), pp. 19564–19568.

Hirose, M., Kuroda, Y. and Murata, E. (2016) 'NGF/TrkA Signaling as a Therapeutic Target for Pain', *Pain Practice*. Blackwell Publishing Inc., 16(2), pp. 175–182. doi: 10.1111/papr.12342.

Hohmann, S. W. *et al.* (2017) 'The G2A receptor (GPR132) contributes to oxaliplatin-induced mechanical pain hypersensitivity', *Scientific Reports*. Nature Publishing Group, 7(1), pp. 1–11. doi: 10.1038/s41598-017-00591-0.

Holzer, P. (2009) 'Acid-sensitive ion channels and receptors', in *Handbook of Experimental Pharmacology*. Routledge, pp. 283–332. doi: 10.1007/978-3-540-79090-7_9.

Hsieh, W. S. *et al.* (2017) 'TDAG8, TRPV1, and ASIC3 involved in establishing hyperalgesic priming in experimental rheumatoid arthritis', *Scientific Reports*. Nature Publishing Group, 7(1), pp. 1–14. doi: 10.1038/s41598-017-09200-6.

Huang, Y. *et al.* (2020) 'A structural overview of the ion channels of the TRPM family', *Cell Calcium*. Elsevier Ltd, p. 102111. doi: 10.1016/j.ceca.2019.102111.

Hunt, S. P. and Mantyh, P. W. (2001) 'The molecular dynamics of pain control', *Nature Reviews Neuroscience*. Nature Publishing Group, 2(2), pp. 83–91. doi: 10.1038/35053509.

Hunt, S. P., Pini, A. and Evan, G. (1987) 'Induction of c-fos-like protein in spinal cord neurons following sensory stimulation', *Nature*. 1987/08/13, 328(6131), pp. 632–634. doi: 10.1038/328632a0.

Ibarra, Y. and Blair, N. T. (2013) 'Benzoquinone reveals a cysteine-dependent desensitization mechanism of TRPA1.', *Molecular pharmacology*. American Society for Pharmacology and Experimental Therapeutics, 83(5), pp. 1120–32. doi: 10.1124/mol.112.084194.

Indo, Y. (2001) 'Molecular basis of congenital insensitivity to pain with anhidrosis (CIPA): Mutations and polymorphisms in TRKA (NTRK1) gene encoding the receptor tyrosine kinase for nerve growth factor', *Human Mutation*. John Wiley & Sons, Ltd, pp. 462–471. doi: 10.1002/humu.1224.

Jaggi, A. S., Jain, V. and Singh, N. (2011) 'Animal models of neuropathic pain', *Fundamental and Clinical Pharmacology*. Fundam Clin Pharmacol, pp. 1–28. doi: 10.1111/j.1472-8206.2009.00801.x.

Jang, Y. *et al.* (2018) 'Nociceptive Roles of TRPM2 Ion Channel in Pathologic Pain'. doi: 10.1007/s12035-017-0862-2.

Janscó, G., Kiraly, E. and Janscó-Gábor, A. (1977) 'Pharmacologically induced selective degeneration of chemosensitive primary sensory neurones', *Nature*. Nature Publishing Group, 270(5639), pp. 741–743. doi: 10.1038/270741a0.

Jaquemar, D., Schenker, T. and Trueb, B. (1999) ‘An Ankyrin-like Protein with Transmembrane Domains Is Specifically Lost after Oncogenic Transformation of Human Fibroblasts’, *Journal of Biological Chemistry* , 274(11), pp. 7325–7333. doi: 10.1074/jbc.274.11.7325.

Jasmin, L. *et al.* (1998) ‘The cold plate as a test of nociceptive behaviors: Description and application to the study of chronic neuropathic and inflammatory pain models’, *Pain*. Pain, 75(2–3), pp. 367–382. doi: 10.1016/S0304-3959(98)00017-7.

Jasti, J. *et al.* (2007) ‘Structure of acid-sensing ion channel 1 at 1.9 Å resolution and low pH’, *Nature*. Nature Publishing Group, 449(7160), pp. 316–323. doi: 10.1038/nature06163.

Jeong, J. Y. *et al.* (2012) ‘One-step sequence-and ligation-independent cloning as a rapid and versatile cloning method for functional genomics Studies’, *Applied and Environmental Microbiology*, 78(15), pp. 5440–5443. doi: 10.1128/AEM.00844-12.

Jeske, N. A. *et al.* (2006) ‘Cannabinoid WIN 55,212-2 Regulates TRPV1 Phosphorylation in Sensory Neurons’, *Journal of Biological Chemistry* , 281(43), pp. 32879–32890. doi: 10.1074/jbc.M603220200.

Jiang, M. C. and Gebhart, G. F. (1998) ‘Development of mustard oil-induced hyperalgesia in rats’, *Pain*. Elsevier, 77(3), pp. 305–313. doi: 10.1016/S0304-3959(98)00110-9.

Jones, N. G. *et al.* (2004) ‘Acid-induced pain and its modulation in humans’, *Journal of Neuroscience*. Society for Neuroscience, 24(48), pp. 10974–10979. doi: 10.1523/JNEUROSCI.2619-04.2004.

Jordt, S.-E. *et al.* (2004) ‘Mustard oils and cannabinoids excite sensory nerve fibres through the TRP channel ANKTM1’, *Nature*. Nature Publishing Group, 427(6971), pp. 260–265. doi: 10.1038/nature02282.

Jordt, S. E. and Julius, D. (2002) ‘Molecular basis for species-specific sensitivity to “hot” chili peppers’, *Cell*. 2002/02/21, 108(3), pp. 421–430. doi: 10.1016/S0092-8674(02)00637-2.

Jordt, S. E., Tominaga, M. and Julius, D. (2000) ‘Acid potentiation of the capsaicin receptor determined by a key extracellular site’, *Proceedings of the National Academy of Sciences of the United States of America*. National Academy of Sciences, 97(14), pp. 8134–8139. doi: 10.1073/pnas.100129497.

Julius, D. (2013) ‘TRP Channels and Pain’, *Annu. Rev. Cell Dev. Biol*, 29, pp. 355–84. doi: 10.1146/annurev-cellbio-101011-155833.

Julius, D. and Basbaum, A. I. (2001) ‘Molecular mechanism of nociception’, *Nature*, 413, pp. 203–210.

Kang, K. *et al.* (2010) ‘Analysis of Drosophila TRPA1 reveals an ancient origin for human chemical nociception’, *Nature*. Nature Publishing Group, 464(7288), pp. 597–600. doi: 10.1038/nature08848.

Kang, K. *et al.* (2011) ‘Modulation of TRPA1 thermal sensitivity enables sensory discrimination in Drosophila’, *Nature*. 2011/12/06, 481(7379), pp. 76–80. doi: 10.1038/nature10715.

Kang, Y., Wu, J.-X. and Chen, L. (2020) ‘Structure of voltage-modulated sodium-selective NALCN-FAM155A channel complex’, *bioRxiv*. Cold Spring Harbor Laboratory, p. 2020.07.26.221747. doi: 10.1101/2020.07.26.221747.

Kania, B. F., Brytan, M. and Tomaszewska, D. (2009) 'Centrally administered verapamil prevents the autonomic reaction to visceral pain in sheep', *Research in Veterinary Science*, 86(1), pp. 121–128. doi: 10.1016/j.rvsc.2008.04.009.

Karashima, Y. *et al.* (2007) 'Bimodal action of menthol on the transient receptor potential channel TRPA1.', *The Journal of neuroscience : the official journal of the Society for Neuroscience*. Society for Neuroscience, 27(37), pp. 9874–84. doi: 10.1523/JNEUROSCI.2221-07.2007.

Kim, B. J. *et al.* (2012) 'Involvement of Na + -leak channel in substance P-induced depolarization of pacemaking activity in interstitial cells of Cajal', *Cellular Physiology and Biochemistry*. Cell Physiol Biochem Press, 29(3–4), pp. 501–510. doi: 10.1159/000338504.

Kim, E. B. *et al.* (2011) 'Genome sequencing reveals insights into physiology and longevity of the naked mole rat', *Nature*, 479(7372), pp. 223–227. doi: 10.1038/nature10533.

Konnerth, A., Lux, H. D. and Morad, M. (1987) 'Proton-induced transformation of calcium channel in chick dorsal root ganglion cells.', *The Journal of Physiology*. John Wiley & Sons, Ltd, 386(1), pp. 603–633. doi: 10.1113/jphysiol.1987.sp016553.

Kopp, M. and Matuszewski, S. (2014) 'Rapid evolution of quantitative traits: Theoretical perspectives', *Evolutionary Applications*. John Wiley & Sons, Ltd, 7(1), pp. 169–191. doi: 10.1111/eva.12127.

Köroğlu, Ç., Seven, M. and Tolun, A. (2013) 'Recessive truncating NALCN mutation in infantile neuroaxonal dystrophy with facial dysmorphism', *Journal of Medical Genetics*, 50(8), pp. 515–520. doi: 10.1136/jmedgenet-2013-101634.

Krapivinsky, G. *et al.* (2014) 'The TRPM7 chanzyme is cleaved to release a chromatin-modifying kinase', *Cell*. Cell Press, 157(5), pp. 1061–1072. doi: 10.1016/j.cell.2014.03.046.

Kremeyer, B. *et al.* (2010) 'A Gain-of-Function Mutation in TRPA1 Causes Familial Episodic Pain Syndrome', *Neuron*. Cell Press, 66(5), pp. 671–680. Available at: https://www.sciencedirect.com/science/article/pii/S0896627310003235 (Accessed: 15 February 2019).

Kschonsak, M. *et al.* (2020) 'Structure of the human sodium leak channel NALCN', *Nature 2020*. Nature Publishing Group, pp. 1–10. doi: 10.1038/s41586-020-2570-8.

Kubisch, C. *et al.* (1999) 'KCNQ4, a novel potassium channel expressed in sensory outer hair cells, is mutated in dominant deafness', *Cell*. Cell Press, 96(3), pp. 437–446. doi: 10.1016/S0092-8674(00)80556-5.

Kumar, R., Mehra, R. and Ray, S. B. (2010) 'L-type calcium channel blockers, morphine and pain: Newer insights', *Indian Journal of Anaesthesia*. Wolters Kluwer -- Medknow Publications, 54(2), pp. 127–131. doi: 10.4103/0019-5049.63652.

Kumar, S. *et al.* (2017) 'TimeTree: a resource for timelines, timetrees, and divergence times', *Molecular Biology and Evolution*, 34, pp. 1812–1819.

Kumar, S. and Subramanian, S. (2002) 'Mutation rates in mammalian genomes', *Proceedings of the National Academy of Sciences of the United States of America*, 99(2), pp. 803–808. Available at: www.pnas.orgcgidoi10.1073pnas.022629899.

Kwan, K. Y. *et al.* (2006) 'TRPA1 Contributes to Cold, Mechanical, and Chemical Nociception but Is Not Essential for Hair-Cell Transduction', *Neuron*. Cell Press, 50(2), pp. 277–289. doi: 10.1016/J.NEURON.2006.03.042.

De La Roche, J. *et al.* (2013) 'The molecular basis for species-specific activation of human TRPA1 protein by protons involves poorly conserved residues within transmembrane domains 5 and 6', *Journal of Biological Chemistry*, 288(28), pp. 20280–20292. doi: 10.1074/jbc.M113.479337.

Latremoliere, A. and Woolf, C. J. (2009) 'Central Sensitization: A Generator of Pain Hypersensitivity by Central Neural Plasticity', *Journal of Pain*. NIH Public Access, pp. 895–926. doi: 10.1016/j.jpain.2009.06.012.

Laursen, W. J., Bagriantsev, S. N. and Gracheva, E. O. (2014) 'TRPA1 Channels: Chemical and Temperature Sensitivity', *Current Topics in Membranes*. Academic Press, 74, pp. 89–112. doi: 10.1016/B978-0-12-800181-3.00004-X.

Lebrun, P., Manil, J. and Colin, F. (2000) 'Formalin-induced central sensitization in the rat: Somatosensory evoked potential data', *Neuroscience Letters*. Elsevier, 283(2), pp. 113–116. doi: 10.1016/S0304-3940(00)00934-4.

Lee, S. P. *et al.* (2008) 'Thymol and related alkyl phenols activate the hTRPA1 channel', *British Journal of Pharmacology*. John Wiley & Sons, Ltd, 153(8), pp. 1739–1749. doi: 10.1038/bjp.2008.85.

Leffler, A. *et al.* (2008) 'The vanilloid receptor TRPV1 is activated and sensitized by local anesthetics in rodent sensory neurons', *Journal of Clinical Investigation*, 118(2), pp. 763–776. doi: 10.1172/JCI32751.

Leffler, A., Mönter, B. and Koltzenburg, M. (2006) 'The role of the capsaicin receptor TRPV1 and acid-sensing ion channels (ASICS) in proton sensitivity of subpopulations of primary nociceptive neurons in rats and mice', *Neuroscience*. doi: 10.1016/j.neuroscience.2005.12.020.

Lewin, G. R. and Moshourab, R. (2004) 'Mechanosensation and pain', *Journal of Neurobiology*. John Wiley & Sons, Ltd, 61(1), pp. 30–44. doi: 10.1002/neu.20078.

Lewin, G. R., Ritter, A. M. and Mendell, L. M. (1993) 'Nerve growth factor-induced hyperalgesia in the neonatal and adult rat', *Journal of Neuroscience*, 13(5), pp. 2136–2148. doi: 10.1523/jneurosci.13-05-02136.1993.

Liao, M. *et al.* (2013) 'Structure of the TRPV1 ion channel determined by electron cryo-microscopy', *Nature*, 504(7478), pp. 107–112. doi: 10.1038/nature12822.

Löken, L. S. *et al.* (2009) 'Coding of pleasant touch by unmyelinated afferents in humans', *Nature Neuroscience*. Nature Publishing Group, 12(5), pp. 547–548. doi: 10.1038/nn.2312.

Losos, J. B., Warheit, K. I. and Schoener, T. W. (1997) 'Adaptive differentiation following experimental island colonization in Anolis lizards', *Nature*. Nature Publishing Group, 387(6628), pp. 70–73. doi: 10.1038/387070a0.

Lu, B. *et al.* (2007) 'The neuronal channel NALCN contributes resting sodium permeability and is required for normal respiratory rhythm', *Cell*. 2007/04/24, 129(2), pp. 371–383. doi: 10.1016/j.cell.2007.02.041.

Lu, B. *et al.* (2010) ‘Extracellular calcium controls background current and neuronal excitability via an UNC79-UNC80-NALCN cation channel complex’, *Neuron*. 2010/11/03, 68(3), pp. 488–499. doi: 10.1016/j.neuron.2010.09.014.

Lynagh, T. *et al.* (2018) ‘Acid-sensing ion channels emerged over 600 Mya and are conserved throughout the deuterostomes’, *Proceedings of the National Academy of Sciences of the United States of America*. National Academy of Sciences, 115(33), pp. 8430–8435. doi: 10.1073/pnas.1806614115.

Macpherson, L. J. *et al.* (2005) ‘The Pungency of Garlic: Activation of TRPA1 and TRPV1 in Response to Allicin’, *Current Biology*. Elsevier, 15(10), pp. 929–934. doi: 10.1016/j.cub.2005.04.018.

Macpherson, L. J. *et al.* (2006) ‘More than cool: Promiscuous relationships of menthol and other sensory compounds’, *Molecular and Cellular Neuroscience*, 32(4), pp. 335–343. doi: https://doi.org/10.1016/j.mcn.2006.05.005.

Macpherson, L. J., Xiao, B., *et al.* (2007) ‘An Ion Channel Essential for Sensing Chemical Damage’, *The Journal of Neuroscience*, 27(42), pp. 11412 LP – 11415. doi: 10.1523/JNEUROSCI.3600-07.2007.

Macpherson, L. J., Dubin, A. E., *et al.* (2007) ‘Noxious compounds activate TRPA1 ion channels through covalent modification of cysteines’, *Nature letters*, 445, pp. 541–545. doi: 10.1038/nature05544.

Maher, M. *et al.* (2008) ‘Activation of TRPA1 by Farnesyl Thiosalicylic Acid’, *Molecular Pharmacology*, 73(4), pp. 1225 LP – 1234. doi: 10.1124/mol.107.042663.

Manitpisitkul, P. *et al.* (2016) ‘TRPV1 antagonist JNJ-39439335 (mavatrep) demonstrates proof of pharmacology in healthy men: A first-in-human, double-blind, placebo-controlled, randomized, sequential group study’, *Pain Reports*. Lippincott Williams and Wilkins, 1(4). doi: 10.1097/PR9.0000000000000576.

Manitpisitkul, P. *et al.* (2018) ‘A multiple-dose double-blind randomized study to evaluate the safety, pharmacokinetics, pharmacodynamics and analgesic efficacy of the TRPV1 antagonist JNJ-39439335 (mavatrep)’, *Scandinavian Journal of Pain*. Walter de Gruyter GmbH, 18(2), pp. 151–164. doi: 10.1515/sjpain-2017-0184.

McCall, W. D., Tanner, K. D. and Levine, J. D. (1996) ‘Formalin induces biphasic activity in C-fibers in the rat’, *Neuroscience Letters*. Elsevier Ireland Ltd, 208(1), pp. 45–48. doi: 10.1016/0304-3940(96)12552-0.

McKemy, D. D. (2007) *TRPM8: The Cold and Menthol Receptor*, *TRP Ion Channel Function in Sensory Transduction and Cellular SignalingCascades*. CRC Press/Taylor & Francis. Available at: http://www.ncbi.nlm.nih.gov/pubmed/21204488 (Accessed: 26 February 2020).

McMahon, S., Bennett, D. and Bevan, S. (2006) ‘Inflammatory mediators and modulators of pain’, in, pp. 49–72. doi: 10.1016/B0-443-07287-6/50008-4.

McNamara, C. R. *et al.* (2007) ‘TRPA1 mediates formalin-induced pain.’, *Proceedings of the National Academy of Sciences of the United States of America*. National Academy of Sciences, 104(33), pp. 13525–30. doi: 10.1073/pnas.0705924104.

Meseguer, V. *et al.* (2008) 'Transient Receptor Potential Channels in Sensory Neurons Are Targets of the Antimycotic Agent Clotrimazole', *The Journal of Neuroscience*, 28(3), pp. 576 LP – 586. doi: 10.1523/JNEUROSCI.4772-07.2008.

Milenkovic, N. *et al.* (2014) 'A somatosensory circuit for cooling perception in mice', *Nature Neuroscience*. Nature Publishing Group, 17(11), pp. 1560–1566. doi: 10.1038/nn.3828.

Mogil, J. S. (2009) 'Animal models of pain: Progress and challenges', *Nature Reviews Neuroscience*. Nature Publishing Group, pp. 283–294. doi: 10.1038/nrn2606.

Montell, C. and Rubin, G. M. (1989) 'Molecular characterization of the drosophila trp locus: A putative integral membrane protein required for phototransduction', *Neuron*. Cell Press, 2(4), pp. 1313–1323. doi: 10.1016/0896-6273(89)90069-X.

Moran, M. M. (2018) 'TRP Channels as Potential Drug Targets', *Annual Review of Pharmacology and Toxicology Annu. Rev. Pharmacol. Toxicol*. doi: 10.1146/annurev-pharmtox.

Moreno-Miralles, I. *et al.* (2011) 'BMPER regulates retinal angiogenesis in vivo in a mouse model of oxygen-induced retinopathy', *Arterioscler Thromb Vasc Biol*, 31(10), pp. 2216–2222. doi: 10.1161/ATVBAHA.

Nagarajan, Y., Rychkov, G. Y. and Peet, D. J. (2017) 'Modulation of TRP Channel Activity by Hydroxylation and Its Therapeutic Potential', *Pharmaceuticals*. MDPI AG, 10(4), p. 35. doi: 10.3390/ph10020035.

Nagata, K. *et al.* (2005) 'Nociceptor and Hair Cell Transducer Properties of TRPA1, a Channel for Pain and Hearing', *The Journal of Neuroscience*, 25(16), pp. 4052 LP – 4061. doi: 10.1523/JNEUROSCI.0013-05.2005.

Nei, M., Xu, P. and Glazko, G. (2001) 'Estimation of divergence times from multiprotein sequences for a few mammalian species and several distantly related organisms', *Proceedings of the National Academy of Sciences of the United States of America*. National Academy of Sciences, 98(5), pp. 2497–2502. doi: 10.1073/pnas.051611498.

Norris, D. K. and Bradford, H. F. (1985) 'On the specificity of verapamil as a calcium channel-blocker', *Biochemical Pharmacology*. Biochem Pharmacol, 34(11), pp. 1953–1956. doi: 10.1016/0006-2952(85)90314-4.

Nozaki-Taguchi, N. and Yaksh, T. L. (1998) 'A novel model of primary and secondary hyperalgesia after mild thermal injury in the rat', *Neuroscience Letters*. Neurosci Lett, 254(1), pp. 25–28. doi: 10.1016/S0304-3940(98)00648-X.

O'Neill, J. *et al.* (2012) 'Unravelling the mystery of capsaicin: a tool to understand and treat pain.', *Pharmacological reviews*. American Society for Pharmacology and Experimental Therapeutics, 64(4), pp. 939–71. doi: 10.1124/pr.112.006163.

Oda, M. *et al.* (2016) 'Sensitivities of Two Zebrafish TRPA1 Paralogs to Chemical and Thermal Stimuli Analyzed in Heterologous Expression Systems', *Chemical Senses*, 41(3), pp. 261–272. doi: 10.1093/chemse/bjv091.

Omerbašić, D. (2014) *Mollecular dissection of sensory phenotypes using the naked mole-rat (Heterocephalus glaber)*.

Omerbašić, D. *et al.* (2016) 'Hypofunctional TrkA Accounts for the Absence of Pain Sensitization

in the African Naked Mole-Rat', *Cell Reports*. doi: 10.1016/j.celrep.2016.09.035.

Paricio-Montesinos, R. *et al.* (2020) 'The Sensory Coding of Warm Perception', *Neuron*, 106(5), pp. 830-841.e3. doi: https://doi.org/10.1016/j.neuron.2020.02.035.

Park, T. J. *et al.* (2008) 'Selective inflammatory pain insensitivity in the African naked mole-rat (Heterocephalus glaber)', *PLoS Biology*, 6(1), pp. 156–170. doi: 10.1371/journal.pbio.0060013.

Park, T. J. *et al.* (2017) 'Fructose-driven glycolysis supports anoxia resistance in the naked mole-rat', *Science (New York, N.Y.)*, 356(6335), pp. 307–311. doi: 10.1126/science.aab3896.

Pattison, L. A. *et al.* (2019) 'Evolution of acid nociception: Ion channels and receptors for detecting acid', *Philosophical Transactions of the Royal Society B: Biological Sciences*. Royal Society Publishing, 374(1785). doi: 10.1098/rstb.2019.0291.

Perraud, A. L. *et al.* (2001) 'ADP-ribose gating of the calcium-permeable LTRPC2 channel revealed by Nudix motif homology', *Nature*. Nature Publishing Group, 411(6837), pp. 595–599. doi: 10.1038/35079100.

De Petrocellis, L. *et al.* (2008) 'Plant-Derived Cannabinoids Modulate the Activity of Transient Receptor Potential Channels of Ankyrin Type-1 and Melastatin Type-8', *Journal of Pharmacology and Experimental Therapeutics*, 325(3), pp. 1007 LP – 1015. doi: 10.1124/jpet.107.134809.

Petrus, M. *et al.* (2007) 'A Role of TRPA1 in Mechanical Hyperalgesia is Revealed by Pharmacological Inhibition', *Molecular Pain*. SAGE Publications Inc, 3, pp. 1740–1744. doi: 10.1186/1744-8069-3-40.

Pogatzki, E. M. and Raja, S. N. (2003) 'A Mouse Model of Incisional Pain', *Anesthesiology: The Journal of the American Society of Anesthesiologists*, 99(4), pp. 1023–1027.

Prato, V. *et al.* (2017) 'Functional and Molecular Characterization of Mechanoinsensitive "Silent" Nociceptors.', *Cell reports*, 21(11), pp. 3102–3115. doi: 10.1016/j.celrep.2017.11.066.

Price, M. P. *et al.* (2001) 'The DRASIC cation channel contributes to the detection of cutaneous touch and acid stimuli in mice', *Neuron*. Cell Press, 32(6), pp. 1071–1083. doi: 10.1016/S0896-6273(01)00547-5.

Puig, S. and Sorkin, L. S. (1996) 'Formalin-evoked activity in identified primary afferent fibers: Systemic lidocaine suppresses phase-2 activity', *Pain*. Elsevier B.V., 64(2), pp. 345–355. doi: 10.1016/0304-3959(95)00121-2.

Purves, D. *et al.* (2001) 'Ion Channels Underlying Action Potentials'. Sinauer Associates.

Ramirez, D. *et al.* (2020) 'Functional ingredients from brassicaceae species: Overview and perspectives', *International Journal of Molecular Sciences*. MDPI AG. doi: 10.3390/ijms21061998.

Reese, R. M. *et al.* (2020) 'Behavioral characterization of a CRISPR-generated TRPA1 knockout rat in models of pain, itch, and asthma'. doi: 10.1038/s41598-020-57936-5.

Ren, D. (2011) 'Sodium leak channels in neuronal excitability and rhythmic behaviors', *Neuron*. 2011/12/27. NIH Public Access, 72(6), pp. 899–911. doi: 10.1016/j.neuron.2011.12.007.

Rohacs, T., Thyagarajan, B. and Lukacs, V. (2008) 'Phospholipase C mediated modulation of TRPV1 channels', *Molecular Neurobiology*. Humana Press, pp. 153–163. doi: 10.1007/s12035-008-8027-y.

Runnels, L. W. (2011) 'TRPM6 and TRPM7: A Mul-TRP-PLIK-cation of channel functions.', *Current pharmaceutical biotechnology*. NIH Public Access, 12(1), pp. 42–53. doi: 10.2174/138920111793937880.

Russell, L. C. and Burchiel, K. J. (1984) 'Neurophysiological effects of capsaicin', *Brain Research Reviews*, pp. 165–176. doi: 10.1016/0165-0173(84)90005-5.

Saha, T. D. *et al.* (2016) 'Nonmedical prescription opioid use and DSM-5 nonmedical prescription opioid use disorder in the United States', *Journal of Clinical Psychiatry*. Physicians Postgraduate Press Inc., 77(6), pp. 772–780. doi: 10.4088/JCP.15m10386.

Saito, S. *et al.* (2014) 'Heat and Noxious Chemical Sensor, Chicken TRPA1, as a Target of Bird Repellents and Identification of Its Structural Determinants by Multispecies Functional Comparison', *Molecular Biology and Evolution*, 31(3), pp. 708–722. doi: 10.1093/molbev/msu001.

Salmon, A. M. *et al.* (2001) 'Altered neuroadaptation in opiate dependence and neurogenic inflammatory nociception in αCGRP-deficient mice', *Nature Neuroscience*. Nat Neurosci, 4(4), pp. 357–358. doi: 10.1038/86001.

Sambongi, Y. *et al.* (2000) 'Caenorhabditis elegans senses protons through amphid chemosensory neurons: Proton signals elicit avoidance behavior', *NeuroReport*. Lippincott Williams and Wilkins, 11(10), pp. 2229–2232. doi: 10.1097/00001756-200007140-00033.

Sawada, Y. *et al.* (2008) 'Activation of transient receptor potential ankyrin 1 by hydrogen peroxide', *European Journal of Neuroscience*. John Wiley & Sons, Ltd, 27(5), pp. 1131–1142. doi: 10.1111/j.1460-9568.2008.06093.x.

Schindelin, J. *et al.* (2012) 'Fiji: an open-source platform for biological-image analysis', *Nature Methods*. Nature Publishing Group, 9(7), pp. 676–682. doi: 10.1038/nmeth.2019.

Schmidt, R. F. and Willis, W. D. (2007) *Encyclopedia of Pain*, *Encyclopedia of Pain*. Springer Berlin Heidelberg. doi: 10.1007/978-3-540-29805-2.

Van Der Schueren, B. J. *et al.* (2007) 'Reproducibility of the capsaicin-induced dermal blood flow response as assessed by laser Doppler perfusion imaging', *British Journal of Clinical Pharmacology*. Wiley-Blackwell, 64(5), pp. 580–590. doi: 10.1111/j.1365-2125.2007.02939.x.

Seltzer, Z., Dubner, R. and Shir, Y. (1990) 'A novel behavioral model of neuropathic pain disorders produced in rats by partial sciatic nerve injury', *Pain*. Pain, 43(2), pp. 205–218. doi: 10.1016/0304-3959(90)91074-S.

Shimizu, N. *et al.* (2004) 'Involvement of peripheral mechanism in the verapamil-induced potentiation of morphine analgesia in mice', *Journal of Pharmacological Sciences*. Elsevier, 95(4), pp. 452–457. doi: 10.1254/jphs.FP0040252.

Singh, B. N., Ellrodt, G. and Peter, C. T. (1978) 'Verapamil: A Review of its Pharmacological Properties and Therapeutic Use', *Drugs*. Springer, 15(3), pp. 169–197. doi: 10.2165/00003495-197815030-00001.

Sinke, A. P. *et al.* (2011) ‘Genetic analysis of mouse strains with variable serum sodium concentrations identifies the Nalcn sodium channel as a novel player in osmoregulation’, *Physiological Genomics*. American Physiological Society, 43(5), pp. 265–270. doi: 10.1152/physiolgenomics.00188.2010.

Skolnick, P. (2018) ‘The Opioid Epidemic: Crisis and Solutions’, *Annual Review of Pharmacology and Toxicology Annu. Rev. Pharmacol. Toxicol*, 58, pp. 143–59. doi: 10.1146/annurev-pharmtox.

Slingsby, P. (2017) *Ants of Southern Africa*.

Smani, T. *et al.* (2015) ‘Functional and physiopathological implications of TRP channels’, *Biochimica et Biophysica Acta (BBA) - Molecular Cell Research*. Elsevier, 1853(8), pp. 1772–1782. doi: 10.1016/J.BBAMCR.2015.04.016.

Smith, E. S. J. *et al.* (2007) ‘Proton binding sites involved in the activation of acid-sensing ion channel ASIC2a’, *Neuroscience Letters*. Elsevier, 426(1), pp. 12–17. doi: 10.1016/j.neulet.2007.07.047.

Smith, E. S. J. *et al.* (2011) ‘The Molecular Basis of Acid Insensitivity in the African Naked Mole-Rat’, *Science*. 2011/12/17, 334(6062), pp. 1557–1560. doi: 10.1126/science.1213760.

Smith, E. S. J. and Lewin, G. R. (2009) ‘Nociceptors: a phylogenetic view.’, *Journal of comparative physiology A*, 195, pp. 1089–1106. doi: 10.1007/s00359-009-0482-z.

Smith, E. S. J., Park, T. J. and Lewin, G. R. (2020) ‘Independent evolution of pain insensitivity in African mole-rats: origins and mechanisms’, *Journal of Comparative Physiology A: Neuroethology, Sensory, Neural, and Behavioral Physiology*. Springer, pp. 313–325. doi: 10.1007/s00359-020-01414-w.

Sneddon, L. U. (2003) ‘The evidence for pain in fish: The use of morphine as an analgesic’, *Applied Animal Behaviour Science*. Elsevier, 83(2), pp. 153–162. doi: 10.1016/S0168-1591(03)00113-8.

Sneddon, L. U. (2018) ‘Comparative Physiology of Nociception and Pain’, *Physiology*. American Physiological Society Bethesda, MD, 33(1), pp. 63–73. doi: 10.1152/physiol.00022.2017.

Song, K. *et al.* (2016) ‘The TRPM2 channel is a hypothalamic heat sensor that limits fever and can drive hypothermia’, *Science*. American Association for the Advancement of Science, 353(6306), pp. 1393–1398. doi: 10.1126/science.aaf7537.

Story, G. M. *et al.* (2003) ‘ANKTM1, a TRP-like channel expressed in nociceptive neurons, is activated by cold temperatures’, *Cell*. 2003/03/26, 112(6), pp. 819–829. Available at: https://www.ncbi.nlm.nih.gov/pubmed/12654248.

Stotz, S. C. *et al.* (2008) ‘Citral Sensing by TRANSient Receptor Potential Channels in Dorsal Root Ganglion Neurons’, *PLOS ONE*. Public Library of Science, 3(5), p. e2082.

Streng, T. *et al.* (2008) ‘Distribution and Function of the Hydrogen Sulfide–Sensitive TRPA1 Ion Channel in Rat Urinary Bladder’, *European Urology*. Elsevier, 53(2), pp. 391–400. doi: 10.1016/j.eururo.2007.10.024.

Stuart, Y. E. *et al.* (2014) ‘Rapid evolution of a native species following invasion by a congener’, *Science*. American Association for the Advancement of Science, 346(6208), pp. 463–466. doi:

10.1126/science.1257008.

Sumoza-Toledo, A. and Penner, R. (2011) ‘TRPM2: a multifunctional ion channel for calcium signalling’, *The Journal of Physiology S*, 589, pp. 1515–1525. doi: 10.1113/jphysiol.2010.201855.

Sun, W.-H. *et al.* (2019) ‘The Transition from Acute to Chronic Pain’, in *The Oxford Handbook of the Neurobiology of Pain*. Oxford University Press. doi: 10.1093/oxfordhb/9780190860509.013.28.

Szallasi, A. *et al.* (2007) ‘The vanilloid receptor TRPV1: 10 years from channel cloning to antagonist proof-of-concept’, *Nature Reviews Drug Discovery*. Nature Publishing Group, pp. 357–372. doi: 10.1038/nrd2280.

Takahashi, N. *et al.* (2008) ‘Molecular characterization of TRPA1 channel activation by cysteine-reactive inflammatory mediators’, *Channels*. Taylor & Francis, 2(4), pp. 287–298. doi: 10.4161/chan.2.4.6745.

Tamaddonfard, E. *et al.* (2014) *Role of opioid system in verapamil-induced antinociception in a rat model of orofacial pain*, *ARTICLE Veterinary Research Forum*. Faculty of Veterinary Medicine, Urmia University. Available at: http://vrf.iranjournals.ir/article_4633.html (Accessed: 22 September 2020).

Tan, C. H. and McNaughton, P. A. (2018) ‘TRPM2 and warmth sensation’, *Pflugers Archiv European Journal of Physiology*. Springer Verlag, pp. 787–798. doi: 10.1007/s00424-018-2139-7.

Taylor-Clark, T., Undem, B. J., *et al.* (2008) ‘Prostaglandin-Induced Activation of Nociceptive Neurons via Direct Interaction with Transient Receptor Potential A1 (TRPA1)’, *Molecular Pharmacology*, 73(2), pp. 274 LP – 281. doi: 10.1124/mol.107.040832.

Taylor-Clark, T., McAlexander, M. A., *et al.* (2008) ‘Relative contributions of TRPA1 and TRPV1 channels in the activation of vagal bronchopulmonary C-fibres by the endogenous autacoid 4-oxononenal’, *The Journal of Physiology*. John Wiley & Sons, Ltd, 586(14), pp. 3447–3459. doi: 10.1113/jphysiol.2008.153585.

Tewksbury, J. J. and Nabhan, G. P. (2001) ‘Seed dispersal: Directed deterrence by capsaicin in chillies’, *Nature*. Nature Publishing Group, 412(6845), pp. 403–404. doi: 10.1038/35086653.

Thompson, J. N. (1998) ‘Rapid evolution as an ecological process’, *Trends in Ecology and Evolution*. Elsevier Ltd, pp. 329–332. doi: 10.1016/s0169-5347(98)01378-0.

Tiemann, L. *et al.* (2018) ‘Distinct patterns of brain activity mediate perceptual and motor and autonomic responses to noxious stimuli’, *Nature Communications*. Nature Publishing Group, 9(1), pp. 1–12. doi: 10.1038/s41467-018-06875-x.

Tominaga, M. *et al.* (1998) ‘The cloned capsaicin receptor integrates multiple pain-producing stimuli’, *Neuron*. Cell Press, 21(3), pp. 531–543. doi: 10.1016/S0896-6273(00)80564-4.

Turcotte, M. M., Reznick, D. N. and Hare, J. D. (2011) ‘The impact of rapid evolution on population dynamics in the wild: experimental test of eco-evolutionary dynamics’, *Ecology Letters*. doi: 10.1111/j.1461-0248.2011.01676.x.

Vandewauw, I. *et al.* (2018) ‘A TRP channel trio mediates acute noxious heat sensing’, *Nature*.

Nature Publishing Group, 555(7698), pp. 662–666. doi: 10.1038/nature26137.

Venkatachalam, K. and Montell, C. (2007) 'TRP Channels'. doi: 10.1146/annurev.biochem.75.103004.142819.

Voets, T. *et al.* (2004) 'The principle of temperature-dependent gating in cold- and heat-sensitive TRP channels', *Nature*. Nature Publishing Group, 430(7001), pp. 748–754. doi: 10.1038/nature02732.

Voets, T. *et al.* (2007) 'TRPM8 voltage sensor mutants reveal a mechanism for integrating thermal and chemical stimuli', *Nature Chemical Biology*. Nature Publishing Group, 3(3), pp. 174–182. doi: 10.1038/nchembio862.

Wang, L. *et al.* (2012) 'Identification of in vivo disulfide conformation of TRPA1 ion channel.', *The Journal of biological chemistry*. American Society for Biochemistry and Molecular Biology, 287(9), pp. 6169–76. doi: 10.1074/jbc.M111.329748.

Wang, Y. Y. *et al.* (2011) 'A TRPA1-dependent mechanism for the pungent sensation of weak acids', *J Gen Physiol*. 2011/05/18, 137(6), pp. 493–505. doi: 10.1085/jgp.201110615.

Waxman, S. G. and Dib-Hajj, S. D. (2019) 'The Two Sides of Na V 1.7: Painful and Painless Channelopathies', *Neuron*. Cell Press, pp. 765–767. doi: 10.1016/j.neuron.2019.02.016.

Weisman, A., Quintner, J. and Masharawi, Y. (2019) 'Congenital Insensitivity to Pain: A Misnomer', *Journal of Pain*. Churchill Livingstone Inc., 20(9), pp. 1011–1014. doi: 10.1016/j.jpain.2019.01.331.

Wemmie, J. A., Taugher, R. J. and Kreple, C. J. (2013) 'Acid-sensing ion channels in pain and disease', *Nature Reviews Neuroscience*. NIH Public Access, pp. 461–471. doi: 10.1038/nrn3529.

Weyer, A. and Lehto, S. (2017) 'Development of TRPM8 Antagonists to Treat Chronic Pain and Migraine', *Pharmaceuticals*. MDPI AG, 10(4), p. 37. doi: 10.3390/ph10020037.

Woller, S. A. *et al.* (2017) 'An overview of pathways encoding nociception.', *Clinical and experimental rheumatology*, 35 Suppl 1(5), pp. 40–46. Available at: http://www.ncbi.nlm.nih.gov/pubmed/28967373 (Accessed: 24 January 2019).

Woolf, C. J. and Ma, Q. (2007) 'Nociceptors—Noxious Stimulus Detectors', *Neuron*. Cell Press, 55(3), pp. 353–364. doi: 10.1016/J.NEURON.2007.07.016.

Wright, A. J. *et al.* (2018) 'Increased hyperpolarized [1-13C] lactate production in a model of joint inflammation is not accompanied by tissue acidosis as assessed using hyperpolarized 13C-labelled bicarbonate', *NMR in Biomedicine*, 31(4), p. e3892. doi: 10.1002/nbm.3892.

Wright, S. H. (2004) 'Generation of resting membrane potential', *Advances in Physiology Education*. American Physiological Society, 28(4), pp. 139–142. doi: 10.1152/advan.00029.2004.

Xu, H., Blair, N. T. and Clapham, D. E. (2005) 'Camphor Activates and Strongly Desensitizes the Transient Receptor Potential Vanilloid Subtype 1 Channel in a Vanilloid-Independent Mechanism', *Journal of Neuroscience*. Society for Neuroscience, 25(39), pp. 8924–8937. doi: 10.1523/JNEUROSCI.2574-05.2005.

Yang, F. *et al.* (2010) ‘Thermosensitive TRP channel pore turret is part of the temperature activation pathway’, *Proceedings of the National Academy of Sciences of the United States of America*. National Academy of Sciences, 107(15), pp. 7083–7088. doi: 10.1073/pnas.1000357107.

Yang, F. *et al.* (2015) ‘Structural mechanism underlying capsaicin binding and activation of the TRPV1 ion channel’, *Nature chemical biology*, 11, pp. 518–526. doi: 10.1038/nchembio.1835.

Yao, J., Liu, B. and Qin, F. (2011) ‘Modular thermal sensors in temperature-gated transient receptor potential (TRP) channels’, *Proceedings of the National Academy of Sciences of the United States of America*. National Academy of Sciences, 108(27), pp. 11109–11114. doi: 10.1073/pnas.1105196108.

Zhang, F. *et al.* (2018) ‘Heat activation is intrinsic to the pore domain of TRPV1.’, *Proceedings of the National Academy of Sciences of the United States of America*. National Academy of Sciences, 115(2), pp. E317–E324. doi: 10.1073/pnas.1717192115.

Zhang, R. X. and Ren, K. (2011) *Animal models of inflammatory pain*, *Neuromethods*. Humana Press, Totowa, NJ. doi: 10.1007/978-1-60761-880-5_2.

Zhang, S. *et al.* (2016) ‘Clinical features for diagnosis and management of patients with PRDM12 congenital insensitivity to pain’, *Journal of Medical Genetics*. BMJ Publishing Group, 53(8), pp. 533–535. doi: 10.1136/jmedgenet-2015-103646.

Zheng, J. (2013) ‘Molecular mechanism of TRP channels.’, *Comprehensive Physiology*. NIH Public Access, 3(1), pp. 221–42. doi: 10.1002/cphy.c120001.

Zurborg, S. *et al.* (2009) *Defining a function for the ion channel TRPA1*, *PhD dissertation*.